DAA/LANGLEY

IN-39

P.166

NAG1-215

CENTER FOR COMPUTER AIDED DESIGN

R-FILE CR

82562

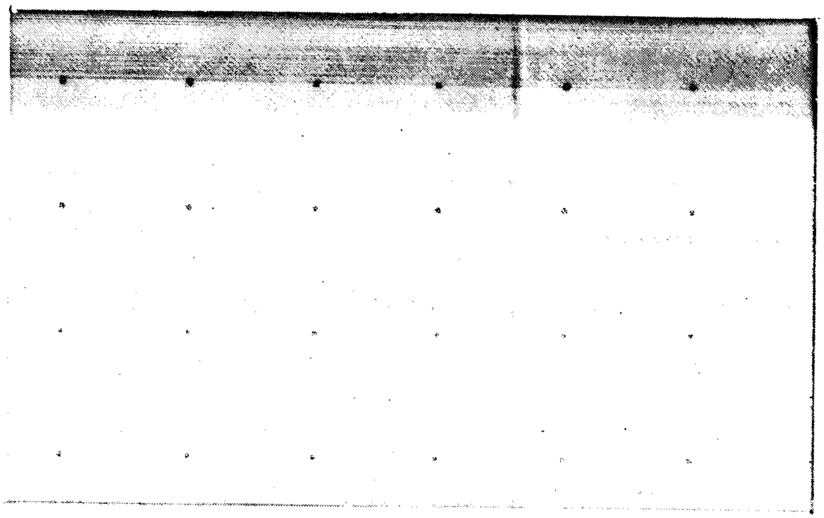

College of Engineering
The University of Iowa
Iowa City, Iowa 52242

(NASA-CR-181100) SHAPE DESIGN SENSITIVITY ANALYSIS USING DOMAIN INFORMATION (Iowa Univ.) 166 p Avail: NTIS HC A08/MF A01 CSCL 20K

N87-27221

Unclas

G3/39 0082562

Technical Report 85-3

SHAPE DESIGN SENSITIVITY ANALYSIS
USING DOMAIN INFORMATION

by

Hwal-Gyeong Seong
and
Kyung K. Choi

Center for Computer Aided Design

College of Engineering
The University of Iowa
Iowa City, Iowa 52242

Research supported by
NASA Grant NAG-1-215

April, 1985

ABSTRACT

A numerical method for obtaining accurate shape design sensitivity information for built-up structures is developed and demonstrated through analysis of examples. Shape design sensitivities in the past have been obtained using a boundary approach to shape design sensitivity analysis and the finite element method of structural analysis. In the boundary approach, shape design sensitivity formulas have been expressed as contour integrals, using integration by parts and boundary and/or interface conditions. Consequently to evaluate shape design sensitivity, all integrals are evaluated as boundary integrals using information obtained from finite element analysis along external boundaries and internal interfaces between components. The boundary approach fails to yield acceptable results for problems with singularities due to unsatisfactory accuracy of boundary information evaluated with the finite element method. The basic character of the finite element method, which gives more accurate domain information than boundary information, is utilized for shape design sensitivity improvement. To do so, a domain approach for shape design sensitivity analysis of built-up structures is derived using the material derivative idea of structural mechanics and the adjoint variable method of design sensitivity analysis. Velocity elements and B-spline curves are introduced to alleviate difficulties in generating domain velocity

fields. Regularity requirements of the design velocity field are studied. Results obtained are applied to the following examples:

(1) Shape design sensitivity analysis of square box and plate-beam-truss built-up structures.

(2) Shape design sensitivity analysis, using a boundary-layer approach, of a simple interface problem and a fillet problem.

Accuracy of shape design sensitivity is shown to be greatly improved using domain information, avoiding data evaluation on external boundaries and internal interfaces.

TABLE OF CONTENTS

LIST OF TABLES

LIST OF FIGURES

LIST OF SYMBOLS

A	Governing matrix operator for control vertex set
$\bar{A}$	Differential operator
A_ℓ	Cross-sectional area of truss member
a	Energy bilinear form
b	Shape parameters B-spline basis functions (Chapter 2.4)
C	Elastic modulus tensor
C^k	The collection of k-times continuously differentiable functions
D	Flexural rigidity of plate
d	Beam width
E	Young's Modulus
F	Function Body force (Chapter 2)
f	Distributed load
G	Shear modulus
g	Function
h	Plate thickness (Chapter 2) Beam height (Chapter 4)
I	Moment of inertia
J	Jacobian matrix Torsion constant (Chapters 2.2 and 5.3)
L	Length
z	Displacement function
β	Beam rotation

Γ	Boundary of a system Outer bounding surface (Chapters 2.4 and 5)
γ	Interface Interface operator Innerbounding surface (Chapter 2.4 and 5)
δ	Variation
$\bar{\delta}$	Dirac measure
ℓ	Load linear form
θ	Beam rotation
λ	Adjoint variable
ν	Possion's ratio
τ	Shear stress Parameter (Chapter 2.2.1)
σ	Stress
ϕ	Constraint function Functional (Chapter 2.2) Function either V^s or V^t (Chapter 2.3)
ξ	Normalized centroid coordinate
η	Normalized centroid coordinate
ψ	Constraint functional
Ω	Domain of the system
∇	Gradient operator
$\bar{L}$	Virtual work
M	Characteristic functions Applied torque (Chapter 2.2)
N	Shape function B-spline basis element (Chapter 2.4)
n	Outward normal vector
P	End point in B-spline approximation

Q	Approximated shape
q	Vector of nodal coordinate
s	Boundary-layer coordinate
T	Traction vector Transformation (Chapter 2.2.1) Kinetic Energy (Chapter 2.2.2)
t	Boundary-layer coordinate Plate thickness (Chapter 4.3) Time (Chapter 2.2)
U	Strain energy
V	Design velocity field
v	Displacement for beam Control vertex set (Chapter 2.4)
W	Product space
$\hat{x}$	Isolated point
Z	Space of kinematically admissible displacement field

I. INTRODUCTION

1.1 Motivation

The theory of structural shape design sensitivity analysis (SDSA) has been extensively developed. Shape design sensitivity formulae have been explicitly expressed as contour integrals, using integration by parts and interface boundary conditions to obtain identities for transformation of domain integrals to contour integrals. In this boundary approach, one uses information evaluated along external boundaries and internal interfaces. This approach has been widely tested in conjunction with the finite element method and it has been found to have difficulties in problems with singular behavior.

The finite element method (FEM) is a powerful tool for solving many analysis problems encountered in the practice of engineering desciplines. However, it is widely known [1] that the accuracy of the boundary information obtained with the finite element method may not be satisfactory for systems with singular characteristics.

If one recalls the nature of the finite element method as a domain approximation method, it is easy to find the reason for conditional accuracy of the boundary approach, when implemented with the finite element method. During the computational process of the finite element analysis, the unknown variables are sought to approximately satisfy the governing equation and the non-kinematic boundary conditions in a domain integral sense.

In the present work, a domain approach to shape design sensitivity analysis is introduced to enhance the accuracy of the shape design sensitivity, by taking advantage of inherent properties of the finite element method. Also, to control the design velocity field within the domain and to save computing time, a boundary-layer approach is introduced and tested.

1.2 Organization

The first two sections of Chapter 2 contain a derivation of the shape design sensitivity formulas, based on the domain approach for built-up structures, using the material derivative idea from continuum mechanics and the adjoint variable method. Built-up structures involve components such as trusses, beams, plane elastic plates, and bending plate components. The last two sections of Chapter 2 present the ideas of boundary-layers and velocity elements. A boundary-layer is a neighborhood of the varied boundary that is isolated from the core of the structure by two bounding surfaces Γ and γ. The outer bounding surface Γ is identical to the structural boundary and the inner bounding surface γ is a pre-set surface chosen by the designer. The principal objective of introducing a boundary-layer is to alleviate the difficulty of generating domain velocity fields. Also, the idea of a boundary-layer can reduce computing cost. A velocity element is a part of the boundary-layer, with two opposite element sides that lie on two bounding surfaces. Using an isoparametric mapping, a velocity element can interpolate the design velocity of interior points, based on a given velocity field along the two bounding surfaces. The bounding surfaces are represented using B-spline curves.

In Chapter 3, regularity properties of the velocity field are studied through a simple example of a uniformly loaded cantilever beam, by introducing internal subdivisions and different design velocity fields. Based on this study, regularity requirements for each design component are drawn and directly applied to a plate-beam-truss built-up structure in Chapter 4.

In Chapter 4, the domain approach to shape design sensitivity analysis of built-up structures is treated. The first example is a square box that is composed of five plane elastic components. The second example is a plate-beam-truss built-up structure with a Hermite cubic design velocity field.

In Chapter 5, shape design sensitivity analysis of structures is presented using the boundary-layer idea. The first example is a simple interface problem. In this problem, singularity can be expected along the interface, due to non-smooth data (material property) across the interface. The capability of this approach is demonstrated by comparing numerical results obtained with the boundary and the domain approaches. The second example studied is a fillet problem. The varied boundary is represented by B-spline curves and the domain velocity field is evaluated using a velocity element idea.

Chapter 6 presents discussion, conclusions, and suggestions for futher research on the domain and boundary-layer approaches.

1.3 Literature Review

The desire to yield maximum performance with a minimum exenditure of resources motivates the continuing developement and growth of structural otimization. In the following, literature is reviewed in the area of shape design sensitivity analysis and optimization, with emphasis on numerical methods.

One of the first treatments of the general problem of optimizing the shape of structures was presented by Zienkiewicz and Campbell [2]. They formulated the shape optimal design problem using a finite element model of the structure and treated the location of nodal points of the finite element model as design variables. They then calculated derivatives of stiffness and load matrices with respect to design parameters, obtained derivatives of structural response measures, and employed sequential linear programming for numerical optimization. Ramakrishnan and Francavilla [3] employed a similar finite element formulation, but they used a a penalty function method for numerical optimization. Francavilla, Ramakrishnan, and Zienkiewicz [4] employed the finite element method of Refs. 2 and 3 for fillet optimization to minimize stress concentration. Schnack [5] and Oda [6] used a finite element formulation for stress calculation in the neighborhood of a stress concentration and iteratively modified the contour to minimize peak stress.

A more basic approach for surface contouring to minimize stress concentration was presented by Tvergaard, for selecting the optimum shape of a fillet [7]. He employed a stress field model of a fillet, with a finite dimensional family of boundary shapes defined in terms of coordinate parameters. He employed a variational analysis of the stress field to obtain derivatives of stress with respect to design parameters and used sequential linear programming to iteratively construct an optimum design. Kristensen and Madsen [8] formulated a class of shape optimal design problems for planar solids that generalize the approach presented by Tvergaard [7]. They used orthogonal polynomials to locate the boundary of the body and treated the coefficients as design parameters. They employed a finite element model of structural response to obtain derivatives of stress with respect to design parameters [9] and employed sequential linear programming to solve the optimization problem. They solved an elementary problem of shape optimization of a hole in a bi-axial stress field, analytically and numerically. They also illustrated the method on more complex problems.

Bhavikatti and Ramakrishnan [10] presented a refinement of the formulation of Refs. 2, 3, and 4 for optimum design of fillets in flat and round tension bars. They also used a polynomial, with coefficients taken as the design variables, to characterize the shape of the fillet and a finite element model to calculate stress within the body. They investigated minimization of stress concentration factor, minimum volume design, and design for uniform stress distribution along the fillet boundary. Derivatives of response measures with respect to design parameters were calculated with a finite element model. Sequential linear programming was employed for numerical optimization. Dems and Mroz [11] presented a quite general approach to shape optimal design.

They used a boundary perturbation analysis to derive optimality criteria and a finite element numerical method to determine the optimum boundary. Dems [12] used this method to formulate and numerically solve a variety of problems of shaft cross-section shape optimization for torsional stiffness.

A function space gradient projection method for optimal design of the shape of two-dimensional elastic bodies was presented by Chun and Haug [13], using design sensitivity analysis methods similar to those presented by Rousselet and Haug [14] and a gradient projection method presented in Ref. 15. The design objective in this work was weight minimization, with constraints on von Mises yield stress and shear stress distribution on the boundary. The above method has been extensively expanded, both theoretically and numerically. Yoo, Haug, and Choi [16] applied the method to several plane elasticity problems of considerable size, such as a dam and a connecting rod, by using sparce matrix techniques [17]. Hou and Benedict [18] applied this method to a torsion problem with shape constraints. Choi and Haug [19] developed shape design sensitivity formulas for five prototype problems of elastic structures. Choi [20] studied shape design sensitivity analysis of displacement and stress constraint functionals, with emphasis on the effect of point and element movement within the domain due to domain perturbation. Haug, Choi and Komkov [21] have developed a unified variational form of structural design sensitivity analysis with a rigorous mathematical foundation. Lee, Choi, and Haug [22] applied the method to build-up structures with constraints on design variables, von

Mises yield stress, displacement, and natural frequency. Yang and Choi [23] improved the accuracy of shape design sensitivity for stress constraints by improving boundary information, using higher order finite elements with more sophistcated function evaluation schemes and smooth boundary representations. The majority of the work in Refs. 17-22 uses the boundary approach of shape design sensitivity analysis.

II. SHAPE DESIGN SENSITIVITY ANALYSIS USING DOMAIN INFORMATION

2.1 Introduction

Shape design sensitivity analysis has generally been done by transforming domain integrals to contour integrals, by integrating by parts and using formal operator equations [19]. This approach, called the boundary approach, has the following features:

(1) It is general and can be applied to a wide variety of problems with regular functions.

(2) The dimension of the boundary, over which integration is performed, is lower by one than the original problem.

(3) The variation of the functional can be obtained by evaluating only normal components of the velocity field on the boundary.

(4) This approach requires accurate data along the boundary, which is difficult to obtain using the finite element method (FEM).

In a majority of the problems tested to date, the boundary approach has given resonable results. However, in (i) problems with irregular functions or (ii) problems with strong singular characteristics, such as build-up structures, the boundary approach may fail to yield acceptable results [22].

In the boundary integral formulation of SDSA, difficulties may arise because of poor accuracy of boundary information, which is obtained by projecting results of FEM analysis from Gauss points of elements in the interior to the boundary, may not be satisfactory. This is caused mainly by the limited order of polynomials used in the finite element [24] and by skin effects [25]. Skin designates discrepancies between the true and approximate boundaries. This behavior is shown to exist near each beam stiffener in the plate-beam-truss built-up structure of Ref. 22.

Considering the intrinsic nature of the FEM as a domain approximation method, one may expect FEM to produce better domain information rather than boundary information. In Section 2.2.1, the domain approach of component shape design sensitivity analysis is derived, after introducing the basic material derivative idea. Components treated are a truss, a beam, a plane elastic plate, and a bending plate. Combinations of these components make up an extensive class of built-up structures. In Section 2.2.2, the domain approach to shape design sensitivity analysis is derived for a built-up structure, using the adjoint variable method. In Section 2.3, the concept of a boundary-layer and a boundary-layer coordinate system is introduced to ease the difficulty of generating a domain velocity field. The boundary-layer is a subdomain, located in a neighborhood of the varied boundary. The boundary-layer is divided into a set of velocity elements that can evaluate the velocity and derivative of velocity of any inside points, using isoparametric mapping. In Section 2.4, the B-spline is introduced to represent an arbitrary smooth boundary.

2.2 Domain Approach to SDSA

2.2.1 Material Derivative of Bilinear Forms of Each Structural Component in One- and Two-Dimensions

A wide range of engineering structures are composed of one- and two-dimensional structural domponents. Such structures maintain integrity through interactions of components along interfaces. The response of structural systems; more specifically, the displacement field in the system, can be characterized by two contributions. The first is contributions from stretching action due to lateral loads. The second is contributions from bending action due to transverse loads. For a given stimulus, these two actions determine the displacement field of the system.

For one dimensional structural components, trusses and beams represent stretching and bending contributions, respectively. For two dimensional structural components, plane elastic plates and bending plates represent stretching and bending contributions, respectively. Mechanical structural systems are collections of a variety of structural components. Combinations of truss, beam, plane elastic plate, and bending plate components make up a large class of engineering structures. Such engineering structures can be considered as being built-up of structural components.

In this section, the material derivative is defined and basic material derivative formulas for one and two dimensional functionals are derived. The material derivative formula of each prototype structural component is derived using basic material derivative formulas [19].

2.2.1.1 Material Derivative. The idea of shape variation and material derivative, presented in Ref. 19 are covered briefly here for convenience and completness. Interested readers may find a more detailed mathematical development in Ref. 19. In shape design sensitivity analysis, shape of a domain is treated as the design variable. It is convenient to think of the domain as a continuous medium and to utilize the material derivative idea to relate a variation in shape to the resulting variation in performance functionals.

Consider a domain Ω in one, two, or three dimensions, shown schematically in Fig. 2.2.1. Suppose that only one parameter τ defines the transformation T, as shown in Fig. 2.2.1. This parameter can be thought as time [19], so that the process of deforming Ω to Ω_τ can be viewed as a dynamic process of deforming a continuum, with the parameter τ playing the role of time. The trajectory of a particle that is initially at x is now defined as the initial-value problem

$$\left.\begin{aligned} \dot{x}_\tau &= V(x_\tau,\tau) \\ x_0 &= x \end{aligned}\right\} \tag{2.2.1}$$

In other words, one can define T by

$$T(x,\tau) = x_\tau(x) \tag{2.2.2}$$

where x_τ is the solution of the initial value problem, if the velocity field $V(x_\tau,\tau)$ is given.

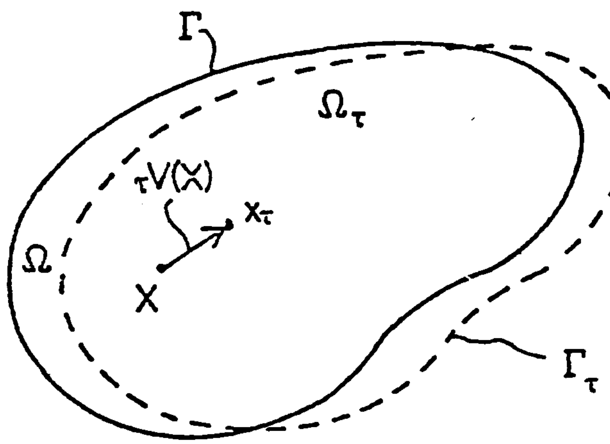

Figure 2.2.1 Domain Variation

Suppose $z_\tau(x_\tau)$ is a smooth classical solution of the following formal operator equation on the deformed domain Ω_τ:

$$\left.\begin{aligned} \bar{A} z_\tau &= f \,, \quad x \quad \Omega_\tau \\ z_\tau &= 0 \,, \quad x \quad \Gamma_\tau \end{aligned}\right\} \tag{2.2.3}$$

The pointwise material derivative, if it exits, at $x \in \Omega$ is defined as

$$\dot{z}(x) = \frac{d}{d\tau} z_\tau(x + \tau V(x))\Big|_{\tau=0} = \lim_{\tau \to 0} \frac{z_\tau(x + \tau V(x)) - z(x)}{\tau} \tag{2.2.4}$$

Consider now a domain functional, defined as an integral over Ω_τ,

$$\phi_1 = \iint_{\Omega_\tau} f_\tau(x_\tau)\, d\Omega_\tau$$

$$= \iint_{\Omega} f_\tau(x + \tau V(x))|J|\, d\Omega \tag{2.2.5}$$

where f_τ is a regular function defined on Ω_τ and J is the Jacobian matrix of the mapping T. The material derivative of ϕ_1 at Ω is [21]

$$\phi_1' = \frac{d}{d\tau} \iint_{\Omega} f_\tau(x + \tau V(x))|J|\, d\Omega$$

$$= \iint_{\Omega} [f'(x) + (\nabla f \cdot V) + f(\nabla \cdot V)]\, d\Omega \tag{2.2.6.a}$$

If the integral over Ω is transformed to a boundary integral, using integration by parts, Eq. (2.2.6.a) can be rewritten as [19]

$$\phi_1' = \iint_{\Omega} f'(x)\, dx + \int_{\Gamma} f(V \cdot n)\, d\Gamma \tag{2.2.6.b}$$

It is important to note that the entire domain velocity V appears in the domain approach of Eq. 2.2.6.a in contrast to only the normal component of the boundary velocity ($V \cdot n$) in the boundary approach of Eq. 2.2.6.b. These two approaches, Eqs. 2.2.6.a and 2.2.6.b, are mathematically identical. However, the values to be evaluated may be significantly different, depending on numerical approximating methods used in the calculation. The boundary approach should be used with a boundary oriented approximation method, such as the boundary element method, and the domain approach matches better with a domain approximation method, such as the finite element method.

In shape design sensitivity analysis of built-up structures, a shape change in a structural component causes movement throughout the entire domain. To predict the effect of a change in shape, one must define the material derivative of a general functional that is given as a one or two dimensional integral. The material derivative of a two dimensional integral is given in Eq. 2.2.6.a and the material derivative of a one dimensional integral is presented below.

Consider a functional that is given as a one dimensional integral

$$\phi_2 = \int_x g \, dx \tag{2.2.7}$$

where g is a regular function and x is a local coordinate system. The material derivative of ϕ_2 is from Eq. 2.2.6.a,

$$\phi_2' = \int_x [g' + g_x V + g V_x] \, dx \tag{2.2.8}$$

with $\dot{g} = g' + g_x V$

<u>2.2.1.2 Truss Component</u>. Consider a truss component with end loads r_0 and r_L shown in Fig. 2.2.2. Note that the end loads r_0 and r_L are generally functions of a shape parameter b which is generally a function of orientation in space, with respect to some coordinate system. The energy bilinear form $a^{(1)}(z^{(1)}, \bar{z}^{(1)})$ for a truss component is

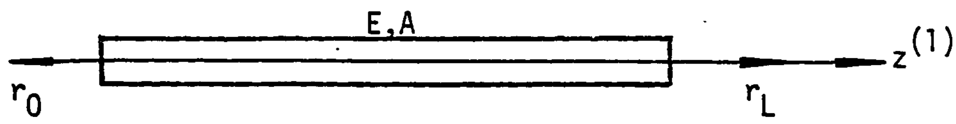

Figure 2.2.2 Truss Component

$$a^{(1)}(z^{(1)}, \bar{z}^{(1)}) = \int_0^L AEz_x^{(1)} \bar{z}_x^{(1)} dx \tag{2.2.9}$$

where A is the cross sectional area of a truss member and the load linear form is

$$\ell^{(1)}(\bar{z}^{(1)}) = r_L(b)\, \bar{z}_{(L)}^{(1)} - r_0(b)\, \bar{z}_{(0)}^{(1)} \tag{2.2.10}$$

where the directions of end loads are as in Fig. 2.2.2.

The material derivative of Eqs. 2.2.9 and 2.2.10 are

$$\begin{aligned}[a^{(1)}(z^{(1)}, \bar{z}^{(1)})]' &= \int_0^L AE[(z_x^{(1)'} \bar{z}_x^{(1)} + z_x^{(1)} \bar{z}_x^{(1)'}) + (z_x^{(1)} \bar{z}_x^{(1)})_x V \\ &\quad + (z_x^{(1)} \bar{z}_x^{(1)}) V_x]\, dx \\ &= \int_0^L AE(\dot{z}_x^{(1)} \bar{z}_x^{(1)})\, dx \\ &\quad - \int_0^L AE(z_x^{(1)} \bar{z}_x^{(1)}) V_x\, dx \end{aligned} \tag{2.2.11}$$

and

$$[\ell^{(1)}(\bar{z}^{(1)})]' = \frac{dr_L(b)}{db}\bar{z}^{(1)}_{(L)} - \frac{dr_0(b)}{db}\bar{z}^{(1)}_{(0)} \quad (2.2.12)$$

where the fact that

$$\dot{\bar{z}}^{(1)} = \bar{z}^{(1)'} + \bar{z}^{(1)}_x V = 0 \quad (2.2.13)$$

has been used.

2.2.1.3 Beam Component. A typical beam with distributed load $q(x)$ and end moment M is shown in Fig. 2.2.3.

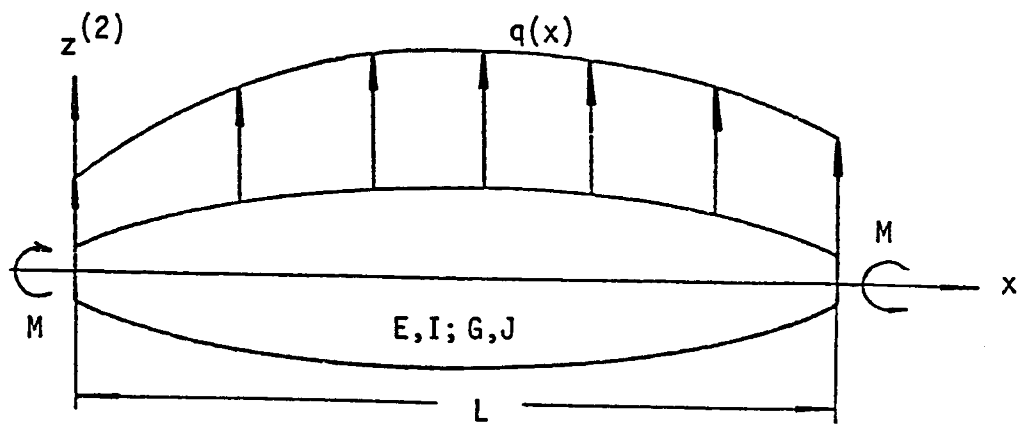

Figure 2.2.3 Beam Component

The energy bilinear form $a^{(2)}(z^{(2)}, \bar{z}^{(2)})$ and load linear form $\ell^{(2)}(\bar{z}^{(2)})$ are, respectively,

$$a^{(2)}(z^{(2)}, \bar{z}^{(2)}) = \int_0^L EI\ (z_{xx}^{(2)}\ \bar{z}_{xx}^{(2)})\ dx + \int_0^L GJ\ (\theta_x \bar{\theta}_x)\ dx \quad (2.2.14)$$

$$\ell^{(2)}(\bar{z}^{(2)}) = \int_0^L q\ \bar{z}^{(2)}\ dx + M[\bar{\theta}(L) - \bar{\theta}(0)] \quad (2.2.15)$$

where the bilinear form $a^{(2)}(z^{(2)}, \bar{z}^{(2)})$ includes both bending and twisting actions, E is Young's modulus, G is shear modulus, I and J are moment of inertia and polar moment of inertia of the beam, respectively, and θ is beam rotation.

The material derivatives of Eqs. 2.2.14 and 2.2.15 are

$$\begin{aligned}[a^{(2)}(z^{(2)}, \bar{z}^{(2)})]' &= \int_0^L EI(\dot{z}_{xx}^{(2)}\ \bar{z}_{xx}^{(2)})\ dx + \int_0^L GJ(\dot{\theta}_x \bar{\theta}_x)\ dx \\ &- \int_0^L EI[3(z_{xx}^{(2)}\ \bar{z}_{xx}^{(2)})V_x + (z_x^{(2)}\ \bar{z}_{xx}^{(2)} + z_{xx}^{(2)}\ \bar{z}_x^{(2)})V_{xx}]\ dx \\ &- \int_0^L GJ(\theta_x \bar{\theta}_x)V_x\ dx \end{aligned} \quad (2.2.16)$$

$$[\ell^{(2)}(\bar{z}^{(2)})]' = \int_0^L q\ \bar{z}^{(2)} V_x\ dx \quad (2.2.17)$$

<u>2.2.1.4 Plane Elasticity Plate Component</u>. In Fig. 2.2.4, a plane elastic plate with traction $T(\underset{\sim}{x})$ and body force $F(\underset{\sim}{x})$ is given. Note that $\underset{\sim}{x}$ is used to designate (x_1, x_2). The energy bilinear form and load linear form are, respectively,

$$a^{(3)}(z^{(3)}, \bar{z}^{(3)}) = \iint_\Omega \sum_{i,j} \sigma_{ij}(z^{(3)})\epsilon_{ij}(\bar{z}^{(3)})\ d\Omega \quad (2.2.18)$$

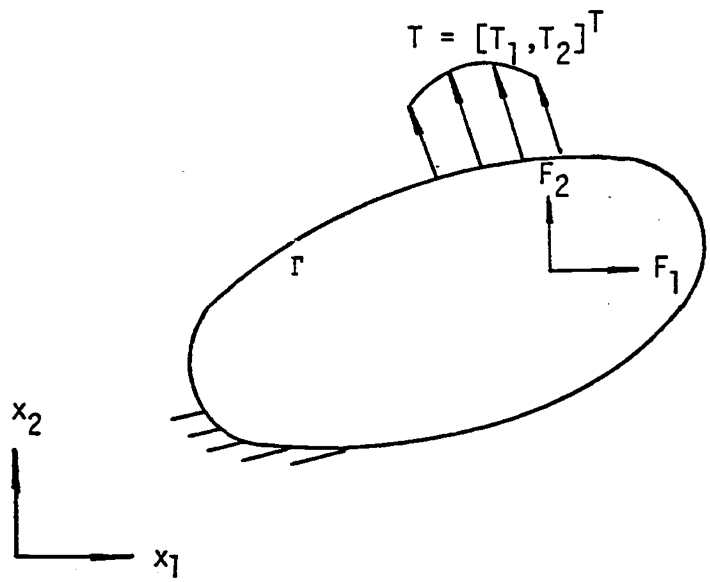

Figure 2.2.4 Plane Elastic Plate Component

$$\ell^{(3)}(\bar{z}^{(3)}) = \iint_{\Omega} (F \cdot \bar{z}^{(3)})\, d\Omega + \int_{\Gamma} (T \cdot \bar{z}^{(3)})\, d\Gamma \tag{2.2.19}$$

Taking variation of Eqs. 2.2.18 and 2.2.19 and the using material derivative idea, one has

$$\begin{aligned}
[a^{(3)}(z^{(3)}, \bar{z}^{(3)})]' &= \iint_{\Omega} \sum_{i,j} \sigma_{ij}(\dot{z}^{(3)}) \epsilon_{ij}(\bar{z}^{(3)})\, d\Omega \\
&- \iint_{\Omega} \sum_{i,j} \sigma_{ij}(z^{(3)}) \, (\nabla \bar{z}_i^{(3)} \cdot \frac{\partial V}{\partial x_j})\, d\Omega \\
&- \iint_{\Omega} \sum_{i,j} \{\sum_{k,\ell} C_{ijk\ell}(\nabla z_K^{(3)} \cdot \frac{\partial V}{\partial x_\ell})\} \, \epsilon_{ij}(\bar{z}^{(3)})\, d\Omega \\
&+ \iint_{\Omega} [\sum_{i,j} \sigma_{ij}(z^{(3)}) \, \epsilon_{ij}(\bar{z}^{(3)})] \, (\nabla \cdot V)\, d\Omega
\end{aligned} \tag{2.2.20}$$

$$[\ell^{(3)}(\overline{z}^{(3)})]' = \iint_\Omega \sum_i [- F_i \ (\nabla \overline{z}_i^{(3)} \cdot V) + (\nabla (F_i \overline{z}_i^{(3)}) \cdot V)$$

$$+ F_i \overline{z}_i^{(3)} (\nabla \cdot V)] \, d\Omega + \int_\Gamma \sum_i (T_i \overline{z}_i^{(3)}) \, d\Gamma \qquad (2.2.21)$$

where C is the elastic modulus tensor, which satisfies $C_{ijk\ell} = C_{k\ell ij}$ and $C_{ijk\ell} = C_{ij\ell k}$, i,j,k,l=1,2.

2.2.1.5 Plate Component. Consider a plate of variable thickness $h(x_1, x_2) \geq h > 0$ with load $f(x_1, x_2)$ shown in Fig. 2.2.5. The energy bilinear form and the load linear form are, respectively,

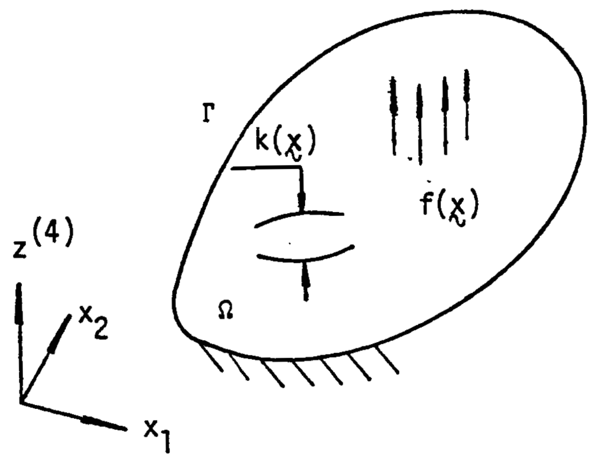

Figure 2.2.5 Bending Plate Component

$$a^{(4)}(z^{(4)}, \bar{z}^{(4)}) = \iint_\Omega D[(z_{11}^{(4)} + \nu z_{22}^{(4)})\,\bar{z}_{11}^{(4)} + (z_{22}^{(4)} + \nu z_{11}^{(4)})\,\bar{z}_{22}^{(4)}$$

$$+ 2(1-\nu)\, z_{12}^{(4)}\,\bar{z}_{12}^{(4)}]\, d\Omega \qquad (2.2.22)$$

and

$$\ell^{(4)}(\bar{z}^{(4)}) = \iint_\Omega (f\,\bar{z}^{(4)})\, d\Omega \qquad (2.2.23)$$

where

$$D = \frac{Eh^3}{12(1-\nu^2)}$$

Taking the material derivative of Eqs. 2.2.22 and 2.2.23, one has

$$[a^{(4)}(\dot{z}^{(4)}, \bar{z}^{(4)})]' = \iint_\Omega D[(\dot{z}_{11}^{(4)} + \nu\dot{z}_{22}^{(4)})\bar{z}_{11}^{(4)} + (\dot{z}_{22}^{(4)} + \nu\dot{z}_{11}^{(4)})\dot{z}_{22}^{(4)}$$

$$+ 2(1-\nu)\dot{z}_{12}^{(4)}\,\bar{z}_{12}^{(4)}]\, d\Omega$$

$$- \iint_\Omega D[\{(\nabla z^{(4)}\cdot V_{11}) \quad + \nu(\nabla z^{(4)}\cdot V)_{22}\}\bar{z}_{11}^{(4)}$$

$$+ \{(\nabla z^{(4)}\cdot V)_{22} + \nu(\nabla z^{(4)}\cdot V)_{11}\}\bar{z}_{22}^{(4)} + 2(1-\nu)(\nabla z^{(4)}\cdot V)_{12}]\, d\Omega$$

$$- \iint_\Omega D[(z_{11}^{(4)} + \nu z_{22}^{(4)})(\nabla\bar{z}^{(4)}\cdot V)_{11} + (z_{22}^{(4)} + \nu z_{11}^{(4)})(\nabla\bar{z}^{(4)}\cdot V)_{22}$$

$$+ 2(1-\nu)z_{12}^{(4)}\,(\nabla\bar{z}^{(4)}\cdot V)_{12}]\, d\Omega \qquad (2.2.24)$$

$$+ \iint_\Omega D \begin{bmatrix} (z^{(4)}_{111}+\nu z^{(4)}_{122})\bar{z}^{(4)}_{11}+(z^{(4)}_{122}+\nu z^{(4)}_{111})\bar{z}^{(4)}_{22}+2(1-\nu)z^{(4)}_{112}\bar{z}^{(4)}_{12} \\ (z^{(4)}_{112}+\nu z^{(4)}_{222})\bar{z}^{(4)}_{11}+(z^{(4)}_{222}+\nu z^{(4)}_{112})\bar{z}^{(4)}_{22}+2(1-\nu)z^{(4)}_{122}\bar{z}^{(4)}_{12} \end{bmatrix}^T \begin{bmatrix} V^1 \\ V^2 \end{bmatrix} d\Omega$$

$$+ \iint_\Omega D \begin{bmatrix} (z^{(4)}_{11}+\nu z^{(4)}_{22})\bar{z}^{(4)}_{111}+(z^{(4)}_{22}+\nu z^{(4)}_{11})\bar{z}^{(4)}_{122}+2(1-\nu)z^{(4)}_{12}\bar{z}^{(4)}_{112} \\ (z^{(4)}_{11}+\nu z^{(4)}_{22})\bar{z}^{(4)}_{112}+(z^{(4)}_{22}+\nu z^{(4)}_{11})\bar{z}^{(4)}_{222}+2(1-\nu)z^{(4)}_{12}\bar{z}^{(4)}_{122} \end{bmatrix} \begin{bmatrix} V^1 \\ V^2 \end{bmatrix} d\Omega$$

$$+ \iint_\Omega D \left[(z^{(4)}_{11}+\nu z^{(4)}_{22})z^{(4)}_{11}+(z^{(4)}_{22}+\nu z^{(4)}_{11})\bar{z}^{(4)}_{22}+2(1-\nu)z^{(4)}_{12}\bar{z}^{(4)}_{12}\right] (\nabla\cdot V)\ d\Omega$$

and

$$[\ell^{(4)}(\bar{z}^{(4)})]' = \iint_\Omega (f\bar{z}^{(4)})\ (\nabla\cdot V)\ d\Omega \tag{2.2.25}$$

where $V = [V^1, V^2]^T$.

2.2.2 Variational Equation for Built-up Structure

The material covered in this sub-section is originated in Ref. 21, which is briefly reviewed here for completeness. As stated previously, a general structure is a collection of structural components that are interconnected by kinematic constraints at their boundaries. Displacement fields in structural components are said to be kinematically admissible if they satisfy kinematic constraints at the interfaces. In an abstract setting, let z denote a composite vector of displacement fields in the components that make up the built-up structure as

$$z = [z^{(1)}, z^{(2)}, \ldots, z^{(r)}]^T \tag{2.2.26}$$

where $z^{(i)} \in [H^{m_i}(\Omega_i)]^{\ell_i}$ represent displacements for the (i)-th component, and r is the number of components that make up the built-up structure. The space of kinematically admissible displacement fields is defined as the set of displacement fields satisfying homogeneous boundary conditions between individual components and the ground reference frame and kinematic interface conditions between components. Symbolically, this is

$$Z = \{z \in W: \ \gamma z = 0 \text{ on } \Gamma, \ \gamma^i z = \gamma^j z \text{ on } \Gamma_{ij}\} \tag{2.2.27}$$

where the product space $W = \pi_i [H^{m_i}(\Omega_i)]^{\ell_i}$ is the space of displacement fields that satisfy the required degree of smothness, γ is a boundary operator [21] that gives the projection of structural displacements and perhaps their derivatives onto the exterior boundary Γ and γ^i and γ^j are interface operators that project displacement fields and perhaps their derivatives from within components i and j onto their common boundary Γ_{ij}.

<u>2.2.2.1 Hamilton's Principle</u> Let the strain energy of the structural system be denoted by

$$U(z) = \frac{1}{2} a(z, z)$$

$$= \frac{1}{2} [\sum_i a^{(i)}(z^{(i)}, z^{(i)})] \tag{2.2.28}$$

where $\frac{1}{2}\, a^{(i)}(z^{(i)}, \bar{z}^{(i)})$ is the strain energy of (i)-th component.

It is presumed that the quadratic strain energy in Eq. 2.2.28 is defined for any displacement in the kinematically admissible displacement field Z. The strain energy U is defined as the sum of strain energies of the components that make up the built-up structure.

Next, define the kinetic energy of the system as

$$T\left(\frac{dz}{dt}\right) = \frac{1}{2}\, d\left(\frac{dz}{dt}\, \frac{dz}{dt}\right)$$

$$= \frac{1}{2}\left[\sum_i d^{(i)}\left(\frac{dz^{(i)}}{dt}, \frac{dz^{(i)}}{dt}\right)\right] \tag{2.2.29}$$

where $\frac{1}{2}\, d^{(i)}(dz^{(i)}/dt, dz^{(i)}/dt)$ is the kinetic energy of (i)-th component where $dz^{(i)}/dt$ denotes the time derivative of displacement $z^{(i)}$. As in the case of strain energy, kinetic energy is obtained by summing kinetic energies of each component in the built-up structure. It is also presumed that the kinetic energy T in Eq. 2.2.29 is defined for all kinematically admissible displacement fields.

Finally, let the virtual work of externally applied forces be defined as

$$\bar{L}(\bar{z}) \equiv \ell(\bar{z})$$

$$= \sum_i \left[\ell^{(i)}(\bar{z}^{(i)})\right] \tag{2.2.30}$$

where $\ell^{(i)}(\bar{z}^{(i)})$ is the virtual work of the (i)-th component, with virtual displacements that satisfy the kinematic boundary conditions; i.e., $\bar{z} \in Z$.

The variational form of Hamilton's principle[21] requires that

$$\int_{t_1}^{t_2} (\bar{U} - \bar{T})\, dt = \int_{t_1}^{t_2} \bar{L}\, dt \tag{2.2.31}$$

for all times t_1 and t_2 and for any kinematically admissible virtual displacements $\bar{z}$ that satisfy the additional conditions

$$\bar{z}(t_1) = \bar{z}(t_2) = 0 \tag{2.2.32}$$

where $\bar{U}$ and $\bar{T}$ are the first variation of the strain and kinematic energy quadratic forms defined as, respectively,

$$\begin{aligned} \bar{U} &= \frac{d}{d\tau} U(z + \tau\bar{z})\Big|_{\tau=0} \equiv a(z, \bar{z}) \\ \bar{T} &= \frac{d}{d\tau} T\left(\frac{dz}{dt} + \tau \frac{d\bar{z}}{dt}\right)\Big|_{\tau=0} \equiv d\left(\frac{dz}{dt}, \frac{d\bar{z}}{dt}\right) \end{aligned} \tag{2.2.33}$$

One may rewrite Eq. 2.2.31 using Eq. 2.2.33 as

$$\int_{t_1}^{t_2} \left[a(z, \bar{z}) - d\left(\frac{dz}{dt}, \frac{d\bar{z}}{dt}\right)\right] dt = \int_{t_1}^{t_2} \ell(\bar{z})\, dt \tag{2.2.34}$$

2.2.2.2 The Principle of virtual Work. Consider the case of static response of a structure to load that does not depend on time. One can obtain the variational form of the governing equation for a built-up structure by suppressing time in Eq. 2.2.34 as

$$a(z, \bar{z}) = \ell(\bar{z}), \qquad \text{for all } \bar{z} \in Z \tag{2.2.35}$$

Note that the energy bilinear form on the left is the summation of bilinear forms of structural components and that the load linear form on the right is the summation of load linear forms of each component making up the built-up structure.

2.2.2.3 First Variation of the Variational Form of the Built-up Structure. The objective is to find a relationship between a shape variation and the resulting variation in the state of the structure. One can define the first variation of Eq. 2.2.35 using Eqs. 2.2.28 and 2.2.30 as

$$[a(z, \bar{z})]' = a(\dot{z}, \bar{z}) + a'(z, \bar{z})$$

$$= \sum_{i=1}^{r} a^{(i)}(\dot{z}^{(i)}, \bar{z}^{(i)}) + \sum_{i=1}^{r} a^{(i)'}(a^{(i)}, \bar{z}^{(i)})$$

$$[\ell(\bar{z})]' = \ell'(\bar{z})$$

$$= \sum_{i=1}^{r} \ell^{(i)'}(\bar{z}^{(i)}) \tag{2.2.36}$$

where $a'(z, \bar{z})$ is the differential of the energy bilinear form with respect to design.

Using material derivatives fo component energy bilinear forms and load linear forms in Eqs. 2.2.11, 2.2.12, 2.2.16, 2.2.17, 2.2.20, 2.2.21, 2.2.24, and 2.2.25, one obtains from Eqs. 2.2.35 and 2.2.36

$$a(\dot{z}, \bar{z}) = \sum_{i=1}^{r} a^{(i)}(\dot{z}^{(i)}, \bar{z}^{(i)})$$

$$= \sum_{i=1}^{r} \ell^{(i)'}(\bar{z}^{(i)}) - \sum_{i=1}^{r} a^{(i)'}(z^{(i)}, \bar{z}^{(i)})$$

$$= \ell'(\bar{z}) - a'(z, \bar{z}) \qquad (2.2.37)$$

2.2.3 Adjoint Variable Method

Consider a general functional that defines performance of a built-up structure as [21]

$$\psi = \sum_{i=1}^{r} \iint_{\Omega_i} g^i(z^{(i)}, \nabla z^{(i)})\, d\Omega \qquad (2.2.38)$$

where $z^{(i)}$ is the displacement field of the (i)-th component and $\nabla z^{(i)} = [\nabla z_1^{(i)}, \nabla z_2^{(i)}]$.

Taking the variation of the above functional, using the material derivative idea, one has

$$\psi' = \frac{d}{d\tau} \psi_{\Omega_\tau}(z_\tau)\Big|_{\tau=0}$$

$$= \sum_{i=1}^{r} \iint_{\Omega_i} (g^i_{z^{(i)}} \dot{z}^{(i)} + \sum_{j=1}^{\ell_i} g^i_{\nabla z_j^{(i)}} \nabla \dot{z}_j^{(i)})\, d\Omega$$

$$+ \sum_{i=1}^{r} \iint_{\Omega_i} \{-g^i_{z^{(i)}} (\nabla z^{(i)} \cdot V^{(i)})$$

$$- \sum_{i=1}^{\ell i} g^i_{\nabla z_j^{(i)}} \nabla(\nabla z_j^{(i)} \cdot V^{(i)})\}\, d\Omega$$

$$+ (\nabla g^i \cdot V^i) + g^i(\nabla \cdot V^i)\}\, d\Omega \qquad (2.2.39)$$

where $z^{(i)} = [z_1^{(i)}, z_2^{(i)}, \ldots, z_{\ell_i}^{(i)}]^T$. In order to take advantage of this result, one must write terms of Eq. 2.2.39 explicitly in terms of the velocity field V. Since $\dot{z}$ cannot generally be determined explicitly, one must resort to a technique such as the adjoint variable method to obtain the desired result.

In order to treat terms on the right of Eq. 2.2.39, one can define an adjoint equation by replacing $\dot{z}$ in Eq. 2.2.39 by a virtual displacement $\bar{\lambda}$ and equate the result to the energy bilinear form, evaluated at the adjoint variable, as

$$a(\lambda, \bar{\lambda}) = \sum_{i=1}^{r} \iint_{\Omega_i} \left(g^i_{z^{(i)}} \bar{\lambda}^{(i)} + \sum_{j=1}^{\ell_i} g^i_{\nabla z_j^{(i)}} \nabla\bar{\lambda}_j^{(i)}\right) d\Omega \qquad (2.2.40)$$

for all $\bar{\lambda} \in Z$, where $\lambda = [\lambda^{(1)}, \lambda^{(2)}, \ldots, \lambda^{(r)}]^T$. Presumming the energy bilinear form is strongly elliptic and that terms on the right of Eq. 2.2.39 is a continuous linear form in $\bar{\lambda}$, this equation can determine λ uniquely [21]. Since $\dot{z}$ satisfies the kinematic admissibility conditions, one may evaluate Eq. 2.2.40 at $\bar{\lambda} = \dot{z}$ and Eq. 2.2.37 at $\bar{z} = \lambda$, to obtain

$$\begin{aligned} \psi' &= \ell'(\lambda) - a'(z, \lambda) \\ &+ \sum_{i=1}^{r} \iint_{\Omega_i} \left\{-g^i_{z^{(i)}}(\nabla z^{(i)} \cdot V^{(i)}) - \sum_{j=1}^{\ell_i} g^i_{\nabla z_j^{(i)}} \nabla(\nabla z_j^{(i)} \cdot V^{(i)})\right\} d\Omega \\ &+ \sum_{i=1}^{r} \iint_{\Omega_i} \left\{(\nabla g^i \cdot V^{(i)}) + g(\nabla \cdot V^{(i)})\right\} d\Omega \end{aligned} \qquad (2.2.41)$$

where $V^{(i)}$ is the velocity field defined on Ω_i.

Note that evaluation of this explicit design sensitivity formula requires solution of Eq. 2.2.40 for adjoint variable λ and evaluation of functionals involving both the state variable and the adjoint variable λ. These calculations are direct and take full advantage of the finite element method for solving both the state and adjoint equations of the built-up structures.

2.2.4 Material Derivative of a Functional Defied as a Local Measure, Using the Domain Approach

Some measures of behavior of state, such as displacement and stress, are not global. They are defined as local measures at an isolated point $\hat{x}$ or over a small test region $\Omega^p \subset \Omega$. With this situation, unlike functionals that define global measures, shape design sensitivity of local functionals may have additional contributions due to movement of point $\hat{x}$ or sub-region Ω^p, called "element velocity terms". This is the case when sub-regions are chosen to be finite elements. If one perturbs the shape of domain Ω, all points in the domain have non-zero velocity. An isolated point $\hat{x}$ moves to $\hat{x}_\tau = \hat{x} + \tau V(\hat{x})$, due to the domain perturbation. Likewise, a small test region Ω^p will move to occupy $\tilde{\Omega}^p$ after perturbation. One must consider contributions from this movement in calculating shape design sensitivity. The idea is given graphically in Fig. 2.2.6 for beam component.

Shape design sensitivity of local functionals was treated in Ref. 20 using a boundary approach. Here, it is treated using the domain approach of SDSA.

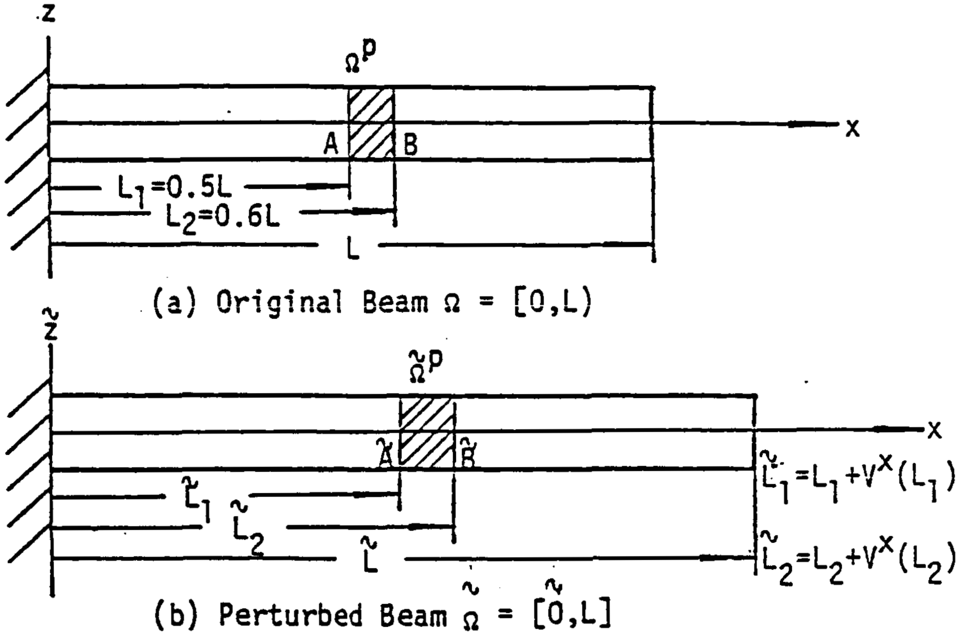

Figure 2.2.6 Element Velocity

Consider a functional defined over a small test region $\Omega^p \subset \Omega$ as

$$\psi = \iint_\Omega f \; M_p \; d\Omega \tag{2.2.42}$$

where f is a regular function and M_p is a characteristic function that has constant value $\overline{M}_p$ on Ω^p and zero on $\Omega\backslash\Omega^p$. The value of $\overline{M}_p$ is

$$\overline{M}_p = \frac{1}{(\iint_{\Omega^p} d\Omega)} \tag{2.2.43}$$

Using Eq. 2.2.43, Eq. 2.2.42 can be re-written as

$$\psi = \frac{(\iint_{\Omega^p} f \, d\Omega)}{(\iint_{\Omega^p} d\Omega)} \tag{2.2.44}$$

One can take the material derivative of Eq. 2.2.42.b to obtain

$$\psi' = \frac{(\iint_{\Omega^p}[f'+(\nabla f \cdot V)+f(\nabla \cdot V)] \, d\Omega)(\iint_{\Omega^p} d\Omega)-(\iint_{\Omega^p} f \, d\Omega)(\iint_{\Omega^p}(\nabla \cdot V) \, d\Omega)}{(\iint_{\Omega^p} d\Omega)^2}$$

$$= \iint_{\Omega^p}[f'+(\nabla f \cdot V)+f(\nabla \cdot V)]M_p \, d\Omega - (\iint_{\Omega^p} f M_p \, d\Omega) \, (\iint_{\Omega^p}(\nabla \cdot V)M_p \, d\Omega) \tag{2.2.45}$$

Note that the first integral is the same as Eq. 2.2.4.a, which is the shape design sensitivity formula for a global functional. Also note that one needs to add the second integral, the element velocity term, for shape design sensitivity of a local functional.

It is important to note that the element velocity term does not necessarily vanish for zero boundary velocity. The element velocity term is non-zero as long as the domain velocity does not vanish, inspite of zero velocity along the boundary.

2.3 Boundary-Layer

The boundary of the domain (or a part of the domain) is parametrized by a set of shape parameters and a boundary representation function. The velocity of the boundary can be defined in terms of its parametrization. Once the velocity of the boundary is given, one can evaluate velocity and its derivative using a mapping called a velocity element. In this section, the concepts of "boundary-layer" and "velocity element" are treated. In the next section, B-spline functions for boundary representation are discussed.

2.3.1 The Boundary-Layer Coordinate System

For shape design sensitivity analysis (SDSA), "mathematical shape modelling" and "velocity field contouring" are interdependent. The shape model and the velocity field must satisfy regularity requirements that are dictated by the problem.

Mathematically speaking, let the domain Ω be a C^k regular open set, with C^k denoting the collection of k-times continuously differentiable functions; i.e., its boundary Γ is a compact manifold of class C^k in R^n ($n = 2, 3$). That is, the boundary is closed and bounded in R^n and can be locally represented by a C^k function. Let the velocity field $V(x)$ R^n be a vector field defined on a neighborhood U of the closure $\overline{\Omega}$ of Ω and let $V(x)$ and its derivative up to order $k > 1$ be continuous. With this hypothesis, it has been shown that the mapping T in Eq. 2.2.1 is a homeomorphism from U to $U_\tau \equiv T(U,\tau)$, for small τ [21].

The boundary of a structure can be modelled using any approximating method [26]. For general shapes, assigning design parameters and defining a compatible velocity field are sometimes awkward or extraodinarily complicated. The simplest and most natural geometric construction is generation of a shape "design" boundary-layer, specified by two bounding surfaces Γ and γ as shown in Fig. 2.3.1.

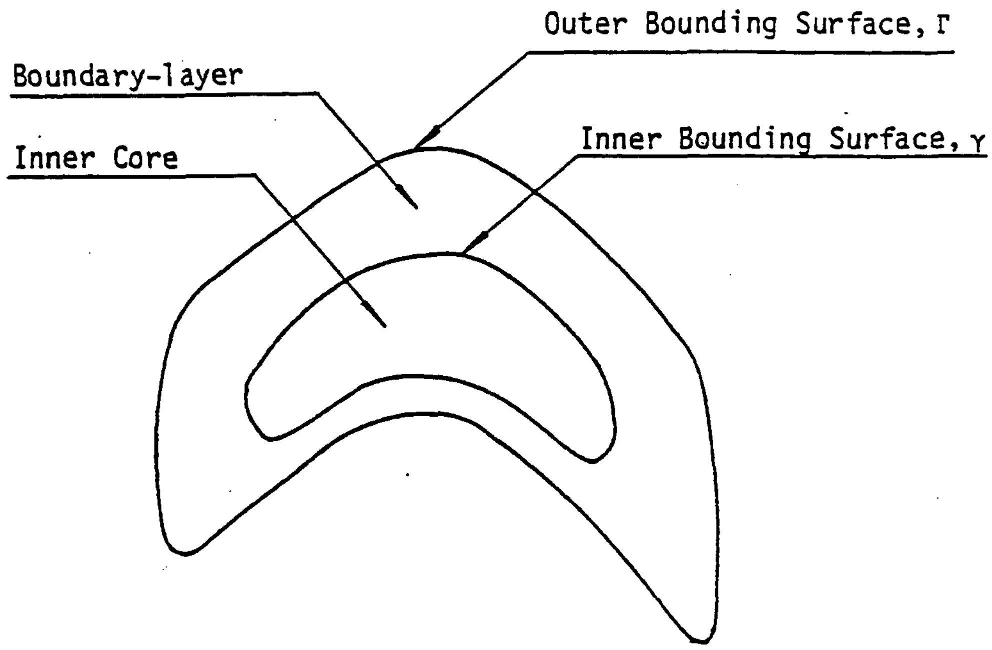

Figure 2.3.1 Shape Design Boundary-layer with Two Defining Surfaces

The inner bounding surface γ isolates the boundary-layer from the inner core of the structure and the outer bounding surface Γ coincides with the structural boundary. A boundary-layer coordinate system, that is orthogonal to the inner bounding surface γ can be established, as shown in Fig. 2.3.2. This coordinate system is particularly useful for shape design sensitivity analysis, due to its "local orthogonality". Local orthogonality menas that the coordinate system is orthogonal only on the pre-set inner bounding surface, but not necessarily elsewhere.

The basic shape of the inner bounding surface should preferably be close to that of the structural boundary. However, too much concavity must be avoided, since the boundary-layer coordinate lines would have intersections among themselves as shown in Fig. 2.3.3. Practically, the inner bounding surface should be defined by a simple analytical function and close to the shape of the structural boundary. Computation can be greatly simplified by using a simple analytical function.

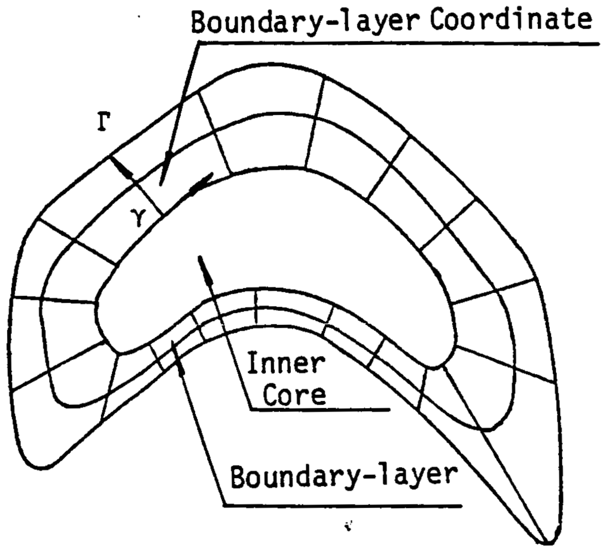

Figure 2.3.2 Shape Design Boundary-layer Coordinate System

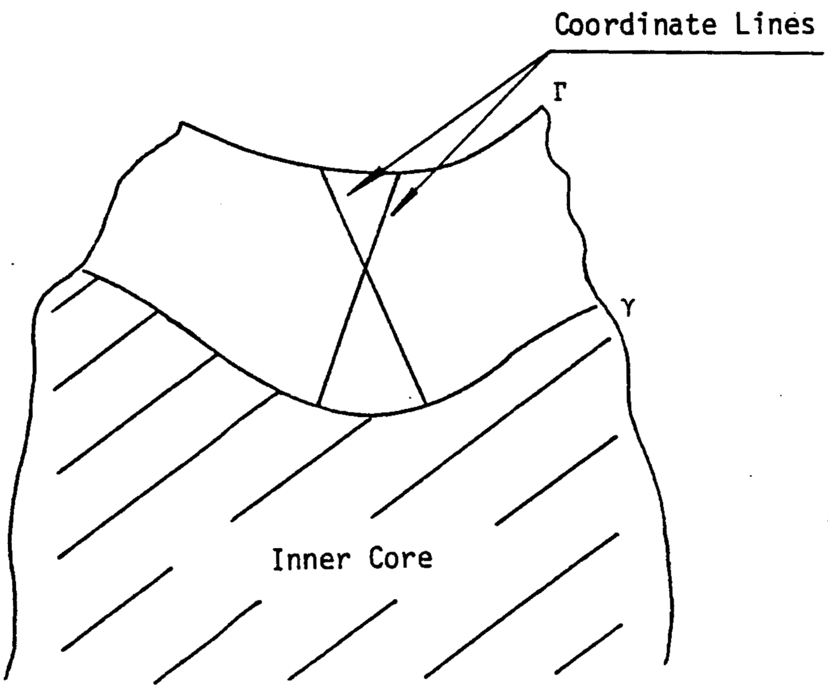

Figure 2.3.3 Intersections of Boundary-layer Coordinate Lines

Shape design variables b can be distances between the two bounding surfaces, measured along the boundary-layer coordinate system, as shown in Fig. 2.3.4. Note that $\hat{n}$ is the outward unit normal to γ.

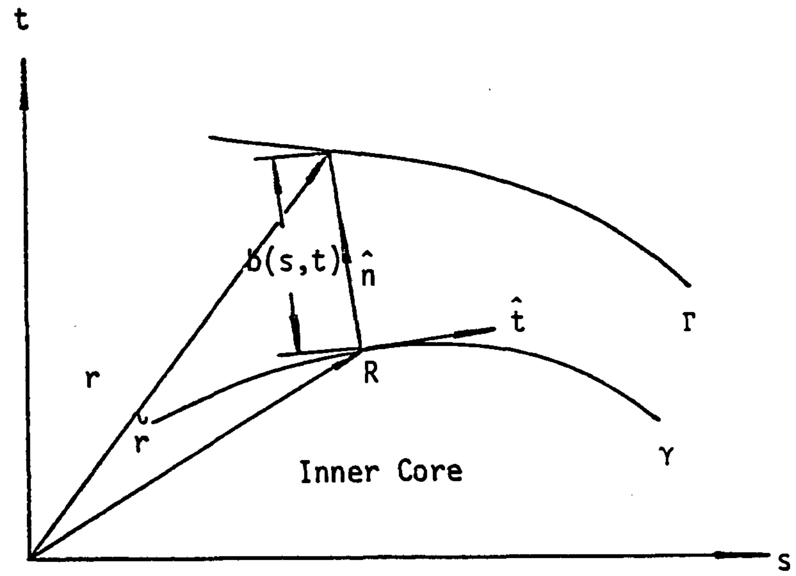

Figure 2.3.4 Definition of Design Variable b

The boundary-layer coordinate system for a two dimensional domain can be formulated mathematically as follows: The equation of a pre-set inner bounding surface γ is given in the form

$$\gamma(s,t) = 0 \tag{2.3.1}$$

where s and t are Cartesian coordinates referred to some origin. Points on the inner boundary surface γ are specified by a vector $\tilde{r}$ from the origin of the coordinate system to the point R on γ as shown in Fig. 2.3.4 In this figure, $\hat{n}$ and $\hat{t}$ are outward unit normal and unit tanget to γ, respectively. The outer bounding surface Γ can be determined by a set of points S that are specified by a vector r,

$$r = \tilde{r} + b(s, t)\,\hat{n} \tag{2.3.2}$$

where $b(s,t)$ is a design variable at (s, t) on γ.

2.3.2 The Velocity Element

As mentioned previously, the domain approach requires velocity and its derivative throughout the domain. For a general shape, velocity and its derivative can be effectively evaluated using shape design velocity elements located within the boundary-layer, as shown in Fig. 2.3.5.

The essential idea underlying development of velocity elements centers on isoparametric mappings [27], based on the Serendipity family [28] of rectangular elements.

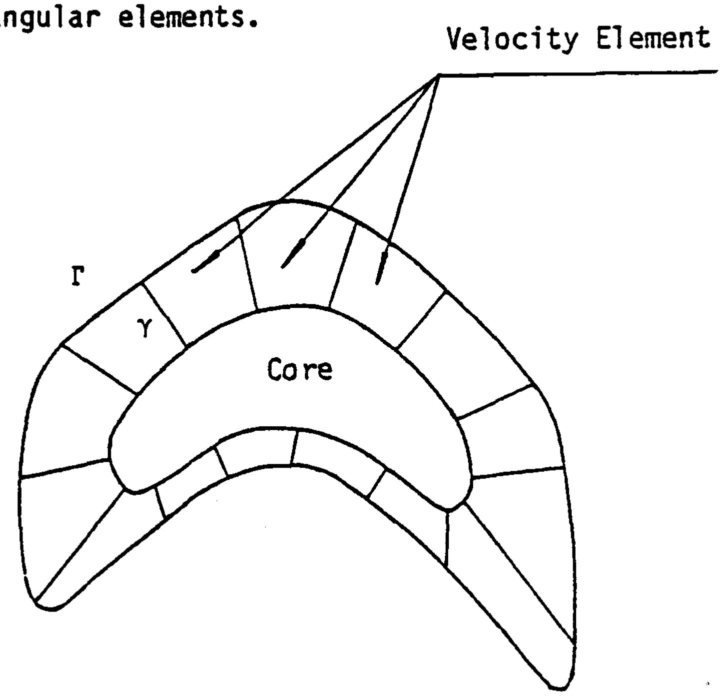

Figure 2.3.5 Boundary-layer with Set of Velocity Elements

The serendipity family of elements contain only exterior nodes, as shown in Fig. 2.3.6.

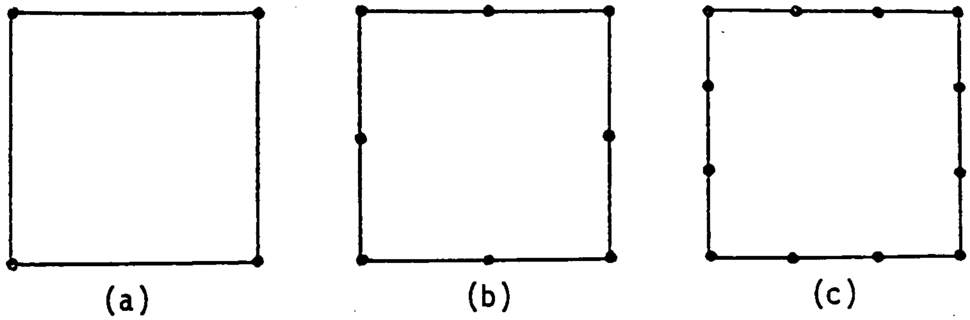

Figure 2.3.6 Some of the Serendipity Family Elements
(a) Linear, (b) Quadratic, (c) Cubic

An isoparametric mapping means that the functional representation of the field variable and the functional representation of the geometry are expressed by shape functions of the same order as in Eqs. 2.3.5 and 2.3.6.

The outer bounding surface Γ can be parametrized by a vector b that locates points on the surface Γ. In terms of the parametrization of the boundary Γ, the velocity of the boundary Γ is defined as

$$V = \frac{d}{d\tau} r(b + \tau\delta b)\Big|_{\tau=0} \delta b = \frac{\partial r}{\partial b} \delta b \qquad (2.3.3)$$

where δb is a design variation, τ is a time-like parameter, and $V = [V^s, V^t]^T$. The velocity along the inner bounding surface γ is defined to be

$$V = 0 \qquad (2.3.4)$$

since γ is not allowed to move.

A velocity element, shown in Fig. 2.3.7, interpolates velocity inside the element, based on specified velocity along γ and Γ, by Eqs. 2.3.3 and 2.3.4. Opposite sides of a velocity element are the inner bounding surface γ and the outer bouding surface Γ, as in Fig. 2.3.7.

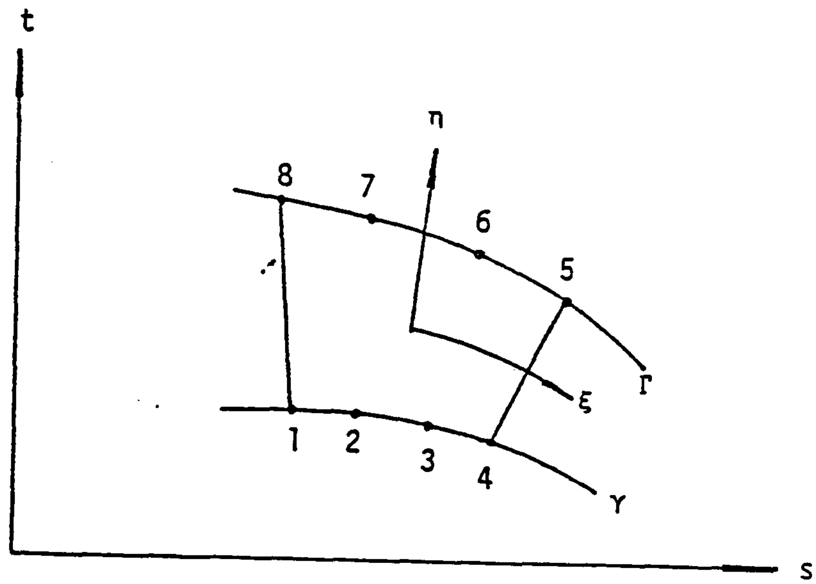

Figure 2.3.7 Velocity Element

As indicated in Fig. 2.3.7, the necessary velocity shape functions should have cubic and linear variations in ξ- and η- directions, respectly.

Note that, due to different orders of approximation along each side, the shape functions for mid-side nodes and corner nodes can be generated as follows:

(i) For mid-side shape functions (N_2, N_3, N_6, and N_7), a simple multiplication of cubic order and first order Lagrangian interpolation suffices.

(ii) For corner shape functions (N_1, N_4, N_5, and N_8), a combination of bilinear corner functions, together with an appropriate fraction of mid-side shapes to ensure zero at appropriate nodes, is required.

The velocity shape functions for cubic/linear variation are listed in Table 2.3.1.

Table 2.3.1 Velocity Element Shape Function

N_i	Shape Functions
N_2	$9(1 - 3\xi)(1 - \eta)(1 - \xi^2)/32$
N_3	$9(1 + 3\xi)(1 - \eta)(1 - \xi^2)/32$
N_6	$9(1 + 3\xi)(1 + \eta)(1 - \xi^2)/32$
N_7	$9(1 - 3\xi)(1 + \eta)(1 - \xi^2)/32$
N_1	$(1 - \xi)(1 - \eta)/4 - 2N_2/3 - N_3/3$
N_4	$(1 + \xi)(1 - \eta)/4 - N_2/3 - 2N_3/3$
N_5	$(1 + \xi)(1 + \eta)/4 - 2N_6/3 - N_7/3$
N_8	$(1 - \xi)(1 + \eta)/4 - N_6/3 - 2N_7/3$

Using an isoparametric mapping, the value of field variables and position within an element may be expressed as

$$\begin{bmatrix} s \\ t \end{bmatrix} = \underline{N}\,\underset{\sim}{q} \tag{2.3.5}$$

$$\begin{bmatrix} V^s \\ V^t \end{bmatrix} = \underline{N}\,\underset{\sim}{V} \tag{2.3.6}$$

where

$$\underline{N} = \begin{bmatrix} N_1 & 0 & N_2 & 0 & N_3 & 0 & N_4 & 0 & \cdots\cdots & N_8 & 0 \\ 0 & N_1 & 0 & N_2 & 0 & N_3 & 0 & N_4 & \cdots\cdots & 0 & N_8 \end{bmatrix}$$

$$q = [s_1, t_1, s_2, t_2, \cdots\cdots, s_8, t_8]$$

$$\underset{\sim}{V} = [V_1^s, V_1^t, V_2^s, V_2^t, \cdots\cdots V_8^s, V_8^t],$$

and (s_i, t_i) and $[V_i^s, V_i^t]^T$ are position and velocity of (i)-th nodes. Note that shape functions N_i, $i = 1, 2, \cdots\cdots, 8$, are given in terms of local coordinates ξ and η, which are dimensionless centroid coordinates with $-1 < \xi, \eta < 1$.

One cannot find derivatives of velocity with respect to s or/and t directly from Eq. 2.3.6, since $\underline{N}$ contains ξ and η, instead of s and t. This requires that the following coordinate transformation of derivatives be invoked [29]: Let ϕ be either V^s or V^t, which are function of s and t. Then, the chain rule yields

$$\begin{bmatrix} \phi,_\xi \\ \phi,_\eta \end{bmatrix} = \underline{J} \begin{bmatrix} \phi,_s \\ \phi,_t \end{bmatrix} \tag{2.3.7}$$

where $\underline{J}$ is the Jacobian matrix obtained using Eq. 2.3.5 as

$$\underline{J} = \begin{bmatrix} s,_\xi & t,_\xi \\ s,_\eta & t,_\eta \end{bmatrix} \tag{2.3.8}$$

The inverse relation, from Eq. 2.3.7, is

$$\begin{bmatrix} \phi,_s \\ \phi,_t \end{bmatrix} = \underline{J}^{-1} \begin{bmatrix} \phi,_\xi \\ \phi,_\eta \end{bmatrix} \quad (2.3.9)$$

The derivative of velocity can be found by the above procedure.

2.4 Mathematical Shape Approximation

2.4.1 Introduction

Creating a mathematical shape model that will adequately represent the domain is one of the fundamental problems of SDSA. For numerical purposes, actual structures can only be represented through mathematical shape modelling. The procedure of SDSA is dependent on shape model creation in two ways. First, structural behavior is analyzed based on the model created. Second, SDSA is performed on the model, using analysis results and shape information such as intrinsic distance [30] and area, etc. Intrinsic distance means distance measured along a surface from point A to point B. In calculating design sensitivity, numerical integrals require shape information along with the design velocity field.

SDSA requires adoption of mathematical shape modelling that is capable of representing geometry of a large class of structural shapes. Linear and the Lagrangian families [31] are too primitive to satisfy continuity and "fairness" requirements. Fairness is related to the absence of unwanted shape deficiencies, particularly oscillations [32]. Shape deficiency is used to designate discrepancy between original shape and approximated shape. The Hermite and the Bezier polynomials [33] have limitations due to continuity. The spline family can provide more flexibility and generality. Among the spline family, polynomial splines and B-splines are the most widely used for shape modelling.

A comparison between polynomial splines and B-splines is summarized in Table 2.4.1. For shape optimization purposes, the "local support" and "variation dimishing" properties are advantages of B-spline [34,35]. Local support means that the effect of perturbing a design component is felt only locally. Consequently, the velocity field associated with a design component is non-zero only locally. The variation diminishing property means that the approximated surface is no less fair than the original surface. The local support and variation diminishing properties of B-spline curves are demonstrated in Fig. 2.4.1. Note that Fig. 2.4.1.a demonstrates the variation diminishing property of a B-spline curves by approximating straight lines exactly. Figure 2.4.1.b shows the local property of B-spline curves. Perturbing a single vertex A of the polygon produces only a local perturbation of the curve in the vicinity of that vertex.

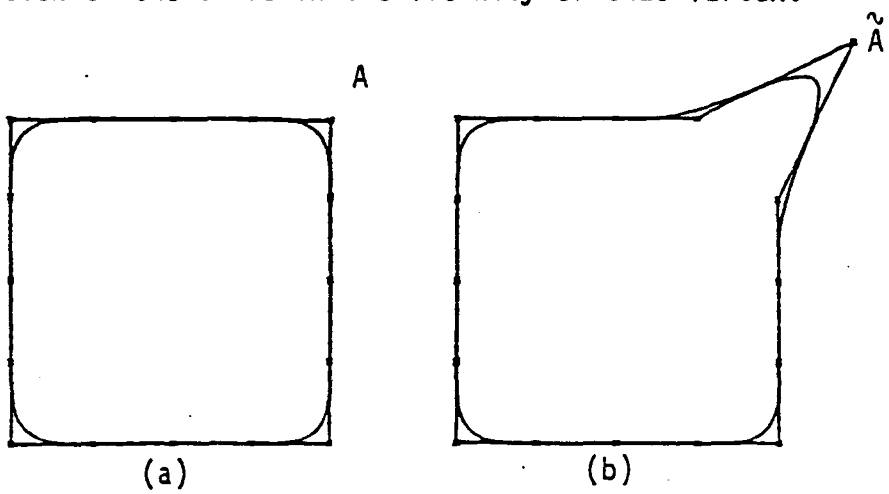

Figure 2.4.1 Local Support and Variation Diminishing Property of B-Spline Curve, (a) Before, (b) After Perturbation

Table 2.4.1 Comparison between Polynomial Spline and B-Spline

Type of Spline	Behavior		Required Data	Design Set
	Perturbation	Modelling		
Polynomial Spline	Global	Interpolation	m positions and 2 end slopes	m position and 2 end data
B-spline	Local	Approximation	Depends on Approx. Method	m position of the control vertex set

If polynomial splines are applied to the above figure, every line segment between nodes will be altered after perturbing a single vertex. This is due to the global nature of the polynomial splines.

Polynomial splines and B-splines can assure the same order of smoothness. However, a surface represented by B-splines is fairer than a surface represented by polynomial splines. The usefulness of B-splines is apparent when one considers to approximate aero-dynamic body such as a vehicle body or an aircraft fuselage or wing surface.

One may conclude that B-splines are superior in representing surfaces. In the following subsection, B-splines are discussed in detail.

2.4.2 B-Spline

B-splines, the common abbreviated name for basis splines first introduced by Schoenberg [36], are a class of piecewise continuous parametric polynomials. The B-splines of order k are polynomials of degree (k-1), which are continuously differentiable (k-2) times at the joints.

As noted in Table 2.4.1, B-splines have approximating features comparable to interpolating features of polynomial splines. An interpolating spline means a spline that passes through its defining points. On the other hand, an approximating spline is a spline curve that may not pass through its defining points, as shown in Fig. 2.4.2. The set of defining points is sometimes called the "control vertex set". The B-spline basis element $N_{i,k}(t)$ can be defined in the interval $t_i<t<t_{i+k}$ by means of the recursive formula of Cox and DeBoor [37]:

For k =1,

$$N_{i,1} = \begin{cases} 1 & \text{for } t_i<t<t_{i+k} \\ 0 & \text{otherwise} \end{cases} \tag{2.4.1}$$

and for k > 1,

$$N_{i,k} = \frac{t - t_i}{t_{i+k-1} - t_i} N_{i,k-1}(t) + \frac{t_{i+k} - t}{t_{i+k} - t_{i+1}} N_{i+1,k-1}(t)$$

where t_i is called the (i)-th knot. Refer to Ref. 37 for definition and details about knots. Note that one should carefully distinguish knots t_i from joints x_j, which are physical junctions between two curve sigments, as shown in Fig. 2.4.2.

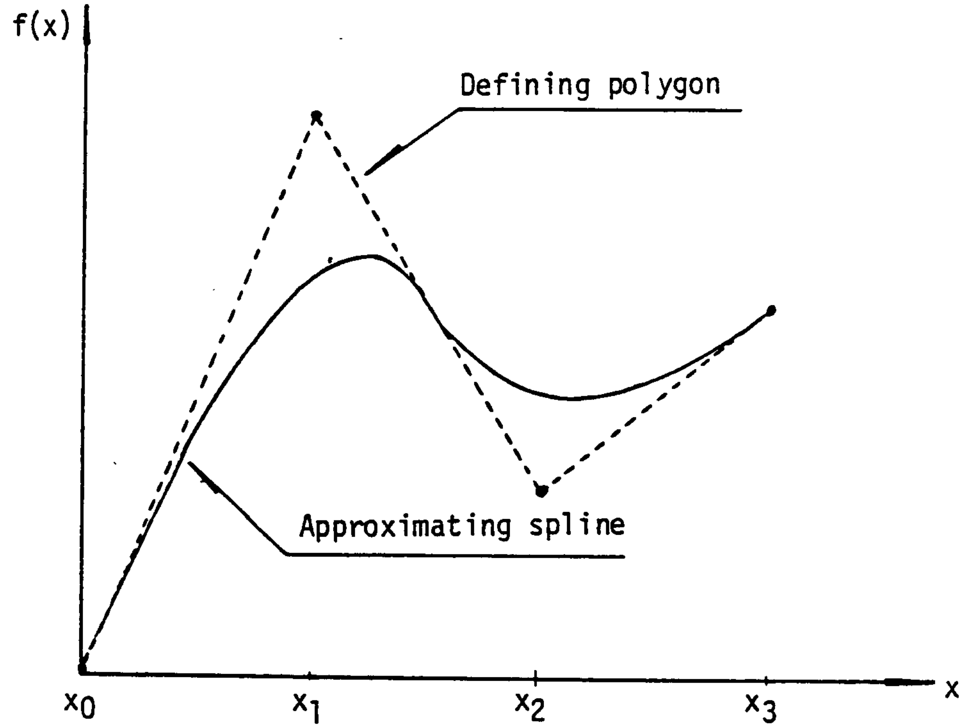

Figure 2.4.2 An Approximating Spline

The recursive formula for $N_{i,k}$ in Eq. 2.4.2 amounts to generating all the entries of the following triangular table:

$$
\begin{array}{ccccc}
N_{i,1}(t) & N_{i-1,2}(t) & \cdots & N_{i-k+2,k-1}(t) & N_{i-k+1,k}(t) \\
 & N_{i,2}(t) & \cdots & N_{i-k+3,k-1}(t) & N_{i-k+2,k}(t) \\
 & & \ddots & \vdots & \vdots \\
 & & & N_{i,k-1}(t) & N_{i-1,k}(t) \\
 & & & & N_{i,k}(t)
\end{array}
$$

Actually, this process yields the complete set of periodic B-spline basis functions of order k, which are cycle translates of a set of basis functions, as shown in Fig. 2.4.3

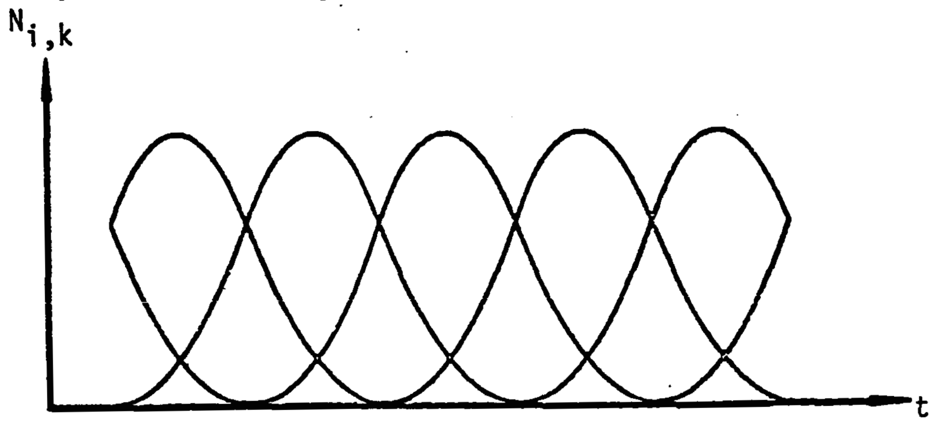

Figure 2.4.3 Complete Sets of B-spline Basis Functions

For cubic B-splines, a set of basis functions are renamed as b_j, $j = -1, 0, 1, 2$, to be used harmoniously as in Eq. 2.4.3. The calculated basis functions b_j are given in Eq. 2.4.2.

$$\left.\begin{aligned} b_{-1} &= (u^3)/6 \\ b_0 &= (1 + 3u + 3u^2 - 3u^3)/6 \\ b_1 &= (4 - 6u^2 + 3u^3)/6 \\ b_2 &= (1 - 3u + 3u^2 - u^3)/6 \end{aligned}\right\} \tag{2.4.2}$$

where u is a parametrization of (x_i, x_{i+1}) with $0<u<1$. In Fig. 2.4.4, the shape of four B-spline basis functions are given. Here, x_i is the (i)-th joint.

A B-spline curve can be constructed in a piecewise manner, where each piece is a curve segment. The entire curve is a mosaic of these

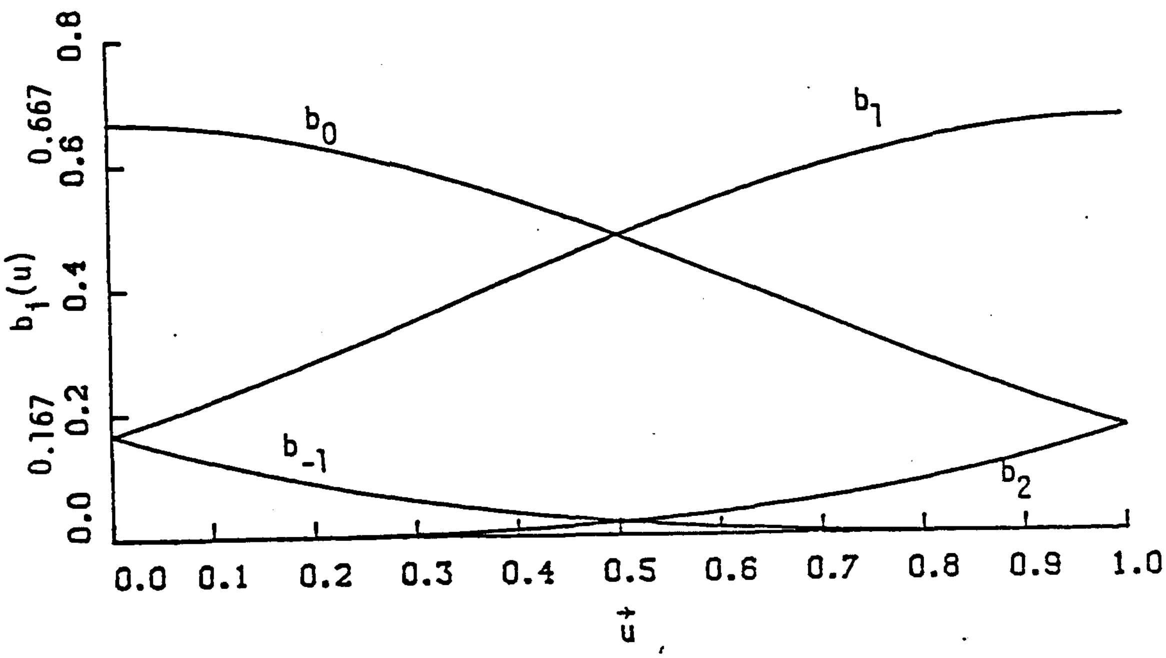

Figure 2.4.4 B-Spline Basis Functions

curve segments that are patched together with appropriate continuity at the joints.

Curve setments are weighted averages of control vertices, using the B-spline basis as weighting (or blending) functions. Consequently, B-splines approximate the control vertices without passing through them. Therefore, one must define a set of control vertices $\underset{\sim}{v} = [v_0, v_1, v_2, \cdots v_m]$ to represent a given curve, as shown in Fig. 2.4.4. A cubic B-spline curve segment is controlled by four control vertices and is not affected by the remaining control vertices. A point on the (i)-th cubic B-spline curve segment is a weighted average of the four adjacent vertices $\{v_{i-1}, v_i, v_{i+1}, v_{i+2}\}$, as shown in Fig. 2.4.5.

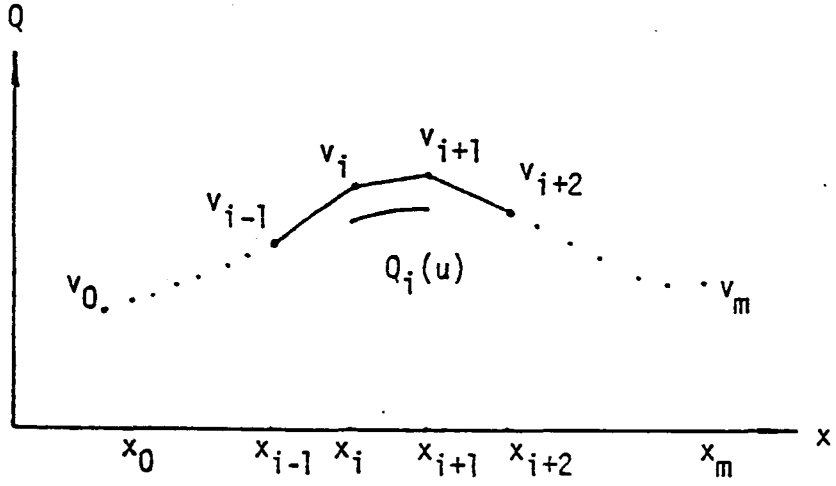

Figure 2.4.5 Pairs of Adjacent Point Forming (i)-th Segment

The mathematical formulation of the (i)-th segment is then [38]

$$Q_i(u) = v_{i-1}b_{-1} + v_ib_0 + v_{i+1}b_1 + v_{i+2}b_2 \qquad (2.4.3)$$

which is a local representation.

As a first step in using B-splines, one must provide a means of obtaining a satisfactory initial approximation to the given starting design, by creating an initial arrangement of control vertices. Once this is done, it is natural to systematically modify the arrangement of control vertices using an optimization technique. The problem is that reduced to determining an appropriate set of B-spline control vertices that will generate a surface, interpolating a specified set of points on the boundary of the starting design.

The one-to-one correspondence between B-spline curves and the control vertex set [33] enables one to carry out the following procedures:

Let S_i, $i = 0, 1, \cdots m$, be boundary points lying on the initial design and v_i, $i = 0, 1, \cdots m$, be control vertices. At the end of the curve, one has

$$\left.\begin{aligned} v_0 &= s_0 \\ v_m &= s_m \end{aligned}\right\} \tag{2.4.4}$$

Using Eq. 2.4.3, one can obtain a system of equations with v_j, $j = 1, 2, \cdots (m-1)$, as unknowns. The resulting matrix equation is

$$\underline{A}\,\underset{\sim}{v} = \underset{\sim}{r} \tag{2.4.5}$$

where $\underline{A}$ is the tri-diagonal matrix

$$\underline{A} = \begin{bmatrix} 4 & 1 & & & & \\ 1 & 4 & 1 & & & \\ & 1 & 4 & 1 & & \\ & & \ddots & \ddots & \ddots & \\ & & & 1 & 4 & 1 \\ & & & & 1 & 4 \end{bmatrix}_{(m-1)\times(m-1)} \tag{2.4.6}$$

$$\underset{\sim}{v} = [v_1, v_2, \cdots v_{m-1}]^T$$

and

$$\underset{\sim}{r} = \begin{bmatrix} r_1 \\ r_2 \\ \vdots \\ r_{m-2} \\ r_{m-1} \end{bmatrix} = \begin{bmatrix} 6s_1 - v_0 \\ 6s_2 \\ \vdots \\ 6s_{m-2} \\ 6s_{m-1} - v_m \end{bmatrix} \tag{2.4.7}$$

One can find a control vertex set $\underset{\sim}{v}$ by solving Eq. 2.4.5.

A B-spline curve segment is the sum of four weighted bases functions, as in Eq. 2.4.3. Thus, (m+1) control vertices $v_0, v_1, \cdots v_m$ can be used to define (m-2) segments, indexed as $Q_1(u), Q_2(u), \cdots, Q_{m-2}(u)$. A B-spline curve does not, in general, begin or end at a control vertex. To obtain better control of the endpoints, one may treat them specially using the following basic features of B-splines.

Basic features of B-splines at the (i)-th joint are

$$\begin{aligned}
&\text{(i)}\ Q_i = (v_i + 4v_{i+1} + v_{i+2})/6 \\
&\text{(ii)}\ dQ_i/du = (-v_i + v_{i+2})/2 \\
&\text{(iii)}\ d^2Q_i/du^2 = (v_i - 2v_{i+1} + v_{i+2})
\end{aligned} \tag{2.4.8}$$

where Q_i is $Q_i(u)$ evaluated at a joint i+1, v_i, v_{i+1}, and v_{i+2} are adjacent control vertices, and u is a parametrization. One can interpret Eq. 2.4.8 more geometrically as follows:

(1) The B-spline curve passes through a point p that is the 1/3 point of the median of the triangle formed by 3 sequential vertices, as shown in Fig. 2.4.6

(2) The first derivative vector at p, dQ_i/du, and the secnd derivative vector at p, d^2Q_i/du^2, can be interpreted geometrically, as shown in Fig. 2.4.6.

Using the above B-spline characteristics, one can make the B-spline curve segment begin or terminate at a desired point. For convenience, two of the techniques are summarized below. More details can be found in Refs. 39 thru 43.

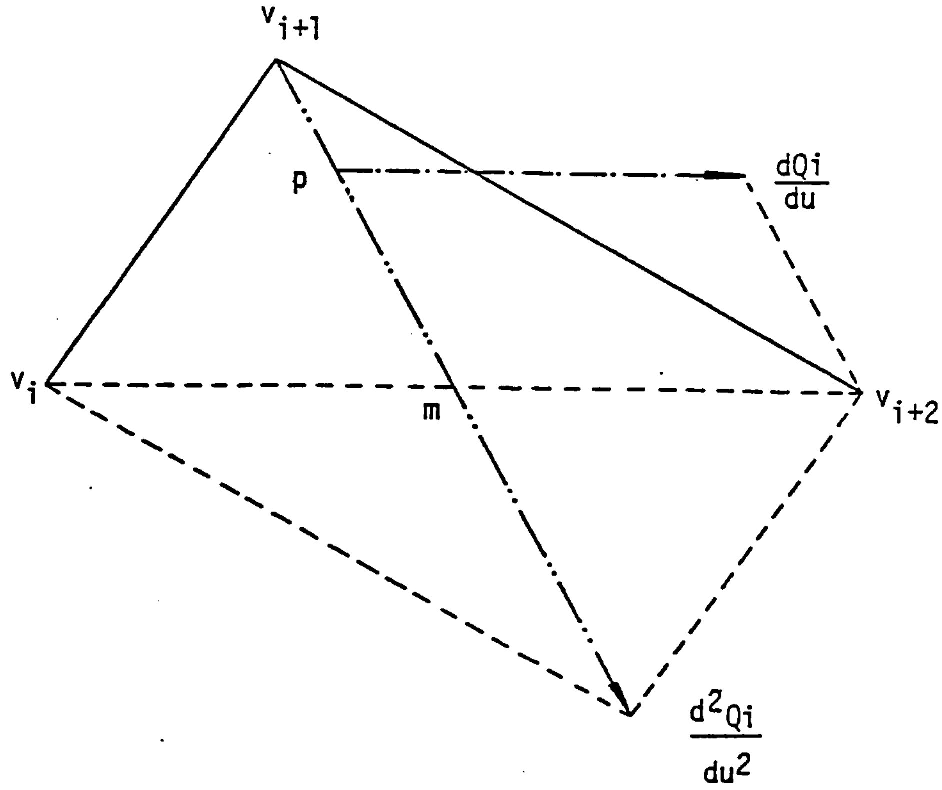

Figure 2.4.6 Geometric Interpretation of B-Spline Basic Features

(i) Triple vertex technique.

One can define two additional segments at the beginning of the curve by

$$\left.\begin{aligned} Q_{-1}(u) &= v_0[b_{-1}(u) + b_0(u) + b_1(u)] + v_1 b_2(u) \\ Q_0(u) &= v_0[b_{-1}(u) + b_0(u)] + v_1 b_1(u) + v_2 b_2(u) \end{aligned}\right\} \tag{2.4.9}$$

The curve then begins at $v_0 = Q_{-1}(0)$. Similarly, one can define two curve segments $Q_{m-1}(u)$ and $Q_m(u)$ to make the curve end at v_m.

(ii) Phantom vertex technique.

An alternative way of controlling the starting or ending point of a curve is to define a phantom vertex and a corresponding curve segment. Let v_{-1} be a phantom vertex for the initial segment and v_{m-1} be a phantom vertex for the terminal segment. Then, the initial curve segment $Q_0(u)$ can be defined as

$$Q_0(u) = v_{-1}b_{-1}(u) + v_0b_0 + v_1b_1(u) + v_2b_2(u) \tag{2.4.10}$$

In a similar way, terminal segment $Q_{m-1}(u)$ can be defined using $\{v_{m-2}, v_{m-1}, v_m, v_{m+1}\}$.

III. REGULARITY OF VELOCITY FIELDS

3.1 Introduction

When a perturbation is given to the boundary Γ, the velocity field inside the domain Ω is not unique. One has great freedom in selecting a design velocity field inside the domain, consistent with smoothness requirements. A sufficient condition for regularity of the velocity field is given in Ref. 21. It is desirable to reduce these requirements for certain class of problems, since a velocity field with lower order regularity is easier to construct and manipulate. One example by Lee and Choi [22] shows that too much relaxation (using a C^0-velocity field in an application in which a C^2-velocity field is suggested by the sufficient condition) can raise difficulty in shape design sensitivity analysis. Therefore, it is helpful to know how much the regularity requirement can be relaxed.

Analytical experiments are performed on a uniformly loaded uniform cantilever beam by introducing domain sub-divisions and different velocity fields, to evaluate regularity requirements on the design velocity field.

Data for this test are as follows: beam length is L, moment of inertia of the beam cross-section is I, Young's modulus is E, and the uniformly distrubuted load is f, as shown in Fig. 3.1.1. The space of kinematically admissible displacements is

$$Z = \{z \in H^2(0,L) : z(0) = z_x(0) = 0\}.$$

The design variable b is the length of the beam, where b_1 and b_2 are the lengths of each sub-domain Ω_i. Also, δb_1 and δb_2 are design variations of b_1 and b_2, respectively.

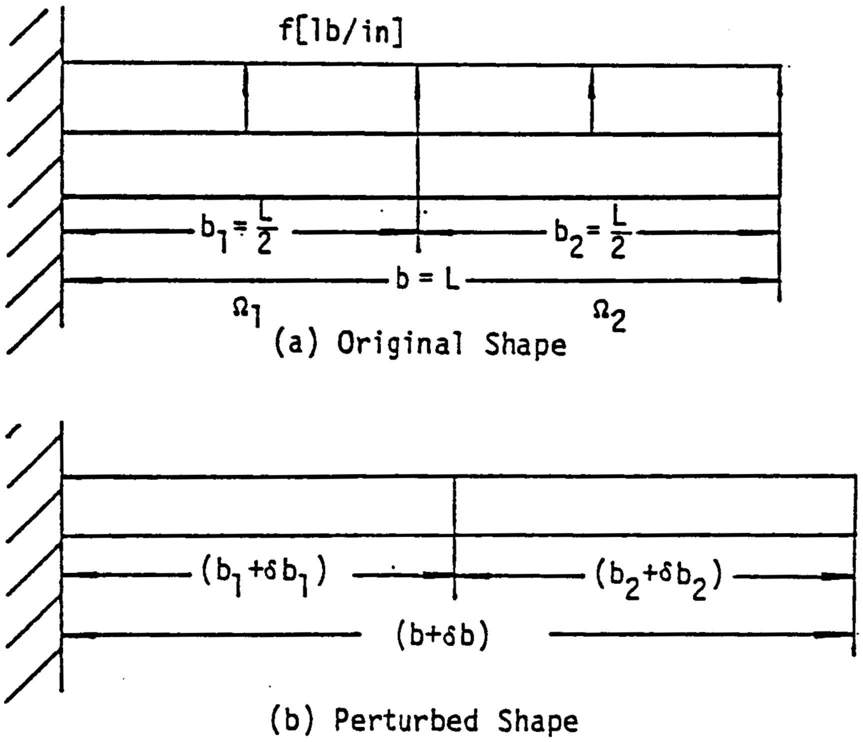

Figure 3.1.1 Beam Configuration

3.2 Formulation

Consider a functional that defines the value of displacement at an isolated point $\hat{x} \in (0,L)$ as

$$\psi = \int_0^L \bar{\delta}(x - \hat{x})z dx \tag{3.2.1}$$

where $\bar{\delta}(x)$ is the Dirac $\bar{\delta}$-measure and $\hat{x}$ is a fixed point in the beam.

Using Eqs. 2.2.16 and 2.2.17 and neglecting torsion, one has [19]

$$\psi' = a(\dot{z},\lambda) - \int_0^L \bar{\delta}(x - \hat{x}) \ (z_x V)dx \tag{3.2.2}$$

where λ is the solution of the adjoint equation

$$a(\lambda,\bar{\lambda}) = \int_0^L \bar{\delta}(x - \hat{x}) \ \bar{\lambda} \ dx, \qquad \text{for all } \bar{z} \in Z \tag{3.2.3}$$

For comparison, one can obtain a shape design sensitivity formula using the boundary approach, which is given in terms of the boundary velocity field as [21]

$$\psi_B' = -EI(z_{xx} \ \lambda_{xx})V\Big|_{x=0} + f\lambda V\Big|_{x=L} \tag{3.2.4}$$

A shape design sensitivity formula can also be derived using the domain approach, which is given in terms of the velocity field and its derivative throughout the domain. Assume the domain is divided into two regions with equal length. Then, the variational form of the governing equation is

$$a(z,\overline{z}) = \ell(\overline{z}), \quad \text{for all } \overline{z} \in Z \tag{3.2.5}$$

where

$$a(z,\overline{z}) = \int_0^L EI(z_{xx}\,\overline{z}_{xx})\,dx$$

$$\ell(\overline{z}) = \int_0^L f\overline{z}\,dx$$

Taking the variation of Eq. 3.2.5 and using Eqs. 2.2.16 and 2.2.17, one obtains

$$\begin{aligned} a(\dot{z},\overline{z}) &= \int_0^L EI(\dot{z}_{xx}\,\overline{z}_{xx})\,dx \\ &= \int_0^L [3EI(z_{xx}\,\overline{z}_{xx})\,V_x + EI(z_x\,\overline{z}_{xx} + z_{xx}\,\overline{z}_x)V_{xx})\,dx \\ &+ \int_0^L (f\overline{z})V_x\,dx, \quad \text{for all } \overline{z} \in Z \end{aligned} \tag{3.2.6}$$

Since $\overline{\lambda} \in Z$ is arbitrary, one may evaluate Eq. 3.2.3 at $\overline{\lambda} = \dot{z}$ to obtain

$$a(\lambda,\dot{z}) = \int_0^L \overline{\delta}(x-\hat{x})\,\dot{z}\,dx \tag{3.2.7}$$

Similarly, one may evaluate Eq. 3.2.6 at $\overline{z} = \lambda$ to obtain

$$\begin{aligned} a(\dot{z},\lambda) &= \int_0^L [3EI(z_{xx}\,\lambda_{xx})V_x + EI(z_x\,\lambda_{xx} + z_{xx}\,\lambda_x)\,V_{xx}]\,dx \\ &+ \int_0^L (f\lambda)\,V_x\,dx \end{aligned} \tag{3.2.8}$$

Since the energy bilinear form a(., .) is symmetric, Eqs. 3.2.2, 3.2.7, and 3.2.8 yield

$$\psi' = \sum_{i=1}^{2} \int_{\Omega_i} [3EI(z^i_{xx}\lambda^i_{xx})V^i_x + EI(z^i_x\lambda^i_{xx} + z^i_{xx}\lambda^i_x)V^i_{xx}]dx$$

$$+ \sum_{i=1}^{2} \int_{\Omega_i} (f\lambda^i)V^i_x \, dx - \int_0^L \overline{\delta}(x - \hat{x})(z_x V^i) \, dx \qquad (3.2.9)$$

as the sum of integrals over two subdomains, since derivatives of design velocity field may be discontinuous at x = L/2.

3.3 Analytic Test

Based on the simple beam theory, the displacement field due to uniformly distributed load can be expressed, as

$$z(x) = \frac{fx^2}{24EI}(x^2 - 4Lx + 6L^2) \qquad 0 < x < L \qquad (3.2.10)$$

The adjoint displacement field due to the adjoint load of Eq. 3.2.3 is

$$\lambda(x) = \frac{1}{6EI}(\langle x - L\rangle^3 - x^3 + 3Lx^2) \qquad 0 < x < L \qquad (3.2.11)$$

Shape design sensitivity of the displacement of point $\hat{x} = L$ is now to be analyzed. A canti-lever beam with internal sub-division at L/2 is shown in Fig. 3.2.2. Also in the figure, three different velocity fields are given, with the following properties:

(i) System - I; piecewise linear velocity field with slope discontinuity at $x = L/2$ (a C^0 velocity field).

(ii) System - II; two quadratic velocity fields joined together to satisfy slope continuity at $x = L/2$ (a C^1 velocity field).

(iii) System III; linear velocity field throughout the domain (a C^1 velocity field).

The analytical expression for the velocity field for each system can be written as follows:

For System I,

$$\left.\begin{aligned} V^1(x) &= \frac{2K\delta b}{L}\,x && 0 < x < \frac{L}{2} \\ V^2(x) &= K\delta b + \frac{2(1-K)\delta b}{L}\left(x - \frac{L}{2}\right) && \frac{L}{2} < x < L \end{aligned}\right\} \qquad (3.2.12)$$

For System II,

$$\left.\begin{aligned} V^1(x) &= -\frac{4\delta b_1}{L^2}\left(x^2 - \frac{L}{2}\,x\right) && 0 < x < \frac{L}{2} \\ V^2(x) &= \delta b_1 + \frac{4\delta b_2}{L^2}\left(x - \frac{L}{2}\right)^2 && \frac{L}{2} < x < L \end{aligned}\right\} \qquad (3.2.13)$$

Finally, for System III,

$$V(x) = \frac{\delta b}{L}\,x \qquad 0 < x < L \qquad (3.2.14)$$

From Eqs. 3.2.10 and 3.2.11, one obtains

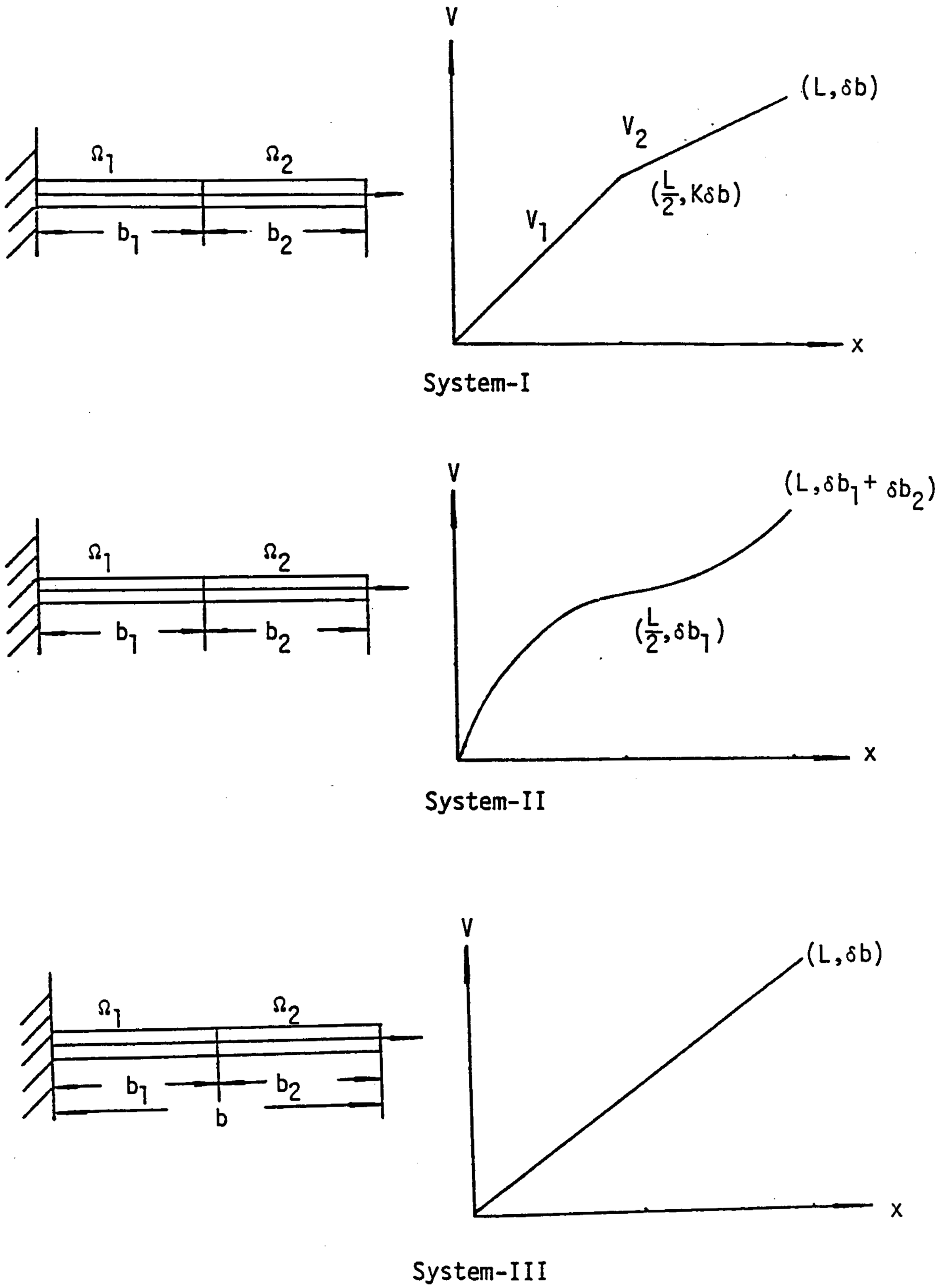

Figure 3.2.1 Three Systems

$$\left.\begin{aligned} z_x &= \frac{f}{6EI}(x^3 - 3Lx^2 + 3L^2x) \\ z_{xx} &= \frac{f}{2EI}(x^2 - 2Lx + L^2) \end{aligned}\right\} \tag{3.2.15}$$

$$\left.\begin{aligned} \lambda_x &= \frac{1}{2EI}(-x^2 + 2Lx) \\ \lambda_{xx} &= \frac{1}{EI}(-x + L) \end{aligned}\right\} \tag{3.2.16}$$

Considering that a perturbation of δb is given at the free end, while the other end remains fixed, the predicted change by the boundary approach can be obtained immediately. Using Eq. 3.2.4, one has

$$\psi_B' = f\lambda V\Big|_{x=L} = f\left(\frac{L^3}{3EI}\right)\delta b \tag{3.2.17}$$

which is the correct result.

Applying the domain approach to System-I, which has a piecewise linear C^0-velocity field, the derivatives of velocity field are, from Eq. 3.2.12,

$$\left.\begin{aligned} V_x^1 &= \frac{2K\delta b}{2} & 0 < x < \frac{L}{2} \\ V_x^2 &= \frac{2(1-K)\delta b}{2} & \frac{L}{2} < x < L \end{aligned}\right\}$$

$$V_{xx}^1 = V_{xx}^2 = 0 \tag{3.2.18}$$

Substituting Eqs. 3.2.15, 3.2.16, and 3.2.18 into Eq. 3.2.9 yields

$$\psi_D' = \int_0^{\frac{L}{2}} 3EI\left(\frac{f}{2EI}\right)(x^2 - 2Lx + L^2)\left(\frac{1}{EI}\right)(-x + L)\,\frac{2K\delta b}{L}\,dx$$

$$+ \int_{\frac{L}{2}}^{L} 3EI\left(\frac{f}{2EI}\right)(x^2 - 2Lx + L^2)\left(\frac{1}{EI}\right)(-x + L)\,\frac{2(1-K)\delta b}{L}\,dx$$

$$+ \int_0^{\frac{L}{2}} f\left(\frac{1}{6EI}\right)(-x^3+3Lx^2)\,\frac{2K\delta b}{L}\,dx + \int_{\frac{L}{2}}^{L} f\left(\frac{1}{6EI}\right)(-x^3+3Lx^2)\,\frac{2(1-K)\delta b}{L}\,dx$$

$$- \left(\frac{fL^3}{6EI}\right)\delta b$$

$$= \left(\frac{fL^3}{6EI}\right)\left(\frac{1}{64}\right)(184K + 36) \qquad (3.2.19)$$

Note that Eq. 3.2.19 is a function of variable parameter K. This result cannot be true, since the state change must be unique once a normal design perturbation is given at the boundary.

Next, the domain approach is applied to system-II, which has a C^1-velocity field. One can obtain the derivatives of the velocity field using Eq. 3.2.13 as

$$\left.\begin{aligned}
V_x^1 &= -\frac{4\,\delta b_1}{L^2}(2x - L) && 0 < x < \tfrac{L}{2}\\
V_x^2 &= -\frac{4\,\delta b_2}{L^2}(2x - L) && \tfrac{L}{2} < x < L\\
V_{xx}^1 &= -\frac{8\,\delta b_1}{L^2} && 0 < x < \tfrac{L}{2}\\
V_{xx}^2 &= \frac{8\,\delta b_2}{L^2} && \tfrac{L}{2} < x < L
\end{aligned}\right\} \qquad (3.2.20)$$

Substituting Eqs. 3.2.15, 3.2.16, and 3.2.20 into Eq. 3.2.9, one has

$$\psi_D' = \int_0^{\frac{L}{2}} EI[3(\frac{f}{2EI})(x^2 - 2Lx + L^2)(\frac{1}{EI})(-x + L)(-\frac{4\delta b_1}{L^2})(2x - L)$$

$$+ (\frac{f}{6EI})(x^3 - 3Lx^2 + 3L^2x)(\frac{1}{EI})(-x + L)(-\frac{8\delta b_1}{L^2})$$

$$+ (\frac{f}{2EI})(x^2 - 2Lx + L^2)(\frac{1}{2EI})(-x^2 + 2Lx)(-\frac{8\delta b_1}{L^2})]\, dx$$

$$+ \int_{\frac{L}{2}}^{L} EI[3(\frac{f}{2EI})(x^2 - 2Lx + L^2)(\frac{1}{EI})(-x + L)(\frac{4\delta b_2}{L^2})(2x - L)$$

$$+ (\frac{f}{6EI})(x^3 - 3Lx^2 + 3L^2x)(\frac{1}{EI})(-x + L)(\frac{8\delta b_2}{L^2})$$

$$+ (\frac{f}{2EI})(x^2 - 2Lx + L^2)(\frac{1}{2EI})(-x^2 + 2Lx)(\frac{8\delta b_2}{L^2})]\, dx$$

$$+ \int_0^{\frac{L}{2}} f(\frac{1}{6EI})(-x^3 + 3Lx^2)(-\frac{4\delta b_1}{L^2})(2x - L)\, dx$$

$$+ \int_{\frac{L}{2}}^{L} f(\frac{1}{6EI})(-x^3 + 3Lx^2)(\frac{4\delta b_2}{L^2})(2x - L)\, dx$$

$$- (\frac{fL^3}{6EI})(\delta b_1 + \delta b_2)$$

$$= (\frac{fL^3}{3EI})\, \delta b \qquad (3.2.21)$$

Note that the result of Eq. 3.2.21 is the same as the result of the boundary approach Eq. 3.2.17, but differs from Eq. 3.2.19.

The velocity field of System-III is a special case of system-I, setting the parameter K = 1/2. Therefore, one can get the predicted change for System-III by evaluating Eq. 3.2.19 with K = 1/2 as

$$\psi_D' = \left(\frac{fL^3}{6EI}\right)\left(\frac{1}{64}\right)\left(184 \cdot \frac{1}{2} + 36\right)\ \delta b$$

$$= \left(\frac{fL^3}{3EI}\right)\ \delta b \qquad (3.2.22)$$

which is the correct result.

Note that the predicted changes are exact for C^1 or more smooth velocity fields, as in Systems-II and -III.

As a theoretical check to see why difficulty arises with only a C^0-velocity field, one can apply the domain approach to System-I, and take the slope dis-continuity at x=L/2 into consideration. The second derivative V_{xx} can be defined as

$$V_{xx} = \frac{2(1-2K)\,\delta b}{L}\ \bar{\delta}\left(x - \frac{L}{2}\right) \qquad (3.2.23)$$

Using Eq. 3.2.23, the predicted displacement change is

$$\psi_D' = \left(\frac{fL^3}{6EI}\right)\left(\frac{1}{64}\right)(184K + 36)$$

$$+ \int_0^L (z_x\ \lambda_{xx} + z_{xx}\ \lambda_x) \cdot \frac{2(1-2K)\,\delta b}{L}\ \bar{\delta}\left(x - \frac{L}{2}\right)\ dx$$

$$= \left(\frac{fL^3}{6EI}\right)\left(\frac{1}{64}\right)(184K + 36)\ \delta b + \left(\frac{fL^3}{6EI}\right)\left(\frac{1}{64}\right)(92 - 184K)\ \delta b$$

$$= \left(\frac{fL^3}{3EI}\right)\ \delta b \qquad (3.2.24)$$

which is correct.

It is shown in Ref. 21 that, if mapping $T(x,\tau)$ of Eq. 2.2.1 is a C^p homeomorphism, the Sobolev space $H^m(\Omega)$ for $m < p$ is preserved by $T(x,\tau)$. In other words, it is sufficient that the design velocity be C^p regular with $p > m$ where $2m$ is the order of the governing differential equation. For the beam problem, $m = 2$ and sufficient regularity is

$$V(x) \in C^p, \text{ with } p > 2 \tag{3.2.25}$$

Results of Systems-II and -III show that a Dirac type of singularity can be avoided by imposing smoothness conditions between sub-domains. For this specific example (beam problem), the design velocity V should have a continuous first derivative and a piecewise continuous second derivative, or V is contained in $C^1 \cap D^2$. These results show that the smoothness requirement for this example is lower by one than the rule of Eq. 3.2.25. However, it must be understood that Eq. 3.2.25 is a sufficient condition that covers a large class of problems, giving a general guideline for selecting the design velocity field.

Note that shape design sensitivity formulas for a beam component in Eq. 2.2.16 and a plate bending component in Eq. 2.2.27 have the same highest order derivatives of the design velocity, both velocity fields should posesses the same order of regularity. The same argument can be applied to the elasticity problem. The design sensitivity formula for a plane elastic component in Eq. 2.2.20 has only a first derivative of design velocity. This means that the design velocity field for an elastic component must be at least C^0.

As a summary, one may use the sufficient condition of Eq. 3.2.25 in constructing design velocity fields. However, in some cases the regularity requirement can be relaxed, as shown above. One should carefully apply this test in each case a lower level of regularity is used, since the range of applicability is still an open question.

This study of regularity of velocity field is applied to the shape design sensitivity analysis of a plate-beam-truss built-up structure in Chapter 4, with success.

IV. NUMERICAL EVALUATION OF THE DOMAIN APPROACH

4.1 Introduction

The domain approach for shape design sensitivity analysis and regularity requirements on the design velocity field developed in Chapters 2 and 3 are applied here to example problems. First, numerical calculation of shape design sensitivity of a square box is presented in Section 4.2. The square box is an extremely simplified model of a wing-box structure. A study of this square box can, however, provide a basis for study of the wing-box. The second example treated is shape design sensitivity analysis of a plate-beam-truss built-up structure in Section 4.3. This problem is geometrically simple. However, it demonstrates singular behavior near component boundaries (interfaces) that may cause trouble when one uses the boundary approach for SDSA with the finite element method [22].

4.2 SDSA of a Square Box

As a first numerical test of the domain approach to shape design sensitivity analysis, a square box is analyzed. Results obtained with the domain approach is compared to results obtained with the boundary approach.

4.2.1 System Description

Consider a square box shown in Fig. 4.2.1. The box consists of five plane elastic components; top, bottom, two sides, and end. Subdomains (or patches) and boundary interfaces are numbered in Fig. 4.2.1 for convinience. Shape design variables of the system are length L, height H, and depth W of the box.

A C^0-velocity field is required on each plane elastic component. It suffices to use piecewise linear velocity fields on each patch, which are given in Table 4.2.1. Note that δL, δH, and δW are design changes.

Table 4.2.1 Velocity Fields on Each Patch

Patch #	Velocity Field Definition
Ω_1 Ω_2	$V^i = (\delta L/L)x_1 + (\delta W/W)x_2 \quad , \quad i = 1,2$
Ω_3 Ω_4	$V^i = (\delta L/L)x_1 + (\delta H/H)x_3 \quad , \quad i = 3,4$
Ω_5	$V^5 = (\delta W/W)x_2 + (\delta H/H)x_3$

External loads are applied along the edges of the top surface, Γ_{13}, Γ_{14}, and Γ_{15}, with constant magnitude T acting in the positive x_3-direction, with units of lb/in. The state variables for this structure are defined for each component as

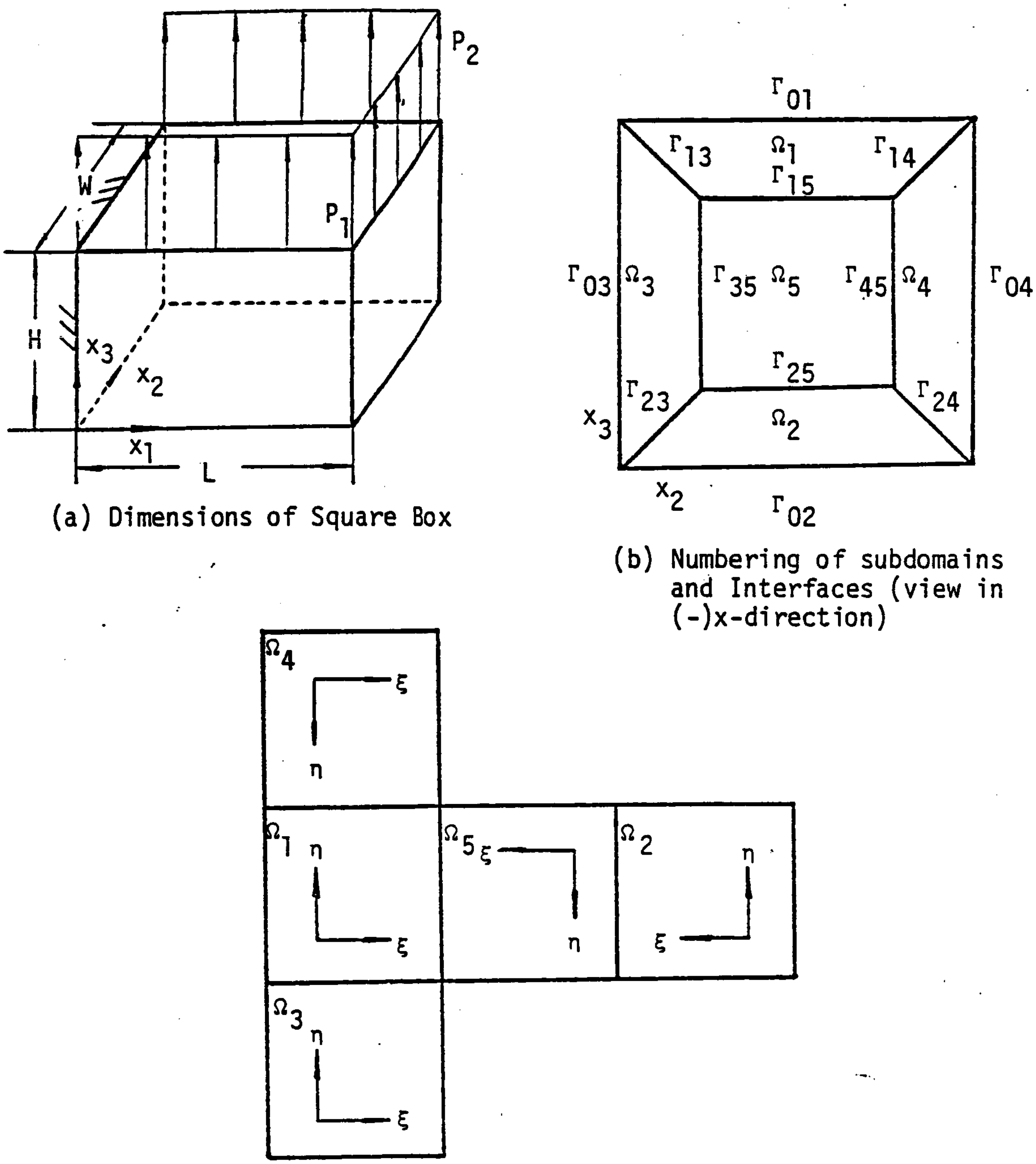

(a) Dimensions of Square Box

(b) Numbering of subdomains and Interfaces (view in (-)x-direction)

(c) Local Coordinate on Developed View

Figure 4.2.1 Square Box

z^1 on Ω^1 (top)

z^2 on Ω^2 (bottom)

z^3 on Ω^3 (side 1)

z^4 on Ω^4 (side 2)

z^5 on Ω^5 (end)

In vector form, the state variable is thus

$$z = [z^1, z^2, z^3, z^4, z^5]^T \tag{4.2.1}$$

Boundary conditions are

$$z^i = 0 \quad \text{along } \Gamma_0 = \Gamma_{01} \cup \Gamma_{02} \cup \Gamma_{03} \cup \Gamma_{04}, \qquad i = 1, 2, 3, 4$$

Interface conditions are

$z_1^1 = z_1^3$ on Γ_{13}

$z_1^1 = z_1^4$ on Γ_{14}

$z_2^1 = z_1^5$ on Γ_{14}

$z_1^2 = z_1^3$ on Γ_{23}

$z_1^2 = z_1^4$ on Γ_{24}

$$z_2^3 = z_2^5 \quad \text{on } \Gamma_{35}$$

$$z_2^4 = z_2^5 \quad \text{on } \Gamma_{45}$$

$$z_2^2 = z_1^5 \quad \text{on } \Gamma_{25}$$

and

$$\sum_i \sigma_{ij}(z^K)n_j^K = T \qquad \text{along } \Gamma_2 = \Gamma_{13} \cup \Gamma_{14} \cup \Gamma_{15}, \qquad k = 3, 4, 5$$

where n_j^K is the outward normal to Γ_{13}, Γ_{14}, Γ_{15} in the plane of Ω_K, and

$$\sum_j \sigma_{ij}(z^\ell)n_j^\ell = 0 \qquad \text{along other interfaces.}$$

One may now define the set Z of kinematically admissible displacement fields as follows :

$$Z = \{z: \; z = (z^1, z^2, z^3, z^4, z^5) \text{ such that all the above boundary interface conditions are satisfied}\}$$

The variational form of the governing equation is

$$a(z, \bar{z}) = \ell(\bar{z}), \qquad \text{for all } \bar{z} \in Z \tag{4.2.2}$$

where

$$a(z, \bar{z}) = \sum_{\ell=1}^{5} \iint_{\Omega_\ell} \sum_{i,j} \sigma_{ij}(z^\ell)\varepsilon_{ij}(\bar{z}^\ell)\, d\Omega \tag{4.2.3}$$

$$\ell(\bar{z}) = \int_{\Gamma_2} [\sum_i T_i \bar{z}_i] \, d\Gamma \tag{4.2.4}$$

with Γ_2 as the boundary on which the uniform line load T is applied. The governing equation is given for completeness. For shape design sensitivity formula derivation, the procedure explained in Chapter 2 is followed.

4.2.2 Shape Design Sensitivity Formula

As explained in Chapter 2, shape design sensivitity coefficients for the assembly of components is obtained by summing design sensitivities associated with each component. However, for this first example, a more detailed procedure is taken for better understanding.

Using Eqs. 2.2.20 and 2.2.36, one obtains the material derivative of the energy bilinear form as the sum of the material derivatives of each component

$$
\begin{aligned}
[a\ (z, \bar{z}]' &= \sum_m [a_m(z^m, \bar{z}^m)]' \\
&= \sum_{m=1}^{5} \iint_{\Omega_m} \sum_{i,j} [\sigma_{ij}(\dot{z}^m)\ \varepsilon_{ij}(\bar{z}^m)]\ d\Omega \\
&- \iint_{\Omega_m} \sum_{i,j} [\sum_{k,\ell} C^m_{ijk\ell}\ (\nabla z^m_K \cdot V^m_\ell)\ \varepsilon_{ij}(\bar{z}^m)]\ d\Omega \\
&- \iint_{\Omega_m} \sum_{i,j} [\sigma_{ij}(z^m)\ (\nabla \bar{z}^m_i \cdot V^m_j)]\ d\Omega \\
&\quad + \iint_{\Omega_m} [\sum_{i,j} \delta_{ij}(z^m)\ \varepsilon_{ij}(\bar{z}^m)](\nabla \cdot V)\ d\Omega]
\end{aligned} \tag{4.2.5}
$$

Similarly, one can obtain the material derivative of load linear form, using Eq. 2.2.21, as

$$
\begin{aligned}
[\ell(\bar{z})]' = & \int_{\Gamma_2} [\sum_i T_i \bar{z}_i]' d\Gamma + \int_{\Gamma_2} [\sum_i (\nabla(T_i \bar{z}_i) \cdot n)](V \cdot n)\, d\Gamma \\
& + (\sum_i T_i \bar{z}_i \; V_T(P_1))\Big|_{x\text{-dir.}} + (\sum_i T_i \; \bar{z}_i \; V_T(P_1))\Big|_{y\text{-dir.}} \\
& + (\sum_i T_i \bar{z}_i \; V_T(P_2))\Big|_{x\text{-dir.}} + (\sum_i T_i \bar{z}_i \; V_T(P_2))\Big|_{y\text{-dir.}}
\end{aligned}
\tag{4.2.6}
$$

where $V_T(P_j)\big|_{k\text{-dir.}}$ is tangential velocity in the k-direction at point P_j. Note that the last four terms denote corner terms due to movement of corner points P1 and P2 in Fig. 4.2.1 [23]. From Eqs. 4.2.5 and 4.2.6, and 2.2.37, one obtains

$$
\begin{aligned}
a(\dot{z}, \bar{z}) = & \sum_m \{\iint_{\Omega_m} \sum_{i,j} [\sigma_{ij}(\dot{z}^m) \varepsilon_{ij} (\bar{z}^m)]\, d\Omega \\
= & \sum_m \{\iint_{\Omega_m} \sum_{i,j} [\sum_{k,\ell} C^m_{ijk\ell} (\nabla z^m_K \cdot V^m_{1\ell})\; \varepsilon_{ij}(\bar{z}^m)]\, d\Omega \\
& + \iint_{\Omega_m} \sum_{i,j} [\delta_{ij}(z^m)\; (\nabla \bar{z}^m_i \cdot V^m_{1j})]\, d\Omega \\
& - \iint_{\Omega_m} [\sum_{i,j} \sigma_{ij}(z^m)\; \varepsilon_{ij}(\bar{z}^m)]\, (\nabla \cdot V)\, d\Omega\} \\
& + \int_{\Gamma_2} [\sum_i T_i \bar{z}_i{}'] \,d\Gamma + \int_{\Gamma_2} [\sum_i (\nabla(T_i \bar{z}_i) \cdot n)](V \cdot n)\, d\Gamma \\
& + (\sum_i T_i \bar{z}_i \; V_T(P_1))\Big|_{x\text{-dir.}} + (\sum_i T_i \bar{z}_i \; V_T(P_1))\Big|_{y\text{-dir.}} \\
& + (\sum_i T_i \bar{z}_i \; V_T(P_2))\Big|_{x\text{-dir.}} + (\sum_i T_i \bar{z}_i \; V_T(P_2))\Big|_{y\text{-dir.}}
\end{aligned}
\tag{4.2.7}
$$

Consider the von Mises yield stress functional, averaged over a small region (or finite element) $\Omega^p \subset \Omega_q$, as

$$\psi = \iint_{\Omega_q} \phi(\sigma(z^q))\, M_p \, d\Omega \tag{4.2.8}$$

where ϕ is the von Mises yield stress with $\phi = [\sigma_{11}^2 + \sigma_{22}^2 + 3\sigma_{12}^2 - \sigma_{11}\sigma_{22}]^{1/2}$ and M_p is a characteristic function on Ω^p, defined as

$$M_p = \begin{cases} \dfrac{1}{(\iint_{\Omega^p} d\Omega)} & \text{on } \Omega^p \\ 0 & \text{on } \Omega \backslash \Omega^p \end{cases}$$

One can find the material derivative of Eq. 4.2.8, using Eq. 2.2.37, the adjoint variable method Eq. 2.2.41, the last term of Eq. 2.2.45, and Eq. 4.2.7, to obtain

$$\begin{aligned}
\psi_D' = \sum_m \{ & \iint_{\Omega_m} \sum_{i,j} [\sigma_{ij}(z^m)(\nabla\lambda_i^m \cdot V_j) + \sigma_{ij}(\lambda^m)(\nabla z_i^m \cdot V_j)]\, d\Omega \\
& - \iint_{\Omega_m} [\sum_{i,j} \sigma_{ij}(z^m)\varepsilon_{ij}(\lambda)]\, (\nabla \cdot V)\, d\Omega] \\
& \quad - \iint_{\Omega_q} \sum_{i,j} \frac{\partial \phi}{\partial \sigma_{ij}} (z^q)\, C_{ijk\ell}^q (\nabla z_K^q \cdot V_\ell)]\, M_p \, d\Omega \\
& + \iint_{\Omega_q} \phi(\nabla \cdot V)\, M_p \, d\Omega - \iint_{\Omega_p} \phi M_p \, d\Omega \iint_{\Omega_q} (\nabla \cdot V)\, M_p \, d\Omega \\
& + \int_{\Gamma_2} [\sum_i (\nabla(T_i\lambda_i) \cdot n)\, (V \cdot n)]\, d\Gamma - \int_{\Gamma_2} \sum_i (\nabla(T_i\lambda_i) \cdot V)\, d\Gamma \\
& + (\sum_i T_i\lambda_i \, V_T(P_1))\Big|_{x\text{-dir.}} + (\sum_i T_i\lambda_i \, V_T(P_1))\Big|_{y\text{-dir.}} \\
& + (\sum_i T_i\lambda_i \, V_T(P_2))\Big|_{x\text{-dir.}} + (\sum_i T_i\lambda_i \, V_T(P_2))\Big|_{y\text{-dir.}}
\end{aligned} \tag{4.2.9}$$

where λ is the solution of the adjoint equation

$$a(\lambda, \bar{\lambda}) = \iint_{\Omega_q} \{ \sum_{i,j} \frac{\partial \phi}{\partial \sigma_{ij}} (z^q) \; (\bar{\lambda}^q) \} \; M_p \; d\Omega, \quad \text{for all } \bar{\lambda} \in Z \quad (4.2.10)$$

For comparison, the boundary approach to SDSA can be derived as [21]

$$\begin{aligned}
\psi_B' = \sum_{s,t} \; & \{ \iint_{\gamma_{st}} \sum_{i,j} [\sigma_{ij}(\lambda^*) n_j ((\nabla z_i^{**} - \nabla z^*) \cdot n) \\
& + \sigma_{ij}(z^*) n_j ((\nabla \lambda_i^{**} - \nabla \lambda_i^*) \cdot n)] \; (\nabla \cdot n) \; d\Gamma \\
& + \iint_{\gamma_{st}} \sum_{i,j} [\sigma_{ij}(z^\bullet) \varepsilon_{ij}(\lambda^*) - \sigma_{ij}(z^{**}) \varepsilon_{ij}(\lambda^{**})] \; (V \cdot n) \; d\Gamma \} \\
& + \int_{\Gamma_p} \phi (V \cdot n) M_p \; d\Gamma - \iint_{\Omega_q} \phi M_p \; d\Omega \int_{\Gamma_p} (V \cdot n) \; M_p \; d\Gamma \\
& + \int_{\Gamma_2} [\sum_i (\nabla(T_i \lambda_i) \cdot n) \; (V \cdot n)] \; d\Gamma - \int_{\Gamma_2} \sum_i (\nabla(T_i \lambda_i) \cdot V) \; d\Gamma \\
& + (\sum_i T_i \lambda_i \; V_T(P_1)) \Big|_{x\text{-dir.}} + (\sum_i T_i \lambda_i \; V_T(P_1)) \Big|_{y\text{-dir.}} \\
& + (\sum_i T_i \lambda_i \; V_T(P_2)) \Big|_{x\text{-dir.}} + (\sum_i T_i \lambda_i \; V_T(P_2)) \Big|_{y\text{-dir.}} \qquad (4.2.11)
\end{aligned}$$

where γ_{st} is a interface between two adjacent components Ω_s and Ω_t, with $\gamma_{st} = \gamma_{ts}$ and z^* and z^{**} are the displacements of these components, respectively. Also, Γ_p is the boundary of Ω^p and n is the outward normal to Γ_p.

4.2.3 Numerical Results

The square box is discretized into 320, 8-noded, isoparametric finite elements, having 993 nodes and 1,886 active degrees-of- freedom. External load is applied along the edge of the top surface, with 4.77 ib/in intensity in the global positive x_3-direction. Young's modulus and Possion's ratio are 1.0×10^7 and 0.316, respectively. The thickness of each member is 0.1 inch.

For comparison, shape design sensitivity analysis is performed using the boundary approach of Eq. 4.2.11 by perturbing the height of the box. Results are given in the Table 4.2.2. Notice that accuracy (ratio between predicted change and actual change) of shape design sensitivity is not acceptable.

The same shape design sensitivity analysis is performed using the domain approach of Eq. 4.2.9. The result is given in Table 4.2.2. Note that the measure of accuracy (ratio between predicted change and actual change) lies in the range of 100 ± 5%, except in elements 274, 282, and 284 of Table 4.2.2. However, one may note that those elements are in low stress regions and the actual changes are small compared to others, thus precision is lost during finite difference calculation of $[\psi(b^0 + \delta b) - \psi(b^0)]/\psi(b^0)$.

In Table 4.2.3, shape design sensitivity analysis results for a second test of the box (length as the design variable) are given. Note that the accuracy measure lies in the same range as before. For elements 185, 188, 257 thru 263, 265, 266, 271, 274, and 285, the predicted values are less accurate than others. However, the magnitudes of actual changes $\Delta\psi = [\psi(b^0 + \delta b) - \psi(b^0)]$ for those elements are

Table 4.2.2 SDSA Result for Square Box Using Boundary Approach (Height as Design)

	Elt #	Von Mises Stress OLD	NEW	Actual Change	Predict Change	Ratio x 100 %
TOP	1	100.634	97.713	-2.921	-1.231	42.131
	2	55.674	53.927	-1.747	-1.260	72.135
	3	39.877	38.607	-1.271	-0.981	77.218
	4	33.640	32.574	-1.066	-0.825	77.361
	9	84.752	82.130	-2.621	-1.806	68.884
	10	54.117	52.396	-1.721	-1.293	75.133
	11	38.092	36.889	-1.203	-0.968	80.464
	12	31.402	30.424	-0.978	-0.739	75.584
	17	71.556	69.202	-2.355	-1.741	73.926
	18	51.390	49.744	-1.646	-1.299	78.913
	19	36.390	35.256	-1.134	-0.932	82.199
	20	29.101	28.223	-0.878	-0.611	69.607
	25	63.926	61.746	-2.180	-1.571	72.046
	26	47.776	46.215	-1.561	-1.544	98.956
	27	33.717	32.671	-1.046	-0.918	87.769
	28	25.627	24.882	-0.745	-0.417	55.990
	33	58.139	56.116	-2.022	-1.841	91.045
	34	43.894	42.435	-1.459	-1.645	112.790
	35	30.186	29.242	-0.944	-0.771	81.655
	36	21.280	20.674	-0.606	-0.176	29.104
	41	52.170	50.354	-1.816	-2.765	152.298
	42	38.922	37.626	-1.296	-1.129	87.097
	43	26.279	25.441	-0.838	-0.480	57.337
	44	18.051	17.498	-0.553	-0.138	24.940
	49	43.708	42.247	-1.461	-2.394	163.781
	50	31.544	30.518	-1.026	-0.783	76.308
	51	23.751	22.926	-0.825	-0.678	82.142
	52	20.094	19.322	-0.773	-0.862	111.533
	57	28.211	27.406	-0.804	-0.505	62.833
	58	26.031	25.078	-0.953	-1.543	161.945
	59	29.026	27.797	-1.229	-2.116	172.175
	60	31.157	29.774	-1.383	-2.373	171.555
SIDE1	129	171.978	167.714	-4.264	-10.550	247.414
	130	144.285	140.276	-4.009	-0.569	14.194
	131	127.953	124.235	-3.718	-1.124	30.219
	132	119.633	115.991	-3.642	-1.050	28.818
	137	129.443	126.595	-2.848	-17.597	617.858
	138	132.988	129.603	-3.385	-3.479	102.780
	139	127.639	123.937	-3.702	-1.394	37.659
	140	120.844	117.044	-3.800	-1.404	36.939
	145	105.705	103.260	-2.445	-17.666	722.498
	146	117.304	114.564	-2.739	-0.764	27.898

Table 4.2.2 continued

	147	118.301	115.132	-3.169	-1.278	40.314
	148	115.086	111.665	-3.421	-1.395	40.764
	153	93.644	91.443	-2.201	-17.710	804.585
	154	103.049	100.693	-2.357	-0.492	20.895
	155	106.120	103.469	-2.651	-1.120	42.230
	156	104.972	102.105	-2.867	-1.103	38.476
	161	84.565	82.598	-1.967	-16.821	855.140
	162	91.349	89.277	-2.072	-0.409	19.761
	163	93.915	91.677	-2.238	-1.537	68.662
	164	93.154	90.803	-2.351	-0.212	9.034
	169	76.844	75.138	-1.707	-16.429	962.725
	170	80.706	78.899	-1.807	0.282	-15.586
	171	81.949	80.053	-1.895	-1.462	77.149
	172	81.234	79.317	-1.917	0.382	-19.906
	177	68.597	67.237	-1.360	-1.233	90.676
	178	69.560	68.041	-1.519	0.346	-22.768
	179	70.093	68.533	-1.560	-7.825	501.744
	180	70.122	68.569	-1.553	0.053	-3.395
	185	55.101	54.259	-0.842	-11.464	1361.241
	186	55.588	54.557	-1.031	1.857	-180.119
	187	59.227	58.043	-1.184	-0.472	39.902
	188	60.898	59.585	-1.314	-0.459	34.920
END	257	43.062	42.964	-0.098	-9.016	9180.063
	258	49.130	48.534	-0.597	-1.017	170.555
	259	53.527	52.527	-1.000	-0.566	56.562
	260	54.320	53.053	-1.268	-0.528	41.679
	261	52.277	50.894	-1.383	-0.622	44.946
	262	47.352	46.036	-1.316	-0.599	45.499
	263	38.161	37.128	-1.032	-0.414	40.079
	264	22.026	21.363	-0.663	-0.260	39.252
	265	42.606	42.417	-0.189	-7.311	3864.989
	266	45.127	44.959	-0.168	-0.683	405.541
	267	47.240	46.638	-0.603	-0.656	108.831
	268	46.147	45.203	-0.944	-0.662	70.104
	269	42.773	41.679	-1.094	-0.609	55.694
	270	37.348	36.309	-1.038	-0.480	46.260
	271	29.527	28.631	-0.896	-0.408	45.469
	272	26.142	25.019	-1.123	-0.749	66.688
	273	44.396	43.911	-0.485	-6.642	1368.251
	274	40.949	40.931	-0.018	-0.298	1637.088
	275	39.797	39.664	-0.133	-0.278	208.631
	276	36.623	36.211	-0.412	-0.326	79.069
	277	31.977	31.350	-0.627	-0.369	58.821
	278	27.134	26.357	-0.777	-0.444	57.154
	279	24.686	23.635	-1.051	-0.710	67.571
	280	31.839	30.339	-1.501	-1.045	69.656
	281	45.666	45.012	-0.654	-6.351	971.712
	282	39.156	39.157	0.001	-0.033	-3246.602
	283	35.136	35.284	0.147	0.048	32.407

Table 4.2.2 continued

284	29.856	29.859	0.003	0.037	1072.141
285	23.974	23.728	-0.246	-0.125	50.610
286	20.182	19.539	-0.644	-0.489	75.990
287	22.733	21.538	-1.195	-0.954	79.764
288	34.960	33.279	-1.681	-1.183	70.385

Table 4.2.3 SDSA Result for Square Box
Using Domain Approach
(Height as Design)

	Elt #	Von Mises Stress OLD	NEW	Actual Change	Predict Change	Ratio x 100 %
TOP	1	100.63443	97.71343	-2.92100	-3.02560	103.58116
	2	55.67394	53.92664	-1.74729	-1.80964	103.56785
	3	39.87734	38.60680	-1.27054	-1.31552	103.54027
	4	33.64000	32.57416	-1.06584	-1.10330	103.51473
	9	84.75172	82.13030	-2.62142	-2.71628	103.61893
	10	54.11750	52.39635	-1.72114	-1.78240	103.55929
	11	38.09229	36.88886	-1.20343	-1.24584	103.52454
	12	31.40171	30.42382	-0.97790	-1.01214	103.50134
	17	71.55644	69.20184	-2.35460	-2.43981	103.61896
	18	51.39030	49.74436	-1.64594	-1.70450	103.55790
	19	36.38969	35.25582	-1.13386	-1.17384	103.52559
	20	29.10066	28.22262	-0.87803	-0.90871	103.49418
	25	63.92617	61.74584	-2.18033	-2.25854	103.58715
	26	47.77615	46.21547	-1.56068	-1.61636	103.56736
	27	33.71692	32.67051	-1.04641	-1.08343	103.53843
	28	25.62709	24.88163	-0.74546	-0.77144	103.48579
	33	58.13858	56.11622	-2.02236	-2.09421	103.55295
	34	43.89400	42.43542	-1.45858	-1.51070	103.57378
	35	30.18578	29.24186	-0.94391	-0.97748	103.55581
	36	21.28009	20.67423	-0.60586	-0.62693	103.47671
	41	52.16973	50.35392	-1.81580	-1.87975	103.52165
	42	38.92171	37.62587	-1.29584	-1.34207	103.56740
	43	26.27852	25.44055	-0.83797	-0.86795	103.57855
	44	18.05108	17.49795	-0.55313	-0.57285	103.56495
	49	43.70809	42.24665	-1.46144	-1.51226	103.47719
	50	31.54422	30.51825	-1.02597	-1.06236	103.54706
	51	23.75135	22.92610	-0.82525	-0.85558	103.67493
	52	20.09424	19.32151	-0.77274	-0.80181	103.76186
	57	28.21065	27.40639	-0.80426	-0.83223	103.47717
	58	26.03146	25.07839	-0.95307	-0.98874	103.74283
	59	29.02616	27.79707	-1.22909	-1.27622	103.83477
	60	31.15718	29.77414	-1.38304	-1.43646	103.86274

Table 4.2.3 continued

BOTTOM	65	86.28385	82.99484	-3.28901	-3.39641	103.26564
	66	49.20760	47.31834	-1.88926	-1.95116	103.27625
	67	35.10166	33.75394	-1.34772	-1.39162	103.25781
	68	29.26721	28.14580	-1.12141	-1.15766	103.23289
	73	75.61336	72.71050	-2.90286	-2.99854	103.29579
	74	47.86338	46.02199	-1.84139	-1.90177	103.27898
	75	33.16758	31.89516	-1.27242	-1.31370	103.24392
	76	26.96837	25.93788	-1.03049	-1.06359	103.21208
	81	65.59970	63.06451	-2.53519	-2.61931	103.31823
	82	45.52028	43.76816	-1.75212	-1.80964	103.28330
	83	31.42032	30.21688	-1.20345	-1.24241	103.23730
	84	24.58127	23.64699	-0.93428	-0.96399	103.18063
	89	59.01335	56.72553	-2.28782	-2.36378	103.32000
	90	42.63218	40.98418	-1.64800	-1.70249	103.30660
	91	29.11188	27.99637	-1.11551	-1.15172	103.24594
	92	21.34630	20.54120	-0.80510	-0.83036	103.13828
	97	53.42710	51.35160	-2.07550	-2.14435	103.31712
	98	39.32319	37.79588	-1.52731	-1.57816	103.32918
	99	26.26198	25.25324	-1.00874	-1.04169	103.26607
	100	17.77022	17.10474	-0.66548	-0.68615	103.10558
	105	47.01331	45.18366	-1.82965	-1.89021	103.30984
	106	34.66051	33.31319	-1.34731	-1.39214	103.32707
	107	23.27783	22.38046	-0.89738	-0.92693	103.29384
	108	16.13709	15.52403	-0.61306	-0.63284	103.22522
	113	37.36988	35.91812	-1.45176	-1.49927	103.27249
	114	27.64675	26.57968	-1.06706	-1.10201	103.27447
	115	22.48638	21.60390	-0.88247	-0.91262	103.41663
	116	20.66130	19.83577	-0.82552	-0.85490	103.55854
	121	21.39204	20.56917	-0.82287	-0.84901	103.17777
	122	25.40962	24.40117	-1.00845	-1.04356	103.48124
	123	31.19434	29.91584	-1.27850	-1.32590	103.70736
	124	34.36406	32.93564	-1.42842	-1.48260	103.79333
SIDE	129	171.97848	167.71438	-4.26410	-4.41063	103.43639
	130	144.28489	140.27579	-4.00910	-4.13931	103.24788
	131	127.95324	124.23535	-3.71789	-3.83449	103.13623
	132	119.63305	115.99074	-3.64231	-3.75305	103.04038
	133	114.31134	110.62116	-3.69018	-3.80276	103.05064
	134	111.82036	107.95628	-3.86407	-3.98556	103.14402
	135	114.85173	110.55992	-4.29181	-4.43088	103.24042
	136	127.43202	122.52440	-4.90762	-5.06634	103.23407
	137	129.44261	126.59456	-2.84805	-2.95053	103.59818
	138	132.98811	129.60304	-3.38506	-3.48761	103.02925
	139	127.63870	123.93687	-3.70183	-3.81286	102.99912
	140	120.84447	117.04449	-3.79998	-3.91629	103.06096
	141	115.99465	112.13318	-3.86147	-3.98045	103.08108
	142	113.02475	109.10592	-3.91883	-4.03815	103.04454
	143	109.97003	106.11951	-3.85052	-3.96507	102.97474
	144	102.30763	98.72379	-3.58384	-3.69474	103.09456
	145	105.70496	103.25986	-2.44509	-2.53832	103.81294

Table 4.2.3 continued

	146	117.30361	114.56425	-2.73937	-2.82433	103.10152
	147	118.30094	115.13183	-3.16911	-3.25755	102.79074
	148	115.08585	111.66459	-3.42127	-3.51647	102.78252
	149	110.95022	107.44962	-3.50061	-3.59917	102.81556
	150	106.22925	102.79248	-3.43676	-3.53362	102.81814
	151	99.14657	95.92302	-3.22355	-3.31679	102.89258
	152	85.65457	82.65421	-3.00035	-3.09651	103.20472
	153	93.64369	91.44257	-2.20111	-2.28507	103.81424
	154	103.04949	100.69251	-2.35698	-2.43365	103.25282
	155	106.11978	103.46860	-2.65119	-2.72399	102.74617
	156	104.97155	102.10465	-2.86690	-2.94150	102.60214
	157	101.32153	98.38944	-2.93210	-3.00942	102.63719
	158	95.62944	92.76005	-2.86939	-2.94810	102.74292
	159	87.25962	84.52179	-2.73783	-2.81852	102.94697
	160	74.98447	72.34916	-2.63531	-2.71972	103.20290
	161	84.56467	82.59761	-1.96706	-2.04206	103.81273
	162	91.34894	89.27698	-2.07196	-2.14015	103.29122
	163	93.91524	91.67677	-2.23847	-2.30128	102.80579
	164	93.15356	90.80305	-2.35051	-2.41224	102.62611
	165	89.80530	87.42771	-2.37759	-2.44060	102.65009
	166	84.06349	81.71003	-2.35346	-2.41896	102.78294
	167	75.93268	73.60904	-2.32364	-2.39284	102.97791
	168	65.60454	63.29090	-2.31364	-2.38734	103.18539
	169	76.84401	75.13751	-1.70650	-1.77203	103.83995
	170	80.70596	78.89944	-1.80652	-1.86651	103.32081
	171	81.94871	80.05344	-1.89527	-1.95133	102.95786
	172	81.23386	79.31704	-1.91682	-1.97041	102.79572
	173	78.26009	76.35330	-1.90678	-1.95968	102.77393
	174	72.71803	70.81259	-1.90544	-1.96003	102.86528
	175	64.95500	63.01863	-1.93637	-1.99462	103.00856
	176	56.29105	54.29555	-1.99550	-2.05872	103.16854
	177	68.59733	67.23706	-1.36027	-1.41412	103.95861
	178	69.56015	68.04109	-1.51906	-1.57245	103.51504
	179	70.09274	68.53318	-1.55956	-1.61089	103.29152
	180	70.12211	68.56864	-1.55346	-1.60041	103.02234
	181	67.85988	66.31273	-1.54715	-1.59164	102.87565
	182	62.55606	61.00636	-1.54970	-1.59491	102.91745
	183	54.55658	52.98256	-1.57401	-1.62196	103.04622
	184	45.73187	44.10885	-1.62302	-1.67479	103.18977
	185	55.10083	54.25866	-0.84218	-0.87811	104.26743
	186	55.58785	54.55671	-1.03114	-1.07550	104.30251
	187	59.22714	58.04332	-1.18383	-1.22911	103.82540
	188	60.89820	59.58460	-1.31360	-1.35720	103.31901
	189	59.44980	58.06919	-1.38061	-1.42205	103.00151
	190	54.46755	53.10190	-1.36565	-1.40555	102.92142
	191	45.66123	44.39744	-1.26379	-1.30200	103.02384
	192	32.61714	31.53561	-1.08153	-1.11627	103.21215
END	257	43.06239	42.96419	-0.09821	-0.10655	108.50170
	258	49.13032	48.53379	-0.59653	-0.62333	104.49200

Table 4.2.3 continued

259	53.52694	52.52667	-1.00027	-1.04084	104.05629
260	54.32027	53.05260	-1.26766	-1.31371	103.63238
261	52.27702	50.89411	-1.38291	-1.42855	103.29994
262	47.35170	46.03594	-1.31576	-1.35624	103.07644
263	38.16057	37.12849	-1.03208	-1.06297	102.99386
264	22.02591	21.36332	-0.66259	-0.68699	103.68263
265	42.60581	42.41664	-0.18917	-0.21486	113.57790
266	45.12722	44.95884	-0.16838	-0.18060	107.26023
267	47.24021	46.63766	-0.60255	-0.62371	103.51193
268	46.14709	45.20271	-0.94438	-0.97535	103.27983
269	42.77325	41.67905	-1.09419	-1.12847	103.13251
270	37.34775	36.30935	-1.03839	-1.07113	103.15215
271	29.52699	28.63060	-0.89639	-0.93170	103.93929
272	26.14174	25.01903	-1.12271	-1.16931	104.15009
273	44.39629	43.91085	-0.48544	-0.52915	109.00276
274	40.94931	40.93111	-0.01820	-0.03538	194.42853
275	39.79717	39.66406	-0.13312	-0.13907	104.47462
276	36.62302	36.21113	-0.41188	-0.42241	102.55573
277	31.97706	31.34971	-0.62736	-0.64641	103.03756
278	27.13442	26.35718	-0.77724	-0.80728	103.86422
279	24.68556	23.63504	-1.05052	-1.09766	104.48742
280	31.83936	30.33886	-1.50051	-1.56030	103.98524
281	45.66577	45.01216	-0.65361	-0.70665	108.11477
282	39.15575	39.15678	0.00103	-0.02103	-2040.93735
283	35.13625	35.28374	0.14750	0.14909	101.07706
284	29.85577	29.85918	0.00341	0.00750	219.60867
285	23.97411	23.72807	-0.24604	-0.25508	103.67386
286	20.18210	19.53853	-0.64357	-0.67564	104.98325
287	22.73317	21.53773	-1.19544	-1.24756	104.36047
288	34.96003	33.27873	-1.68131	-1.74729	103.92415

Table 4.2.4 SDSA Result for Square Box
Using Domain Approach
(Length as Design)

	Elt #	Von Mises Stress OLD	NEW	Actual Change	Predict Change	Ratio x 100 %
TOP	1	100.63443	103.78530	3.15087	3.07549	97.60764
	2	55.67394	58.23363	2.55969	2.50390	97.82047
	3	39.87734	42.20731	2.32996	2.29028	98.29699
	4	33.64000	35.95122	2.31122	2.28113	98.69797
	9	84.75172	86.95996	2.20825	2.14499	97.13557
	10	54.11750	56.63499	2.51750	2.47243	98.21000
	11	38.09229	40.50634	2.41405	2.37384	98.33412
	12	31.40171	33.73828	2.33657	2.30087	98.47234
	17	71.55644	73.28717	1.73073	1.67965	97.04853
	18	51.39030	53.53043	2.14013	2.10877	98.53464

Table 4.2.4 continued

	19	36.38969	38.66464	2.27495	2.24349	98.61675
	20	29.10066	31.38476	2.28411	2.25004	98.50847
	25	63.92617	65.38354	1.45737	1.42286	97.63145
	26	47.77615	49.51865	1.74250	1.72446	98.96468
	27	33.71692	35.65189	1.93497	1.91733	99.08855
	28	25.62709	27.63564	2.00855	1.98508	98.83146
	33	58.13858	59.36943	1.23085	1.21307	98.55525
	34	43.89400	45.30579	1.41179	1.40998	99.87154
	35	30.18578	31.68205	1.49627	1.49238	99.74015
	36	21.28009	22.79503	1.51493	1.50010	99.02083
	41	52.16973	53.22842	1.05869	1.04999	99.17791
	42	38.92171	40.07670	1.15500	1.17203	101.47506
	43	26.27852	27.32058	1.04206	1.04642	100.41790
	44	18.05108	18.91286	0.86178	0.84558	98.12008
	49	43.70809	44.61852	0.91043	0.92291	101.37149
	50	31.54422	32.41523	0.87101	0.88778	101.92468
	51	23.75135	24.28852	0.53717	0.53220	99.07399
	52	20.09424	20.33228	0.23804	0.22397	94.09153
	57	28.21065	28.74663	0.53597	0.59021	110.11999
	58	26.03146	26.38137	0.34990	0.33047	94.44750
	59	29.02616	29.23143	0.20527	0.19831	96.60794
	60	31.15718	31.30541	0.14823	0.15058	101.58780
	61	31.15718	31.30541	0.14823	0.15058	101.58780
	62	29.02616	29.23143	0.20527	0.19831	96.60794
	63	26.03146	26.38137	0.34990	0.33047	94.44750
	64	28.21065	28.74663	0.53597	0.59021	110.11999
BOTTOM	65	86.28385	89.52932	3.24548	3.17833	97.93089
	66	49.20760	51.70151	2.49391	2.44280	97.95028
	67	35.10166	37.35064	2.24899	2.21072	98.29852
	68	29.26721	31.49583	2.22862	2.19866	98.65573
	73	75.61336	78.01060	2.39724	2.34965	98.01466
	74	47.86338	50.30632	2.44294	2.40017	98.24920
	75	33.16758	35.46582	2.29825	2.25789	98.24419
	76	26.96837	29.18948	2.22111	2.18423	98.33964
	81	65.59970	67.47185	1.87214	1.83760	98.15480
	82	45.52028	47.63719	2.11691	2.08787	98.62810
	83	31.42032	33.59012	2.16979	2.13633	98.45749
	84	24.58127	26.74014	2.15887	2.12160	98.27359
	89	59.01335	60.55661	1.54326	1.52421	98.76615
	90	42.63218	44.38781	1.75563	1.74194	99.22044
	91	29.11188	30.98445	1.87257	1.85249	98.92778
	92	21.34630	23.26564	1.91934	1.89200	98.57533
	97	53.42710	54.71222	1.28512	1.28203	99.75935
	98	39.32319	40.76850	1.44531	1.44731	100.13849
	99	26.26198	27.73868	1.47670	1.47071	99.59451
	100	17.77022	19.23274	1.46252	1.44528	98.82123
	105	47.01331	48.10625	1.09294	1.10137	100.77178
	106	34.66051	35.85638	1.19587	1.20787	101.00332
	107	23.27783	24.31058	1.03275	1.03340	100.06302

Table 4.2.4 continued

	108	16.13709	16.92466	0.78757	0.77243	98.07728
	113	37.36988	38.29384	0.92397	0.93633	101.33766
	114	27.64675	28.51542	0.86867	0.87661	100.91393
	115	22.48638	22.95476	0.46838	0.46698	99.70162
	116	20.66130	20.81388	0.15259	0.14922	97.79369
	121	21.39204	21.86005	0.46801	0.47243	100.94410
	122	25.40962	25.63305	0.22343	0.22547	100.91448
	123	31.19434	31.31165	0.11731	0.12479	106.37442
	124	34.36406	34.46283	0.09877	0.11078	112.15702
SIDE	129	171.97848	174.92077	2.94229	2.83083	96.21181
	130	144.28489	147.17610	2.89121	2.72701	94.32052
	131	127.95324	130.60632	2.65307	2.55823	96.42536
	132	119.63305	122.23507	2.60202	2.52531	97.05197
	133	114.31134	116.95689	2.64555	2.57766	97.43403
	134	111.82036	114.60309	2.78273	2.71857	97.69435
	135	114.85173	117.97635	3.12462	3.05748	97.85138
	136	127.43202	130.94177	3.50974	3.43456	97.85795
	137	129.44261	131.12998	1.68736	1.63050	96.63030
	138	132.98811	135.18474	2.19663	2.13853	97.35510
	139	127.63870	130.19786	2.55916	2.49756	97.59316
	140	120.84447	123.52891	2.68444	2.61374	97.36630
	141	115.99465	118.74030	2.74565	2.68257	97.70237
	142	113.02475	115.79395	2.76920	2.71224	97.94317
	143	109.97003	112.59708	2.62705	2.57702	98.09553
	144	102.30763	104.61563	2.30800	2.25407	97.66333
	145	105.70496	107.07836	1.37340	1.30398	94.94527
	146	117.30361	118.88574	1.58213	1.53328	96.91255
	147	118.30094	120.29037	1.98943	1.94144	97.58745
	148	115.08585	117.32766	2.24181	2.19249	97.79982
	149	110.95022	113.27138	2.32116	2.27480	98.00300
	150	106.22925	108.47626	2.24701	2.20489	98.12533
	151	99.14657	101.16379	2.01721	1.97823	98.06733
	152	85.65457	87.45312	1.79855	1.75770	97.72890
	153	93.64369	94.81903	1.17534	1.12334	95.57512
	154	103.04949	104.29693	1.24744	1.19562	95.84590
	155	106.11978	107.59368	1.47390	1.43087	97.08052
	156	104.97155	106.62767	1.65611	1.61890	97.75267
	157	101.32153	103.03800	1.71647	1.68149	97.96232
	158	95.62944	97.29838	1.66894	1.63633	98.04628
	159	87.25962	88.82320	1.56358	1.53344	98.07268
	160	74.98447	76.45953	1.47505	1.44836	98.19018
	161	84.56467	85.55652	0.99185	0.94271	95.04516
	162	91.34894	92.35470	1.00576	0.95899	95.35052
	163	93.91524	94.99255	1.07730	1.03854	96.40147
	164	93.15356	94.28181	1.12825	1.09605	97.14540
	165	89.80530	90.94592	1.14062	1.11172	97.46585
	166	84.06349	85.20942	1.14593	1.11992	97.73080
	167	75.93268	77.10497	1.17229	1.15121	98.20215
	168	65.60454	66.80416	1.19962	1.18618	98.87979

Table 4.2.4 continued

	169	76.84401	77.65623	0.81222	0.75988	93.55582
	170	80.70596	81.50506	0.79910	0.75524	94.51046
	171	81.94871	82.70473	0.75602	0.72246	95.56134
	172	81.23386	81.91789	0.68403	0.65822	96.22771
	173	78.26009	78.90258	0.64249	0.61966	96.44573
	174	72.71803	73.39538	0.67735	0.65803	97.14800
	175	64.95500	65.75554	0.80054	0.78729	98.34549
	176	56.29105	57.23964	0.94859	0.94555	99.67962
	177	68.59733	69.21429	0.61696	0.53167	86.17570
	178	69.56015	70.15992	0.59977	0.56805	94.71189
	179	70.09274	70.53774	0.44500	0.41914	94.18829
	180	70.12211	70.41920	0.29709	0.28300	95.25776
	181	67.85988	68.09515	0.23527	0.22166	94.21444
	182	62.55606	62.83363	0.27757	0.26628	95.93328
	183	54.55658	54.99360	0.43702	0.43011	98.41811
	184	45.73187	46.41994	0.68807	0.69057	100.36360
	185	55.10083	55.48157	0.38073	0.05267	13.83486
	186	55.58785	55.81064	0.22279	0.29350	131.73681
	187	59.22714	59.30341	0.07627	0.06558	85.99149
	188	60.89820	60.90101	0.00281	0.00516	184.09342
	189	59.44980	59.43476	-0.01504	-0.01861	123.72023
	190	54.46755	54.48607	0.01852	0.01608	86.83648
	191	45.66123	45.77325	0.11203	0.11082	98.92143
	192	32.61714	32.92948	0.31234	0.31473	100.76460
END	257	43.06239	43.02243	-0.03996	0.06560	-164.15975
	258	49.13032	49.09116	-0.03916	0.00872	-22.28038
	259	53.52694	53.50754	-0.01940	-0.00629	32.43450
	260	54.32027	54.31034	-0.00992	-0.00222	22.39806
	261	52.27702	52.27824	0.00122	0.00657	537.81326
	262	47.35170	47.36369	0.01200	0.01579	131.61393
	263	38.16057	38.16603	0.00546	0.00782	143.22216
	264	22.02591	22.00883	-0.01708	-0.01706	99.88791
	265	42.60581	42.62436	0.01855	0.02982	160.72709
	266	45.12722	45.11601	-0.01121	-0.02510	223.82650
	267	47.24021	47.26791	0.02770	0.03331	120.26333
	268	46.14709	46.19714	0.05005	0.05727	114.42115
	269	42.77325	42.82741	0.05416	0.06086	112.37168
	270	37.34775	37.38730	0.03956	0.04516	114.17577
	271	29.52699	29.53403	0.00704	0.01035	146.99528
	272	26.14174	26.19295	0.05121	0.05454	106.51004
	273	44.39629	44.47833	0.08203	0.08544	104.15643
	274	40.94931	40.96752	0.01822	0.01337	73.40770
	275	39.79717	39.82967	0.03250	0.03146	96.80740
	276	36.62302	36.66663	0.04361	0.04665	106.96071
	277	31.97706	32.01814	0.04108	0.04544	110.61912
	278	27.13442	27.16644	0.03201	0.03652	114.08903
	279	24.68556	24.73067	0.04511	0.04968	110.12954
	280	31.83936	31.99465	0.15529	0.16361	105.36131
	281	45.66577	45.78814	0.12237	0.12677	103.59741

Table 4.2.4 continued

282	39.15575	39.19432	0.03857	0.03718	96.39331
283	35.13625	35.16403	0.02779	0.02644	95.14028
284	29.85577	29.87675	0.02098	0.02200	104.88641
285	23.97411	23.98394	0.00983	0.01220	124.06492
286	20.18210	20.19824	0.01614	0.01924	119.19564
287	22.73317	22.80974	0.07657	0.08197	107.05609
288	34.96003	35.17924	0.21920	0.23069	105.24148

smaller than others. Thus, the finite differences may not be accurate.

4.2.4 Discussion

The above results indicate that accuracy of the boundary approach for built-up structures is poor, whereas accuracy of the domain approach is excellent. Note also that derivation of shape design sensitivity formulas is greatly simplified by using the domain approach. None of the integration by parts, formal operator equations, or boundary interface conditions are necessary during derivation. Sensitivity results are obtained by simply adding contributions from each component, as long as a legitimate design velocity field (satisfying regularity requirements) is used throughout the domain.

4.3 Plate-Beam-Truss Built-up Structure

In this section, shape design sensitivity analysis of a plate-beam-truss built-up structure is performed, using the domain approach for shape design sensitivity analysis. The same problem was treated by the boundary approach in Ref. 22.

4.3.1 System Description

Consider a built-up structure made up of plates, beams, and trusses, as shown in Fig. 4.3.1. It is a modeled shape of a beam-plate grillage supported by four sets of four-bar trusses. The dotted lines are supporting trusses, and solid lines are beam stiffners. Due to symetry of the structure, only one quarter of the structure is shown in the figure. It is assumed that plates and beams are welded together so that energy is not dissipated during deformation. Design variables for this built-up structure are thickness $t_i(x,y)$ of each plate component, width $d_{\tilde{j}}(x)$ and the height $h_{\tilde{j}}(x)$ of each longitudinal beam component, width $d_k(y)$ and height $h_k(\acute{y})$ of each transverse beam component, constant cross-sectional area A_ℓ of the 4-bar truss components, positions b_1 and b_2 of transverse beams, and positions b_3 and b_4 of longitudinal beams. In vector form, this is

$$\underset{\sim}{b} = [t_i, \tilde{d}_j, \tilde{h}_j, d_K, h_K, A_\ell, b_1, b_2, b_3, b_4]^T$$

It is assumed that the lengths of the trusses are fixed, but that they may change their ground positions, and that the outside boundary of the entire structure does not vary, i.e., only locations b_i, i=1, 2, 3, 4 of the beams are shape variables.

Dimensions of the structure and the numbering and spacing of beams in both directions are shown in Fig. 4.3.1. Coordinates of intersection points of beams and plates are supposed to be in the mid-planes of the plates and neutral axes of the beams.

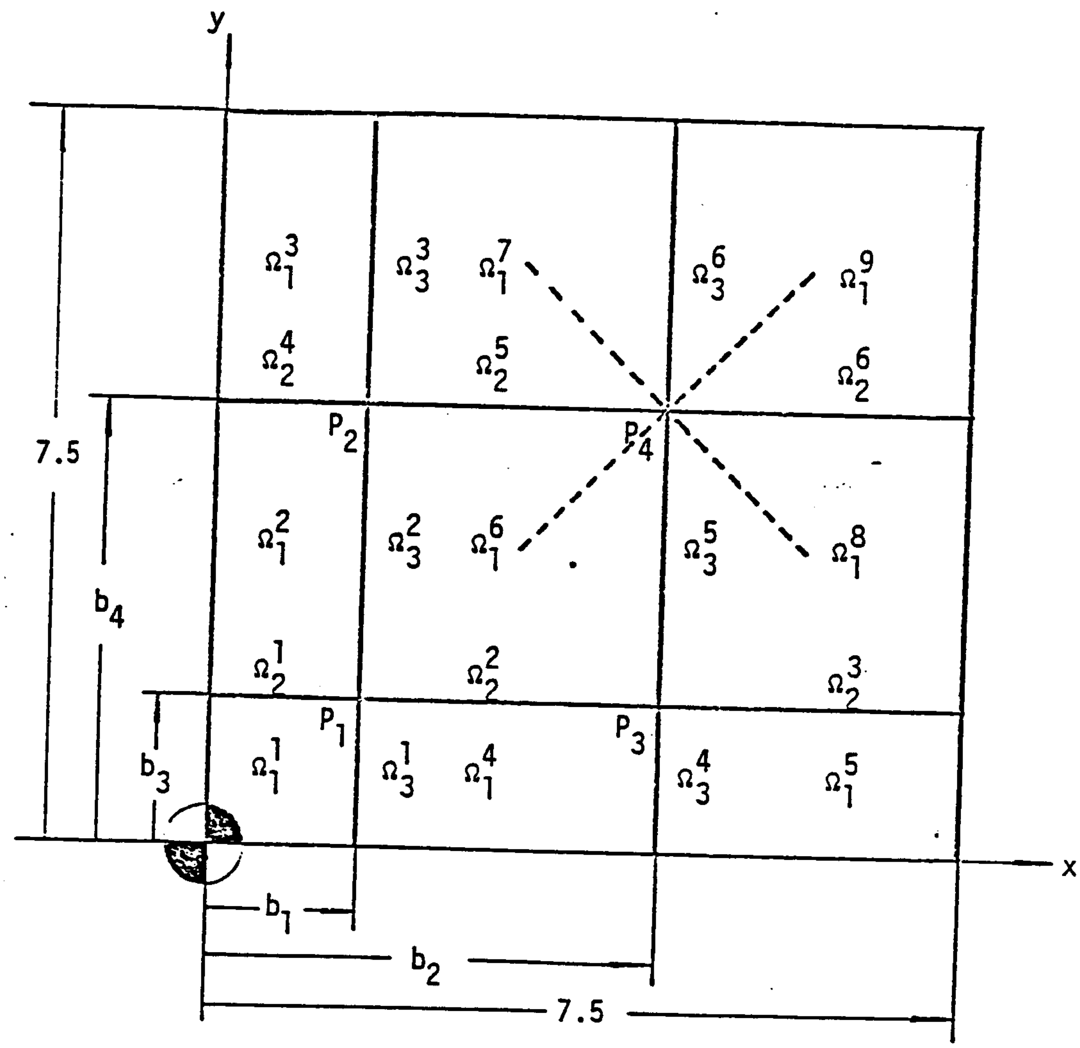

Figure 4.3.1 Dimension and Numbering of Quarter Plate

Applied loads are

$$f_i \in L^2(\Omega_1^i), \qquad i = 1, 2, \ldots, 9$$

where $f_i(x,y)$ are defined as distributed loads on the plate and the numbering convention on the sub-domains are also shown in Fig. 4.3.1. Domains of plates, longitudinal beams, and transverse beams are denoted, respectively, as follows:

plate	Ω_1^i
longitudinal beams	Ω_2^i
transverse beams	Ω_3^K
truss	Ω_4^ℓ

The state variables for this built-up structure consist of displacements z^i of each plate component, displacements w^i and rotations β^i of each longitudinal beam component, displacements v^k and rotation θ^k of each transverse beam component, and displacements u^ℓ of truss members, as follows :

z^i	on Ω_1^i
w^j and β^j	on Ω_2^j

v^K and θ^K on Ω_3^K

u^ℓ on Ω_4^ℓ

The following interface conditions are enforced in the finite element model: At interfaces between plate and beam components, lateral deflections of plate and beam components are the same. That is, for longitudinal beams,

$$w^1(x) = z^1(x,b_3) = z^2(x,b_3)$$

$$w^2(x) = z^4(x,b_3) = z^6(x,b_3)$$

$$w^3(x) = z^5(x,b_3) = z^8(x,b_3)$$

$$w^4(x) = z^2(x,b_4) = z^3(x,b_4)$$

$$w^5(x) = z^6(x,b_4) = z^7(x,b_4)$$

$$w^6(x) = z^8(x,b_4) = z^9(x,b_4)$$

and for transvers beams,

$$v^1(y) = z^1(b_1,y) = z^4(b_1,y)$$

$$v^2(y) = z^2(b_1,y) = z^6(b_1,y)$$

$$v^3(y) = z^3(b_1,y) = z^7(b_1,y)$$

$$v^4(y) = z^4(b_2,y) = z^5(b_2,y)$$

$$v^5(y) = z^6(b_2,y) = z^8(b_2,y)$$

$$v^6(y) = z^7(b_2,y) = z^9(b_2,y)$$

The normal slopes of plate components are the same as the torsion angles of beams that are attached at the interfaces. For the plates and longitudinal beams,

$$\beta^1 = z_y^1 = z_y^2$$

$$\beta^2 = z_y^4 = z_y^6$$

$$\beta^3 = z_y^5 = z_y^8$$

$$\beta^4 = z_y^2 = z_y^3$$

$$\beta^5 = z_y^6 = z_y^7$$

$$\beta^6 = z_y^8 = z_y^9$$

and for the plates and transvers beams,

$$\theta^1 = z_x^1 = z_x^4$$

$$\theta^2 = z_x^2 = z_x^6$$

$$\theta^3 = z_x^3 = z_x^7$$

$$\theta^4 = z_x^4 = z_x^5$$

$$\theta^5 = z_x^6 = z_x^8$$

$$\theta^6 = z_x^7 = z_x^9$$

The torsional angles of transverse beams and the axial slopes of longitudinal beams must be the same at the intersections of beams; i.e., at points p_i,

$$P_1: \quad \theta^1 = w_x^1 = w_x^2$$

$$P_2: \quad \theta^2 = w_x^4 = w_x^5$$

$$P_3: \quad \theta^4 = w_x^2 = w_x^3$$

$$P_4: \quad \theta^5 = w_x^5 = w_x^6$$

Similarly, the torsional angles of longitudinal beams and axial slopes of transverse beams must be the same at intersentions of beams; i.e., at points p_i,

$$P_1: \quad \beta^1 = v_y^1 = v_y^2$$

$$P_2: \quad \beta^4 = v_y^2 = v_y^3$$

$$P_3: \quad \beta^2 = v_y^4 = v_y^5$$

$$P_4: \quad \beta^5 = v_y^5 = v_y^6$$

It is assumed that each lateral displacement is evaluated at the middle plane of the plates and at the neutral axes of beams. Then, the lateral deflections of crossing beams and trusses must be the same, at the intersection points; i.e., at points p_i,

$$P_1:\ v^1 = v^2,\ v^1 = w^2,\ v^2 = w^2$$

$$P_2:\ v^2 = v^3,\ v^2 = w^4,\ v^3 = w^5$$

$$P_3:\ v^4 = v^5,\ v^4 = w^2,\ v^5 = w^2$$

$$P_4:\ v^5 = v^6,\ v^5 = w^5,\ v^6 = w^6$$

With the assumption that there are no in-plane deformations in the plates and beams, the plate-beam structure that rests on the 4-bar trusses is pressumed to move as a rigid body in the plane of plates. Finally, the displacement of the bottom of each truss component is zero, since it is fastened to a rigid foundation.

One can now define the set Z of kinematically admissible displacement field as

$$Z = \{a:\ a=(z^i, w^i, \beta^j, v^K, \theta^K, u^\ell) \text{ such that all the above boundary interface conditions are satisfied}\}$$

4.3.2 Shape Design Sensisitivty Analysis

Applying the design component idea, shape design sensitivity coefficients of the built-up structure are obtained by adding shape design sensitivities of each component in the structure. Using Eqs. 2.2.11, 2.2.16, 2.2.20, 2.2.24, 2.2.25, 2.2.36, and 2.2.37, one obtains

$$
\begin{aligned}
a(\dot{z},\bar{z}) = \sum_i \iint_{\Omega_1^i} D^i [& 4(z^i_{xx}\bar{z}^i_{xx}V^x_x + z^i_{yy}\bar{z}^i_{yy}V^y_y) + \nu(z^i_{xx}\bar{z}^i_{yy} + z^i_{yy}\bar{z}^i_{zz})(V^x_x + V^y_y) \\
& - (z^i_{xx}\bar{z}^i_{xx} + z^i_{yy}\bar{z}^i_{yy})\ (V^x_x + V^y_y) + (z^i_x\ \bar{z}^i_{xx}) + z^i_{xx}\bar{z}^i_x)\ V^x_{xx} \\
& + (z^i_y\ \bar{z}^i_{yy} + z^i_{yy}\bar{z}^i_y)\ V^y_{yy} + 2(1-\nu)\ z^i_{xy}\bar{z}^i_{xy}\ (V^x_x + V^y_y) \\
& \nu\ (z^i_x\ \bar{z}^i_{yy} + z^i_{yy}\bar{z}^i_x)\ V^x_{xx} + \nu\ (z^i_y\ \bar{z}^i_{xx} + z^i_{xx}\bar{z}^i_y)\ V^y_{yy}]\ d\Omega_1 \\
+ \sum_j \int_{\Omega_2^j} & G\hat{J}^j(\beta^j_x\ \bar{\beta}^j_x)\ V^x_x\ d\Omega_2 \\
+ \sum_K \int_{\Omega_3^K} & GJ^K(\theta^K_y\ \bar{\theta}^K_y)\ V^y_y\ d\Omega_3 \\
+ \sum_j \int_{\Omega_2^j} & E\hat{I}^j[3(w^j_{xx}\bar{w}^j_{xx})\ V^x_x + (w^j_x\ \bar{w}^j_{xx} + w^j_{xx}\bar{w}^j_x)\ V^x_{xx}]\ d\Omega_2 \\
+ \sum_K \int_{\Omega_3^K} & EI^K[3(v^K_{yy}\bar{v}^K_{yy})\ V^y_y + (v^K_y\ \bar{v}^K_{yy} + v^K_{yy}\bar{v}^K_y)\ V^y_{yy}]\ d\Omega_3 \\
+ \sum_i \iint_{\Omega_1^i} & (f_i\bar{z}_i)\ (\nabla \cdot V)\ d\Omega_1 \qquad (4.3.1)
\end{aligned}
$$

where

E = Young's modulus

G = Shear modulus

$D^i \quad = Et_i^3/12(1-\nu^2)$

$\hat{J}^j, J^K$ = Torsion constant

$\hat{I}^i, I^K$ = Moment of inertia

The stress constraint functional can be defined, using the characteristic function approach on $\Omega^p \subset \Omega_q$, as

$$\psi = \iint_{\Omega_q} \phi(\sigma(z^q))\, M_p \, d\Omega \tag{4.3.2}$$

where ϕ is the von Mises failure criterion, as

$$\phi = [\sigma_{xx}^2 + \sigma_{yy}^2 + 3\sigma_{xy}^2 - \sigma_{xx}\sigma_{yy}]^{1/2}$$

The shape design sensitivity formula can be derived using Eqs. 2.2.37, 2.2.41, the last term of Eq. 2.2.45, and Eq. 4.3.1 as

$$\begin{aligned}
\psi' = \sum_i \iint_{\Omega_1^i} D^i [& 4(z_{xx}^i \lambda_{xx}^i V_x^x + z_{yy}^i \lambda_{yy}^i V_y^y) + \nu(z_{xx}^i \lambda_{yy}^i + z_{yy}^i \lambda_{xx}^i)(V_x^x + V_y^y) \\
& - (z_{xx}^i \lambda_{xx}^i + z_{yy}^i \lambda_{yy}^i)(\nabla \cdot V) + 2(1-\lambda)\, z_{xy}^i \lambda_{xy}^i \,(\nabla \cdot V) \\
& + (z_x^i \lambda_{xx}^i + z_{xx}^i \lambda_y^i)\, V_{xx}^x + (z_y^i \lambda_{yy}^i + z_{yy}^i \lambda_y^i)\, V_{yy}^y \\
& + \nu(z_x^i \lambda_{yy}^i + z_{yy}^i \lambda_x^i)\, V_{xx}^x + \nu(z_y^i \lambda_{xx}^i + z_{xx}^i \lambda_y^i)\, V_{yy}^y]\, d\Omega_1
\end{aligned}$$

$$+ \sum_j \int_{\Omega_2^i} G^j \hat{J}^j (w_{xy}^j \lambda_{xy}^j)\, d\Omega_2 + \sum_2 \int_{\Omega_3^K} G^K J^K (v_{xy}^K \lambda_{xy}^K)\, d\Omega_3$$

$$+ \sum_j \int_{\Omega_2^j} E^j \hat{I}^j \left[3\, w_{xx}^j \lambda_{xx}^j V_x^x + (w_x^j \lambda_{xx}^j + w_{xx}^j \lambda_x^j)\, V_{xx}^x\right] d\Omega_2$$

$$+ \sum_K \int_{\Omega_3^K} E^K I^K \left[3\, v_{yy}^K \lambda_{yy}^K V_y^y + (v_y^K \lambda_{yy}^K + v_{yy}^K \lambda_y^K) V_{yy}^y\right] d\Omega_3$$

$$- \iint_{\Omega_2^q} \frac{1}{2\phi} \left[4A^2(1-\nu+\nu^2)({z_{xx}^q}^2 V_x^x + {z_{qq}^q}^2 V_y^y) - 2A^2(1-4\nu+\nu^2)(z_{xx}^q z_{yy}^q)(\nabla \cdot V)\right.$$

$$+ 2A^2(1-\nu+\nu^2)(z_{xx}^q z_x^q V_{xx}^x + z_{yy}^q z_y^q V_{yy}^y) - A^2(1-4\nu+\nu^2)(z_{yy}^q z_x^q V_{xx}^x + z_{xx}^q z_y^q V_{yy}^q)$$

$$\left. + 6B^2 {z^q_{xy}}^2 (\nabla \cdot V)\right] M_p\, d\Omega_1$$

$$+ \iint_{\Omega_1^q} \phi(\nabla \cdot V)\, M_p\, d\Omega_1 + \sum_i \iint_{\Omega_1^i} (f^i \lambda^i)\, (\nabla \cdot V)\, d\Omega_1$$

$$- \iint_{\Omega_1^q} \phi\, M_p\, d\Omega \iint_{\Omega_1^q} (\nabla \cdot V)\, M_p\, d\Omega_1 \qquad (4.3.3)$$

where λ is the solution of the adjoint equation of Eq. 2.2.40, which can be rewritten for this problem as

$$a(\lambda, \bar{\lambda}) = \iint_{\Omega_1^q} \sum_{i,j} \frac{\partial \phi}{\partial \sigma_{ij}} (z^q)\, \sigma_{ij}(\bar{\lambda})\, M_p\, d\Omega_1, \quad \text{for all } \bar{\lambda} \in Z$$

and

$$A = -\frac{Et^2}{(1-\nu^2)}, \quad B = -\frac{Et^2}{(1+\nu)}$$

Due to Symmetry, only one quarter of the structure is considered. The quarter plate is divided into 9 sub-domains(or patches) and 400 non-conforming rectangular plate elements with 12 degrees-of-freedom [27] are used to discretize the quadrant. Eighty beam elements are used to model the four beam stiffners. Four-bar trusses are used as supports. The total number of active degrees-of-freedom of the system is 1281.

The result of Chapter 3 is applicable for constructing the design velocity field. Beam and bending plate components require C^1-regular velocity fields between patches. Hermite cubic polynomials, which assure C^1 continuity at interfaces, are used to generate design velocity fields. In Fig. 4.3.2, velocity $V^x(x)$ in the x-direction is plotted. Note that a C^1 velocity field is obtained by imposing zero slope at each interface.

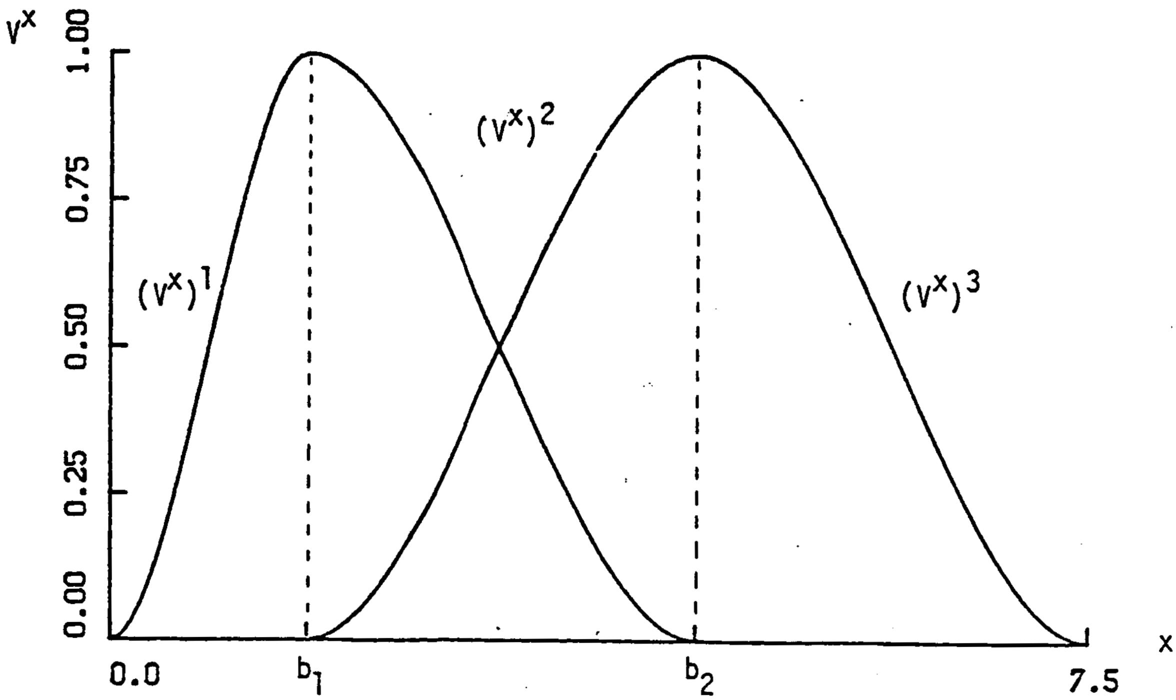

Figure 4.3.2 Design Velocity V^x Along x-Axes

The beam stiffners are allowed to move transversally only. Consequently, the x-direction component V^x of velocity V is a function of x only and the y-direction component V^y is a function of y only. The velocity fields in each patch can be written as in Table 4.3.1, where

Table 4.3.1 Velocity in Each Patch

Patch No.	V^x	V^y
Ω_1^1	$(V^x)^1$	$(V^y)^1$
Ω_1^2	$(V^x)^1$	$(V^y)^2$
Ω_1^3	$(V^x)^1$	$(V^y)^3$
Ω_1^4	$(V^x)^2$	$(V^y)^1$
Ω_1^5	$(V^x)^3$	$(V^y)^1$
Ω_1^6	$(V^x)^2$	$(V^y)^2$
Ω_1^7	$(V^x)^2$	$(V^y)^3$
Ω_1^8	$(V^x)^3$	$(V^y)^2$
Ω_1^9	$(V^x)^3$	$(V^y)^3$

$$(V^x)^1 = -\left(\frac{2}{a^3}\right) \xi^2 \left(\xi - \frac{3a}{2}\right) \delta b_1$$

$$(V^x)^2 = \left(\frac{2}{a^3}\right) \xi^2 \left(\xi - \frac{3a}{2}\right) \left(\delta b_1 - \delta b^2\right) + \delta b_1$$

$$(V^x)^3 = \left(\frac{2}{a^3}\right) \xi^3 \left(\xi - \frac{3a}{2}\right) \delta b_2 + \delta b_2$$

$$(V^y)^1 = -\left(\frac{2}{b^3}\right) \eta^2 \left(\eta - \frac{3b}{2}\right) \delta b_3$$

$$(V^y)^2 = \left(\frac{2}{b^3}\right) \eta^2 \left(\eta - \frac{3b}{2}\right) (\delta b_3 - \delta b_4) + \delta b_3$$

$$(V^y)^3 = \left(\frac{2}{b^3}\right) \eta^2 \left(\eta - \frac{3b}{2}\right) \delta b_4 + \delta b_4$$

with

(ξ, η): a patch coordinate system originated at the lower left corner of each patch, and

a,b: dimensions of each patch in x- and y-directions as shown in Fig. 4.3.3.

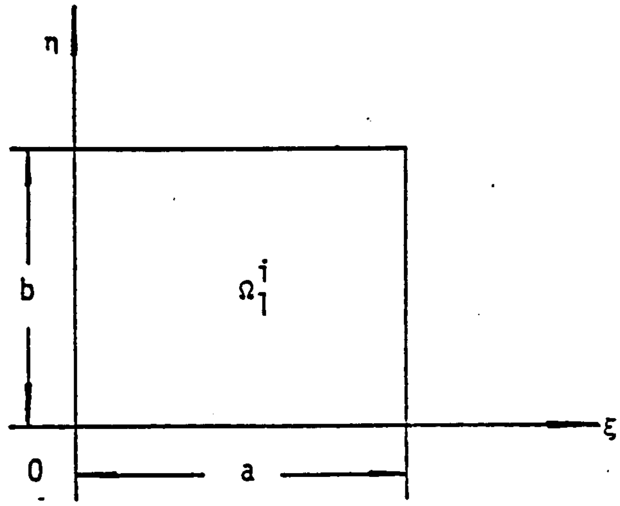

Figure 4.3.3 Patch Coordinate System

This problem was solved by Lee and Choi [22], using the boundary approach, with considerable difficulty in handling boundary elements of each patch. The accuracy of those boundary elements deteriorate with ratio (between predict and actual changes times 100) ranging from -98.2 to 515.5. SDSA results obtained using domain approach are given in Table 4.3.2. The perturbation is a 0.25% change of each design parameter. The ratio between predicted change and actual change is excellent for all elements located inside and adjacent to the beam stiffners. This shows that the domain approach of SDSA can handle singular behavior across the beam stiffners much better than the boundary approach.

Next, as a test, a piecewise linear velocity field is used without considering slope discontinuity at each interface, to see the numerical effect of terms associated with slope jumps. As explained in Chapter 3, a piecewise linear velocity field can be used only after considering singular behavior along the interfaces. A part of the SDSA result is given in Table 4.3.3. This clearly indicates that regularity of the design velocity field in the domain is a crucial factor of the domain approach of SDSA.

Table 4.3.2 SDSA Results for Truss-Beam-Plate Built-up Structure Using the Domain Approach

Element Number	Von Mises Stress OLD	NEW	Actual Change	Predict Change	Ratio %
81	49.128	50.043	0.915	0.915	100.101
83	40.429	41.289	0.860	0.861	100.103
85	34.279	34.881	0.602	0.600	99.634
87	50.331	51.190	0.858	0.858	100.008
89	62.143	63.067	0.925	0.924	99.927
91	67.841	68.765	0.924	0.923	99.928
93	77.076	77.949	0.873	0.871	99.818
95	83.610	84.604	0.994	0.994	100.036
97	92.755	93.843	1.088	1.090	100.161
99	102.907	104.158	1.251	1.253	100.208
102	44.262	45.153	0.891	0.891	99.955
104	33.034	33.809	0.776	0.775	99.878
106	42.663	43.440	0.778	0.776	99.835
108	55.944	56.826	0.882	0.880	99.878
110	63.522	64.437	0.914	0.913	99.820

Table 4.3.2 continued

112	69.646	70.537	0.891	0.889	99.723
114	77.930	78.891	0.961	0.960	99.866
116	85.518	86.577	1.060	1.060	100.043
118	91.868	93.039	1.171	1.172	100.067
120	104.643	106.009	1.367	1.374	100.576
122	39.542	40.401	0.859	0.858	99.917
124	33.332	34.143	0.811	0.810	99.918
126	44.281	45.046	0.765	0.763	99.702
128	52.498	53.329	0.831	0.830	99.917
130	58.526	59.389	0.862	0.861	99.843
132	67.527	68.410	0.883	0.881	99.722
134	75.498	76.477	0.979	0.978	99.864
136	79.045	80.149	1.104	1.104	100.019
138	81.265	82.434	1.169	1.170	100.061
140	89.832	91.166	1.334	1.340	100.472
145	38.362	39.116	0.754	0.749	99.406
147	44.882	45.626	0.744	0.744	99.935
149	46.061	46.804	0.743	0.742	99.867
151	56.025	56.826	0.801	0.800	99.944
153	70.749	71.663	0.914	0.911	99.697
155	68.378	69.490	1.112	1.112	99.967
157	67.127	68.334	1.207	1.209	100.125
159	65.011	66.196	1.185	1.189	100.362
165	38.300	39.039	0.740	0.738	99.787
167	40.579	41.250	0.670	0.669	99.769
169	47.855	48.520	0.665	0.663	99.704
171	60.184	60.932	0.748	0.744	99.436
173	67.866	68.758	0.892	0.889	99.631
175	64.113	65.214	1.101	1.100	99.934
177	62.719	64.012	1.293	1.294	100.081
179	64.430	65.898	1.468	1.471	100.248
186	43.048	43.773	0.726	0.725	99.870
188	51.596	52.317	0.721	0.719	99.742
190	59.144	59.893	0.749	0.745	99.568
192	62.228	62.978	0.749	0.745	99.348
194	56.037	56.965	0.928	0.924	99.657
196	57.209	58.333	1.124	1.124	99.973
198	59.270	60.553	1.283	1.284	100.086
200	65.318	66.805	1.487	1.490	100.151
208	55.122	55.881	0.759	0.756	99.694
210	58.260	59.010	0.750	0.746	99.513
212	59.139	59.726	0.587	0.581	98.980
214	48.012	48.846	0.834	0.830	99.447
216	47.049	48.106	1.057	1.056	99.883
218	49.752	50.954	1.203	1.203	100.000
220	56.823	58.228	1.405	1.408	100.195
229	55.504	56.252	0.747	0.744	99.522
231	53.218	53.793	0.575	0.569	99.025
233	55.546	55.983	0.437	0.430	98.454
235	37.003	37.871	0.868	0.863	99.421

Table 4.3.2 continued

237	35.140	36.218	1.078	1.077	99.867
239	37.897	39.123	1.226	1.226	99.998
249	52.077	52.764	0.687	0.683	99.347
251	48.867	49.239	0.372	0.365	98.032
253	56.294	56.509	0.215	0.208	96.745
255	32.700	33.318	0.618	0.608	98.390
257	23.383	24.298	0.915	0.907	99.142
259	23.267	24.329	1.062	1.056	99.478
270	45.287	45.655	0.368	0.360	97.893
272	61.326	61.258	-0.068	-0.075	109.851
274	47.757	47.886	0.129	0.120	93.134
276	32.009	32.264	0.255	0.240	94.039
278	27.041	27.324	0.283	0.263	93.002
280	34.813	35.190	0.377	0.364	96.534
291	53.166	53.065	-0.101	-0.109	108.029
292	67.683	67.463	-0.220	-0.226	102.722
293	67.215	67.053	-0.162	-0.167	103.331
294	60.173	60.055	-0.118	-0.125	106.060
296	53.350	53.241	-0.109	-0.118	107.688
297	53.724	53.624	-0.099	-0.108	108.923
298	55.290	55.228	-0.062	-0.071	114.797
299	57.632	57.626	-0.007	-0.016	241.315
300	65.729	65.812	0.083	0.077	93.336
309	58.271	58.413	0.142	0.135	94.890
311	67.683	67.463	-0.220	-0.226	102.722
313	81.478	81.173	-0.304	-0.312	102.463
315	82.704	82.424	-0.280	-0.285	101.642
317	90.044	89.857	-0.187	-0.189	101.419
319	100.980	101.057	0.077	0.075	97.485
329	56.294	56.509	0.215	0.208	96.745
331	67.215	67.053	-0.162	-0.167	103.331
333	82.051	81.674	-0.377	-0.382	101.415
335	79.509	79.143	-0.366	-0.369	100.925
337	90.039	89.689	-0.350	-0.352	100.411
339	101.657	101.295	-0.362	-0.364	100.572
349	42.011	42.430	0.419	0.410	97.833
351	60.173	60.055	-0.118	-0.125	106.060
353	78.037	77.663	-0.374	-0.379	101.275
354	67.361	66.997	-0.364	-0.368	101.176
355	62.299	61.961	-0.338	-0.342	101.065
356	61.299	60.986	-0.313	-0.316	100.931
357	62.680	62.383	-0.297	-0.300	100.804
358	64.853	64.565	-0.288	-0.290	100.717
359	67.503	67.225	-0.279	-0.281	100.738
360	75.326	75.037	-0.289	-0.293	101.558
366	56.141	57.173	1.032	1.030	99.846
368	37.003	37.871	0.868	0.863	99.421
380	49.342	49.141	-0.201	-0.205	102.234
397	29.770	29.560	-0.210	-0.214	102.002
399	27.894	27.717	-0.177	-0.182	102.481

Table 4.3.2 continued

417	21.848	21.623	-0.225	-0.230	102.151
419	18.109	17.866	-0.243	-0.248	101.974
438	14.556	14.247	-0.309	-0.313	101.186
440	14.939	14.640	-0.299	-0.302	100.982
460	12.189	11.934	-0.255	-0.255	100.106
480	8.471	8.315	-0.156	-0.154	99.114

Table 4.3.3 SDSA Results for Truss-Beam-Plate Built-up Structure Using the Domain Approach with Piece-wise Linear Velocity, without Compensation

Element Number	Von Mises Stress OLD	NEW	Actual Change	Predict Change	Ratio %
81	49.128	50.043	0.915	0.777	84.918
83	40.429	41.289	0.860	0.684	79.535
85	34.279	34.881	0.602	0.468	77.741
87	50.331	51.190	0.858	0.673	78.438
89	62.143	63.067	0.925	0.706	76.324
91	67.841	68.765	0.924	0.647	70.022
93	77.076	77.949	0.873	0.549	62.671
95	83.610	84.604	0.994	0.607	61.066
97	92.755	93.843	1.088	0.679	62.408
99	102.907	104.158	1.251	0.807	64.508

With the sensitivity coefficients obtained in the previous step, one can now apply a nonlinear programming method to find an improved design. The linearization method [44] of iterative optimization is chosen. Minimum cost (total mass) of the built-up structure, subject to stress constraints on plate and beam elements and a displacement constraint is considered. The initial design is chosen to be a uniform plate (thickness = 0.1 inch) and uniform beam (height = 0.5 inch, depth = 0.15 inch), with shape parameters $b_1 = b_3 = 1.5$ and $b_2 = b_4 = 4.5$. The lower bounds on plate thickness, beam height, and beam depth are 0.05, 0.25, and 0.075, respectively. Beam stiffners are allowed to move freely, without coalescence or passing each other. Upper bounds for stress constraints are 400 psi for beam elements and 100 psi for plate elements. Center point vertical displacement is limited by 0.0006 inch downward. Consequently, this problem has 292 design variables and 251 constraints, without including design bound constraints.

The cost function history achieved is plotted in Fig. 4.3.4. Due to excessive computing cost (35,000 CPU second/iteration in a PRIME 750), the algorithm is terminated after the 22nd iteration, after which one may expect a series of small design changes that lead to an optimum.

Figure 4.3.4 Cost Function History

The shape given in Fig. 4.3.5 is the 22nd improved design, with a 36% cost reduction. Maximum violation is reduced from 0.1140 to 0.0035, and the norm of the direction vector is reduced from 0.1170 to 0.021. The design process shows the following trend: Beam height changes slightly, except in Ω_2^4 and Ω_2^{10}, where height increases considerably. Beam depth generally decreases, except in Ω_2^4 and Ω_2^{10}. The beam stiffners move inward (see Fig. 4.3.5.b), resulting in decreases in plate thickness in patches Ω_1^1, Ω_1^2, Ω_1^4, and Ω_1^6. The plate elements in the remaining patches are adjusted in thickness, to compensate for beam movement. Plate elements on the free boundary tend to approach the lower bound.

4.3.3 Discussion

The domain approach for shape design sensitivity analysis yields excellent results given in Table 4.3.1. Accuracy problems arise, however, in the same analysis result using the boundary approach in Ref. 22. The reasons for poor sensitivity are partly due to the nature of the boundary approach, which requires accurate information along the interfaces, and partly due to the design velocity field used in the analysis. Test results of Chapter 3 and Table 4.3.3 demonstrate that the regularity requirement of the design velocity field must be met. Otherwise, singular behavior should be considered at the interfaces.

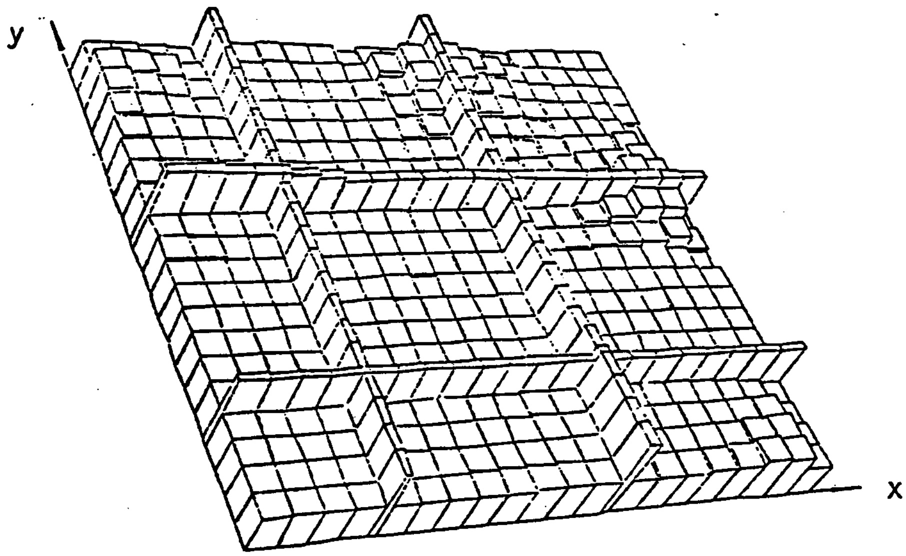

(a) Perspective View

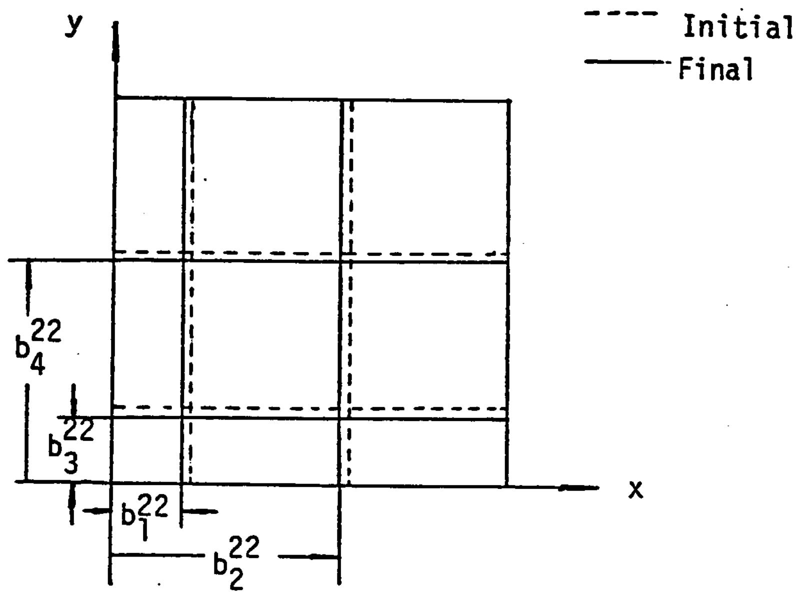

(b) Beam Positions

Figure 4.3.5 Shape of Built-Up Structure at Twenty-Second Iteration

V. NUMERICAL EVALUATION OF THE BOUNDARY-LAYER APPROACH

5.1 Introduction

As outlined in Section 2.3, the purpose of establishing a boundary-layer within the domain is two fold:

(i) Direct control over the velocity field within the domain, and

(ii) Reduce computing cost, without sacrificing accuracy of the domain approach.

In this chapter, two examples are solved by the boundary-layer approach. The first example is a simple interface problem, composed of two plane elastic plates with different material properties. This simple example shows the efficiency and reliability of the boundary-layer approach, compared to the boundary approach.

The second example is a fillet. The idea of velocity element is tested in conjunction with a B-spline boundary curve. Using B-spline functions, design velocity along the outer bounding surface Γ (see Section 2.3) is obtained. Design velocity within the boundary-layer is then found using the velocity element idea.

5.2 A Plane Stress Interface Problem

For elliptic boundary-value problems, singularities may occur when the boundary or the data is not smooth. The latter type of singularity may arise in interface problems such as elasticity problems with composite materials. Shape design sensitivity analyses are performed on examples of this kind using the boundary-layer approach and results are compared to the domain and boundary approaches to show good performance of the boundary-layer method. This problem was studied by Yang and Choi [23], using the boundary approach.

5.2.1 System Discription and Formulation

A plane elasticity problem that is composed of two plane elastic plate components with different material properties is chosen to be analyzed. The major concerns are: (i) To perform shape design sensitivity analysis with $E_2/E_1 = 7.65$, using the boundary-layer approach, and to show effectivness of the boundary-layer approach by comparing results obtained by boundary and domain approaches. Young's modulus is then changed to $E_2/E_1 = 500$, to evaluate validity of the boundary-layer approach under a severe condition. (ii) To see the effect of mesh refinement on singular behavior, using the boundary-layer approach.

The geometry of the problem studied is shown in Fig. 5.2.1. The domain is the union of sub-domains Ω_1 and Ω_2, with material properties are given in Table 5.2.1.

Table 5.2.1 Material Properties of Interface Problem

i	E_i	ν_i
Ω_1	2.3 GPa	0.3
Ω_2	17.6 GPa	0.3

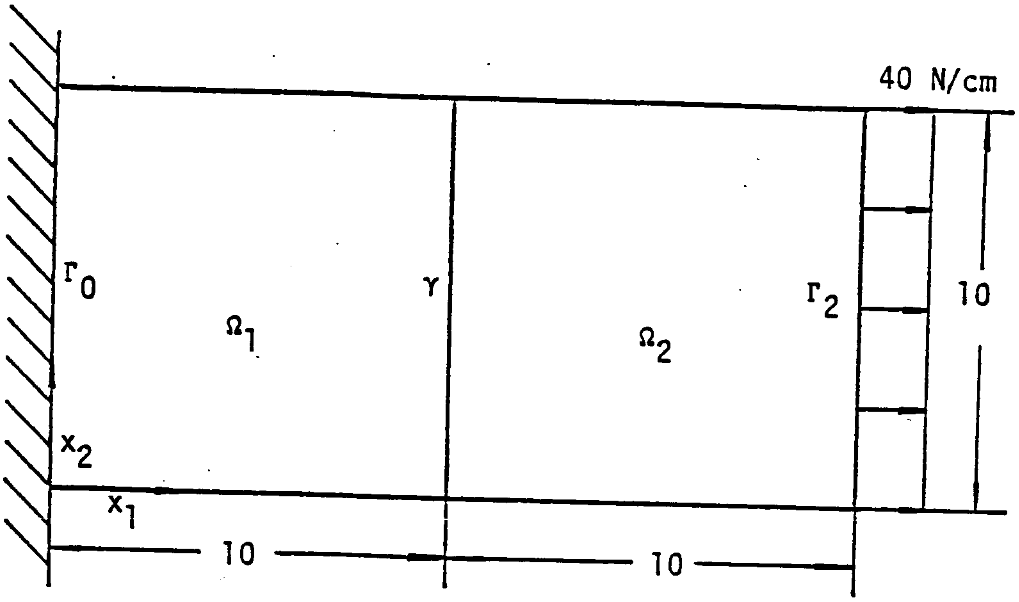

Figure 5.2.1 Geometry of Interface Problem (Length in [cm])

The space of kinematically admissible displacement field is

$$Z = \{z = (z_1, z_2) \in [H^1(\Omega^1)]^2 \times [H^2(\Omega_2)]^2:$$

$$z_1^1 = z_2^1 = 0, \ x \in \Gamma_0, \ z_i^1 = z_i^2, \ i = 1, 2, \ x \in \gamma\}$$

where Γ_0 is the fixed end and γ is the interface.

Applying the design component idea, one obtains, using Eqs. 2.2.20, 2.2.36, and 2.2.37,

$$a(\dot{z}, \bar{z}) = \sum_m \{\iint_{\Omega_m} \sum_{i,j} [\sum_{k,\ell} C^m_{ijk\ell} (\nabla z^m_k \cdot V^m_\ell) \, d\Omega$$

$$+ \iint_{\Omega_m} \sum_{i,j} [\sigma_{ij}(z^m) (\nabla z^m_i \cdot V^m_j)] \, d\Omega$$

$$- \iint_{\Omega_m} [\sum_{i,j} \sigma_{ij}(z^m) \, \epsilon_{ij} (\bar{z}^m) (\nabla \cdot V^m) \, d\Omega\} \qquad (5.2.1)$$

A stress constraint of the following type is considered:

$$\psi = \iint_{\Omega_q} \phi(\sigma(z^q))\, M_p \, d\Omega \tag{5.2.2}$$

where M_p is a characteristic function on test region $\Omega^p \subset \Omega_q$ and ϕ is the von Mises yield criterion,

$$\phi = [\sigma_{11}{}^2 + \sigma_{22}{}^2 + 3\,\sigma_{12}{}^2 - \sigma_{11}\,\sigma_{22}]^{1/2}$$

The variation of the constraint functional of Eq. 5.2.2 is, using Eqs. 2.2.37, 2.2.41, the last term of Eq. 2.2.45 and Eq. 5.2.1,

$$\begin{aligned}
\psi' = \sum_{m=1}^{2} \{ & \iint_{\Omega_m} \sum_{i,j} [\sum_{k,\ell} C^m_{ijk\ell}\, (\nabla z^m_k \cdot V^m_\ell)\, \varepsilon_{ij}(\lambda^m)]\, d\Omega \\
& + \iint_{\Omega_m} \sum_{i,j} [\sigma_{ij}(z^m)(\nabla \lambda^m_i \cdot V^m_j)]\, d\Omega \\
& - \iint_{\Omega_m} [\sum_{i,j} \sigma_{ij}(z^m)\, \varepsilon_{ij}(\lambda^m)]\, (\nabla \cdot V^m)\, d\Omega \} \\
& - \iint_{\Omega_q} [\sum_{i,j} \{\sum_{k,\ell} \frac{\partial \phi}{\partial \sigma_{ij}} (z^q)\, C^q_{ijk\ell}\, (\nabla z^q_k \cdot V^q_\ell)\}\, M_p]\, d\Omega \\
& + \iint_{\Omega_q} \phi\, (\nabla \cdot V^q)\, M_p\, d\Omega - \iint_{\Omega_q} \phi\, M_p\, d\Omega \iint_{\Omega_q} (\nabla \cdot V^q)\, M_p\, d\Omega
\end{aligned} \tag{5.2.3}$$

The plate of Fig. 5.2.1 is discretized into a 32-element, 121-node finite element model, in which 8-node isoparametric finite elements are used.

5.2.2 SDSA of a Interface Problem Using Boundary-layer Approach

For a body of given geometry there are a large number of possible boundary-layers some of which are better than others, from the viewpoint of accuracy and economy. It is difficult to estmate the size and location of the best boundary-layers in advance. They can be determined by analyzing the state and/or applying a test shape design sensitivity analysis.

The boundary-layer is chosen to include elements 13 thru 20 in Fig. 5.2.2. The design variable b for this case is distance between node 51 and node 65 in Fig. 5.2.2. Consequently, regions outside the boundary layer remain unchanged. Numerical results with a 3% design change are shown in Table 5.2.2 for the boundary-layer approach and in Table 5.2.3 for the boundary approach. Due to symmetry, the lower half of shape design sensitivity analysis results are shown. One can see from these results that the boundary-layer approach gives excellent results, whereas accuracy of the boundary approach is not acceptable. The poor design sensitivity obtained with the boundary approach is caused by

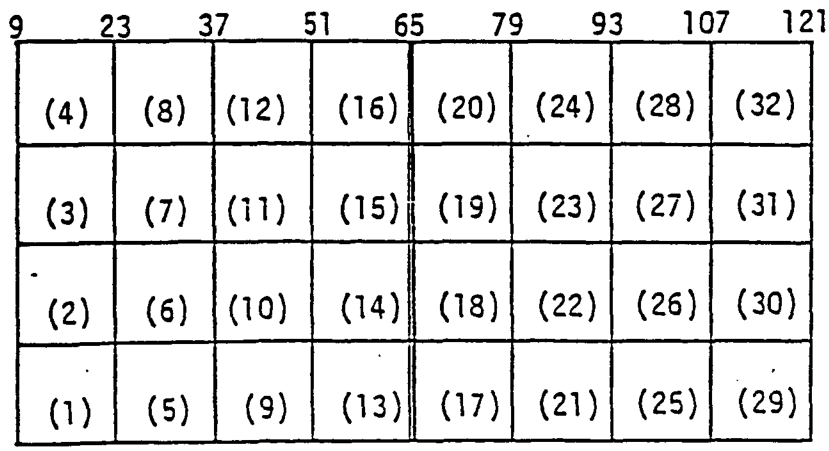

Figure 5.2.2 32-Element Coarse Model

unsatisfactory finite element analysis on the interface, due to an abrupt change in material properties, since the boundary approach requires integration over the interface. Note that, for the boundary approach, the best possible techniques, such as projection from the Gauss points to the boundary [23], are used to evaluate data on the interface. One can avoid data evaluation at the interface by using the boundary-layer (also domain) approach and obtain accurate sensitivity results. This can be of great advantage for complex problems with singular behavior along interfaces. In Table 5.2.4, numerical results with a 3% design change for the domain apporach are given. The design variable for this case is the distance between node 9 and node 65 in Fig. 5.2.2. Note that design variables are not the same for boundary-layer and domain approaches. Notice that thickening the boundary-layer in this problem does not significantly improve results.

Table 5.2.2 SDSA Result of the Coarse Model with 4 - 4 Elements in Each Boundary-Layer (E_2/E_1 = 7.65)

Elt #	Von Mises Stress OLD	NEW	Actual Change	Predict Change	Ratio x 100 %
1	393.013040	393.079670	0.066630	0.067700	101.608
2	364.378670	364.295420	-0.083250	-0.084120	101.047
5	388.075140	388.203440	0.128300	0.129160	100.674
6	402.269030	402.196330	-0.072700	-0.071260	98.027
9	386.434610	386.476870	0.042270	0.041030	97.078
10	407.146120	407.465710	0.319600	0.329540	103.113
13	388.596340	388.703000	0.106660	0.108340	101.578
14	379.042760	379.524870	0.482100	0.485900	100.787
17	441.685240	442.170080	0.484840	0.476150	98.207
18	424.058200	425.317170	1.258970	1.236360	98.204
21	424.190150	424.442700	0.252540	0.256800	101.685
22	378.854330	378.994590	0.140250	0.119020	84.861
25	407.715280	407.991050	0.275770	0.272480	98.807
26	387.873040	387.597780	-0.275260	-0.275400	100.049

Table 5.2.2 continued

29	400.610140	400.625710	0.015570	0.015430	99.059
30	394.617050	394.454610	-0.162440	-0.161040	99.138

Table 5.2.3 SDSA Result of the Coarse Model Using Boundary Approach (E_2/E_1 = 7.65)

Elt #	von Mises Stress OLD	NEW	Actual Change	Predict Change	Ratio x 100 %
1	393.01304	393.17922	0.16618	0.20403	122.77621
2	364.37867	364.76664	0.38796	0.67218	173.25764
5	388.07514	388.36215	0.28701	0.56684	197.49962
6	402.26903	402.83406	0.56503	0.42080	74.47325
9	386.43461	386.84976	0.41515	-0.08520	-20.52248
10	407.14612	407.48249	0.33637	0.14159	42.09417
13	388.59634	388.95414	0.35780	-0.53089	-148.37419
14	379.04276	379.25247	0.20971	-1.90134	-906.64762
17	441.68524	442.25032	0.56507	-13.85905	-2452.60502
18	424.05820	425.22910	1.17089	-13.63066	-1164.12453
21	424.19015	424.70840	0.51825	-0.21408	-41.30779
22	378.85433	378.97497	0.12064	0.76770	636.37320
25	407.71528	408.23368	0.51840	0.49878	96.21538
26	387.87304	387.32342	-0.54962	-0.48837	88.85661
29	400.61014	400.60112	-0.00903	0.01423	-157.65640
30	394.61705	394.00702	-0.61003	-0.57794	94.73960

Table 5.2.4 SDSA Result of the Coarse Model Using Domain Approach (E_2/E_1 = 7.65)

Elt #	von Mises Stress OLD	NEW	Actual Change	Predict Change	Ratio x 100 %
1	393.013040	393.179220	0.166180	0.179540	108.036
2	364.378670	364.766640	0.387960	0.378400	97.535
5	388.075140	388.362150	0.287010	0.286710	99.898
6	402.269030	402.834060	0.565030	0.596340	105.540
9	386.434610	386.849760	0.415150	0.417480	100.562
10	407.146120	407.482490	0.336370	0.368570	109.573
13	388.596340	308.954140	0.357800	0.375490	104.940
14	379.042760	379.252470	0.209710	0.201590	96.125
17	441.685240	442.250320	0.565070	0.570690	100.994
18	424.058200	425.229100	1.170890	1.128710	96.397
21	424.190150	424.708400	0.518250	0.539190	104.042
22	378.854330	378.974970	0.120640	0.063960	53.017
25	407.715280	408.233680	0.518400	0.517100	99.749
26	387.873040	387.323420	-0.549620	-0.560830	102.040

Table 5.2.4 continued

29	400.610140	400.601120	-0.009030	-0.002980	33.025
30	394.617050	394.007020	-0.610030	-0.585290	95.945

Next, to test validity of the boundary-layer approach, Young's modulus is changed to $E_1 = 0.20 \times 10^6$ and $E_2 = 1.00 \times 10^8$ for Ω_1 and Ω_2, respectively. In other words, the ratio between E_2 and E_1 is raised to 500, from 7.65, to check a more severe condition. Design sensitivity results are given in Table 5.2.5. Accuracy of design sensitivity is still acceptable. For elements 9 and 22, accuracy is marginal. However, the magnitude of actual change for these elements is small, so finite differences may not be correct. Numerical results obtained by the boundary approach are given in Table 5.2.6, which indicates that worse results may arise if the ratio E_2/E_1 increases.

Table 5.2.5 SDSA Result of the Coarse Model with 4 - 4 Elements in Each Boundary-Layer (E_2/E_1 = 500)

Elt #	Von Mises Stress OLD	Von Mises Stress NEW	Actual Change	Predict Change	Ratio x 100 %
1	392.305570	392.393590	0.088020	0.089260	101.402
2	365.243520	365.143840	-0.099670	-0.100470	100.798
5	386.631130	386.771990	0.140860	0.141380	100.367
6	402.936370	402.898860	-0.037520	-0.034770	92.675
9	386.580370	386.563300	-0.017060	-0.020160	118.181
10	403.053380	403.582140	0.528760	0.541500	102.410
13	392.165070	392.154620	-0.010460	-0.010330	98.844
14	365.554090	366.176380	0.622290	0.625520	100.518
17	477.041220	478.185420	1.144200	1.119430	97.835
18	440.116980	442.560250	2.443270	2.392580	97.925
21	442.638980	443.092150	0.453170	0.464520	102.503
22	362.566640	362.675590	0.108950	0.071170	65.322
25	412.834660	413.321420	0.486760	0.480000	98.611
26	379.905050	379.413550	-0.491490	-0.490330	99.763

Table 5.2.5 continued

29	401.088180	401.118770	0.030590	0.030310	99.078
30	391.196160	390.922130	-0.274030	-0.271580	99.106

Table 5.2.6 SDSA Result of the Course Model Using Boundary Approach (E_2/E_1 = 500)

Elt #	von Mises Stress OLD	NEW	Actual Change	Predict Change	Ratio x 100 %
1	392.30557	392.54946	0.24389	0.26360	108.07921
2	365.24352	365.56549	0.32197	0.61127	189.85235
5	386.63113	386.95951	0.32838	0.60857	185.32250
6	402.93637	403.56356	0.62719	0.41597	66.32254
9	386.58037	386.91161	0.33124	-0.46177	-139.40854
10	403.05338	403.67621	0.62283	0.25995	41.73644
13	392.16507	392.41381	0.24874	-0.97467	-391.85058
14	365.55409	365.87331	0.31923	-1.70688	-534.69096
17	477.04122	478.28537	1.24415	-999.01813	-80297.17435
18	440.11698	442.55272	2.43574	-995.38437	-40865.88759
21	552.63898	443.60941	0.97043	55.21655	5689.89566
22	362.56664	362.60856	0.04192	65.58310	156445.07974
25	412.83466	413.76383	0.92917	-1.39687	-150.33495
26	379.90505	378.94170	-0.96335	16.78425	-1742.28044
29	401.08818	401.08822	0.00004	1.93765	53656.13681
30	391.19616	390.18924	-1.00692	-3.09688	307.55910

5.2.3 Effect of Mesh Refinement

As stated earlier, there exists a singularity along the interface, due to an abrupt change of material properties accross the interface γ. It is known that mesh refinement is an effective way of dealing with singularities. The plate is discretized into a 128-element, 433-node refined finite element model, which has 832 active degrees-of-freedom. The type of finite element is not changed. Young's modulus is 0.20×10^6 and 1.00×10^8 for Ω_1 and Ω_2, respectively, which gives E_2/E_1 = 500.

As a test of the refined model, 16 elements are assigned to the boundary-layer, which means that the thickness of the boundary-layer is half of that for the coarse model (4 elements in Ω^1 and 4 elements in Ω^2). Shape design sensitivity results are given in Table 5.2.7, due to a 3% change in design variables. Results given in Table 5.2.7 show very good agreement between predicted change ψ' and actual change $\Delta\psi$, except in elements 27 and 74. However, note that the actual change for these elements is smaller than for others and may not accurate.

Table 5.2.7 SDSA Result of the Refined Model with 8 - 8 Elements in Each Boundary-Layer (E_2/E_1 = 500)

Elt #	Von Mises Stress OLD	Von Mises Stress NEW	Actual Change	Predict Change	Ratio x 100 %
1	422.968950	423.030780	0.061830	0.062350	100.846
2	370.248170	370.256580	0.008400	0.008460	100.716
3	353.546740	353.513190	-0.033550	-0.033760	100.631
4	349.312770	349.256790	-0.055990	-0.056320	100.588
9	391.927430	392.016470	0.089030	0.089590	100.620
10	390.900270	390.912700	0.012430	0.012510	100.601
11	382.152430	382.112240	-0.040190	-0.040310	100.300
12	377.526930	377.461990	-0.064940	-0.065110	100.262
17	376.610900	376.723970	0.113070	0.113540	100.416
18	396.657330	396.671200	0.013870	0.013920	100.394
19	399.654010	399.620250	-0.033760	-0.033610	99.559
20	398.967700	398.918750	-0.048960	-0.048660	99.384
25	373.940010	374.064670	0.124650	0.124760	100.083
26	396.719880	396.732840	0.012960	0.012980	100.143
27	406.807520	406.809000	0.001480	0.002230	151.212
28	409.659310	409.676590	0.017270	0.018530	107.256
33	373.926350	374.018230	0.091880	0.090960	99.002
34	396.718570	396.728700	0.010130	0.010260	101.351
35	406.839680	406.937690	0.098010	0.099980	102.016
36	409.713020	409.882140	0.169120	0.171800	101.587
41	376.556490	376.497720	-0.058780	-0.062680	106.633
42	396.653040	396.687610	0.034570	0.036180	104.651
43	399.763400	400.072850	0.309460	0.313430	101.284
44	399.139530	399.561830	0.422300	0.426120	100.906
49	391.670150	391.060950	-0.609200	-0.619550	101.699
50	390.953600	391.272470	0.318870	0.326640	102.436
51	382.375090	383.034650	0.659560	0.664520	100.753
52	377.826960	378.521860	0.694910	0.697740	100.408
57	422.383440	421.874110	-0.509330	-0.512000	100.524
58	370.378660	370.824220	0.445560	0.448860	100.742
59	353.887750	354.289930	0.402180	0.402300	100.029

Table 5.2.7 continued

60	349.700820	350.069920	0.369100	0.369160	100.014
65	541.075820	542.298610	1.222780	1.189130	97.248
66	477.244240	479.974620	2.730380	2.678890	98.114
67	467.075570	468.562640	1.487070	1.475510	99.223
68	468.364240	469.681620	1.317370	1.311190	99.530
73	512.541210	512.828520	0.287310	0.309710	107.797
74	393.697000	393.893700	0.196690	0.157320	79.984
75	389.864860	391.207420	1.342560	1.314160	97.885
76	394.797640	396.408680	1.611030	1.590090	98.700
81	477.399940	478.347540	0.947600	0.944510	99.674
82	404.565300	404.307630	-0.257670	-0.252210	97.882
83	370.947110	371.020010	0.072890	0.063110	86.574
84	363.098310	363.514950	0.416640	0.403200	96.774
89	451.214570	451.926190	0.711620	0.709130	99.650
90	406.665410	406.678550	0.013140	0.014770	112.373
91	374.694670	374.499580	-0.195090	-0.196570	100.760
92	360.740810	360.598020	-0.142790	-0.147740	103.463
97	429.574850	430.053980	0.479140	0.476340	99.417
98	405.132400	405.197000	0.064600	0.064790	100.304
99	382.155770	381.964630	-0.191140	-0.190990	99.922
100	369.595660	369.321610	-0.274060	-0.275070	100.371
105	414.632090	414.893470	0.261380	0.259630	99.332
106	402.520380	402.565190	0.044810	0.044580	99.484
107	388.544580	388.401100	-0.143480	-0.143100	99.738
108	380.039180	379.800650	-0.238530	-0.238190	99.856
113	405.031330	405.130580	0.099250	0.098480	99.227
114	399.987550	399.990320	0.002770	0.002710	98.007
115	392.712790	392.605950	-0.106830	-0.106370	99.568
116	388.068180	387.898250	-0.169930	-0.169270	99.612
121	400.394620	400.402900	0.008280	0.008210	99.169
122	397.935420	397.894640	-0.040780	-0.040480	99.267
123	394.037150	393.930650	-0.106510	-0.105830	99.365
124	391.373530	391.225420	-0.148110	-0.147240	99.411

5.2.4 Discussion

The results given in this section clearly show that the boundary approach may have considerble difficulties in handling problems with singular characteristics. The accuracy of the boundary approach rapidly deteriorates in the vicinity of a singularity. On the other hand, the boundary-layer approach can give acceptable design sensitivity results throughout the domain.

For this specific problem, 56 per cent of cpu time is saved by using the boundary-layer approach, instead of the domain approach, without sacrificing accuracy of design sensitivity.

Mesh refinement is one of the techniques to deal with singular problems. It is confirmed that one can get a similar result with smaller boundary-layer by introducing a refined model.

5.3 Fillet Problem

5.3.1 Introduction

Finding the best shape of a fillet in a tension member has attracted many engineers with different methods. Quite recently, Yang and Choi [23] studied the problem using the boundary approach and smooth boundary representation by polynomial splines.

In this section, shape design sensitivity analysis of a fillet is performed with the boundary-layer approach of SDSA and B-spline boundary repesentation. The velocity element idea is also used to find the velocity and derivative of velocity in the boundary-layer.

Numerous tests show that the boundary approach to SDSA may be adequate for component design (without singularity) but may not be satisfactory for built-up structures. The boundary approach to SDSA yields excellent shape design sensitivity analysis results for this fillet problem, using 8-noded isoparametric finite elements, numerical integration based on Gauss point data, and polynomial spline boundary representation [23]. The major concern here is to test validity of velocity approximation by velocity element and boundary approximation by B-spline functions, in the boundary-layer approach to SDSA.

Two designs (shapes) are chosen to be analyzed:

(i) The initial design with straight boundary.

(ii) The near optimum design of Ref. 23.

Shape design sensitivity analysis results are then compared to results obtained with the boundary approach.

5.3.2 System Discription and Formulation

Consider first a fillet with straight boundary, shown in Fig. 5.3.1. The design for this problem is the shape of varying boundary between points A and B, without moving these two points. Due to symmetry, only the upper half of a fillet is analyzed. Dimensions of the structure and applied loads are given in Fig. 5.3.1. The segment Γ_3 is the center-line of the fillet and Γ_2 is the uniformly loaded edge.

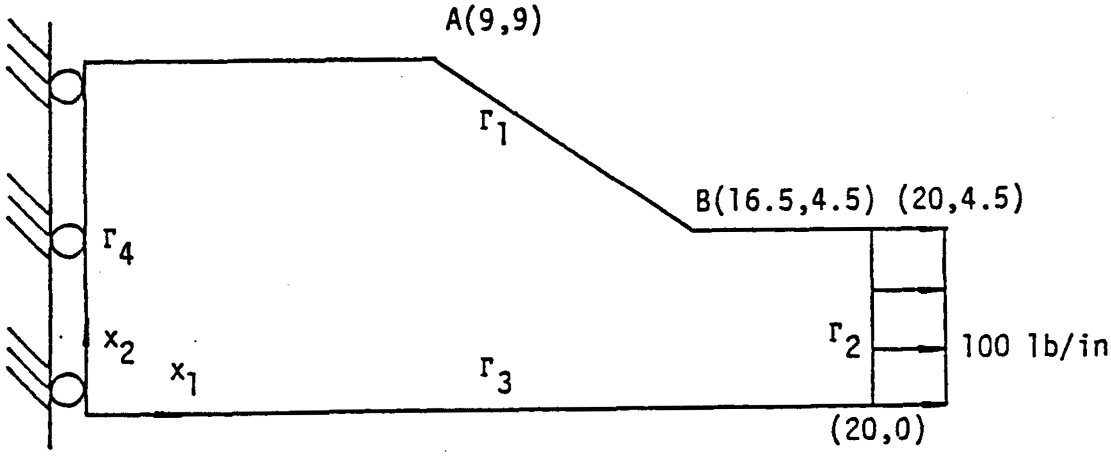

Figure 5.3.1 Fillet with Straight Boundary

Next, a design shown in Fig. 5.3.2 which is near the optimum of Ref. 23 is chosen to be analyzed. Notice the almost vertical slope near point A and horizontal slope near point B. This shape, especially near point A, causes distortion in the finite element mesh for analysis.

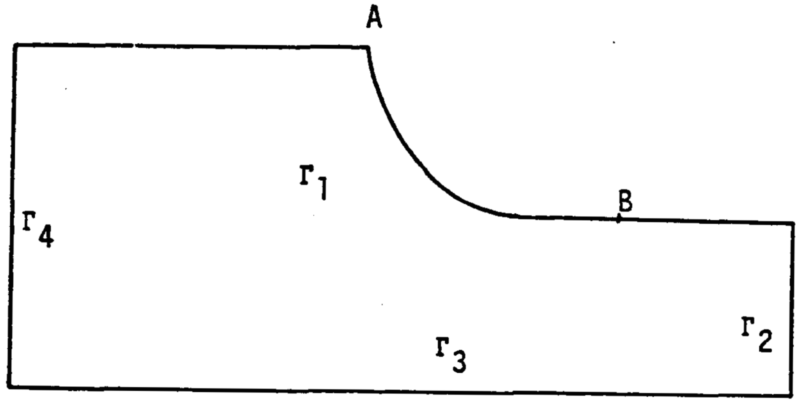

Figure 5.3.2 Fillet at Optimum

Kinematical boundary conditions are

$$\left.\begin{aligned} z_1 &= 0 \quad \text{for } x \in \Gamma_4 \\ z_2 &= 0 \quad \text{for } x \in \Gamma_3 \end{aligned}\right\} \tag{5.3.1}$$

where z_1 and z_2 denote displacements in x_1 and x_2 directions, respectively. The traction boundary condition is

$$T_i = \sum_{j=1}^{2} \sigma_{ij}(z)\, n_j \quad \text{for } x \in \Gamma_2 \tag{5.3.2}$$

where n_j is the (j)-th component of the outward normal to Γ_2 and T_1 and T_2 are x_1 and x_2 components of surface traction. The space of kinematically admissible displacements is defined as

$$Z = \{z = (z_1, z_2) \in [H^1(\Omega)]^2 : z_1 = 0,\ x \in \Gamma_4 \text{ and } z_2 = 0,\ x \in \Gamma_3\} \tag{5.3.3}$$

The variational form of the governing equation is

$$a(z, \bar{z}) = \ell(\bar{z}), \qquad \text{for all } \bar{z} \in Z \tag{5.3.4}$$

where

$$a(z, \bar{z}) = \iint_\Omega [\sum_{i,j} \sigma_{ij}(z)\ \varepsilon_{ij}(\bar{z})]\ d\Omega \tag{5.3.5}$$

$$\ell(\bar{z}) = \int_{\Gamma_2} [\sum_i T_i\ \bar{z}_i]\ d\Gamma \tag{5.3.6}$$

Stress constraint functionals of the following type are considered:

$$\psi = \iint_\Omega \phi\ (\sigma(z))\ M_p\ d\Omega \tag{5.3.7}$$

where M_p is a characteristic function and ϕ is von Mises yield stress. Following the procedure of Chapter 2, one obtains the shape design sensitivity formula

$$\psi' = \iint_\Omega \sum_{i,j} [\sum_{k,\ell} C_{ijk\ell}\ (\nabla z_k \cdot V_\ell)\ \varepsilon_{ij}\ (\lambda)]\ d\Omega$$

$$+ \iint_\Omega \sum_{i,j} [\sigma_{ij}\ (z)\ (\nabla \lambda_i \cdot V_\ell)]\ d\Omega$$

$$- \iint_\Omega [\sum_{i,j} \sigma_{ij}\ (z)\ \varepsilon_{ij}\ (\lambda)]\ (\nabla \cdot V)\ d\Omega$$

$$- \iint_{\Omega} \Big[\sum_{i,j} \Big\{\sum_{k,\ell} \frac{\partial \phi}{\partial \sigma_{ij}} (z)\; C_{ijk\ell}\; (\nabla z_k \cdot V_\ell)\Big\}\Big]\; M_p\; d\Omega$$

$$+ \iint_{\Omega} \phi\; (\nabla \cdot V)\; M_p\; d\Omega$$

$$- \iint_{\Omega} \phi\; M_p\; d\Omega \iint_{\Omega} (\nabla \cdot V)\; M_p\; d\Omega \tag{5.3.8}$$

where λ is the solution of the adjoint equation of Eq. 2.2.40, which can be rewritten for this problem as

$$a(\lambda, \overline{\lambda}) = \iint_{\Omega} \Big[\sum_{i,j} \Big\{\frac{\partial \phi}{\partial \sigma_{ij}} (z)\; \sigma_{ij}\; (\overline{\lambda})\Big\}\; M_p\Big]\; d\Omega, \qquad \text{for all } \overline{\lambda} \in Z$$

Notice that only first derivatives of the velocity field appear in Eq. 5.3.8, requiring only a C^0 design velocity field (see Chapter 3).

5.3.3 Numerical Test

The first step in using the boundary-layer approach to SDSA is to determine the best possible size and location of boundary-layer in the domain. For this purpose, one may discretize the whole domain into relatively fine mesh, for finite element analysis. Based on this analysis result, one can construct suitable size for the boundary-layer after isolating critical regions by measuring strain energy density [45] near the varied boundary. The boundary-layer chosen (27% of the total area) is shown in Fig. 5.3.3 with its (s,t) boundary-layer coordinate system. In Fig. 5.3.4, the finite element model with 319 elements and

1994 active degrees-of-freedom is shown. The element type used is an 8-noded isoparametric element.

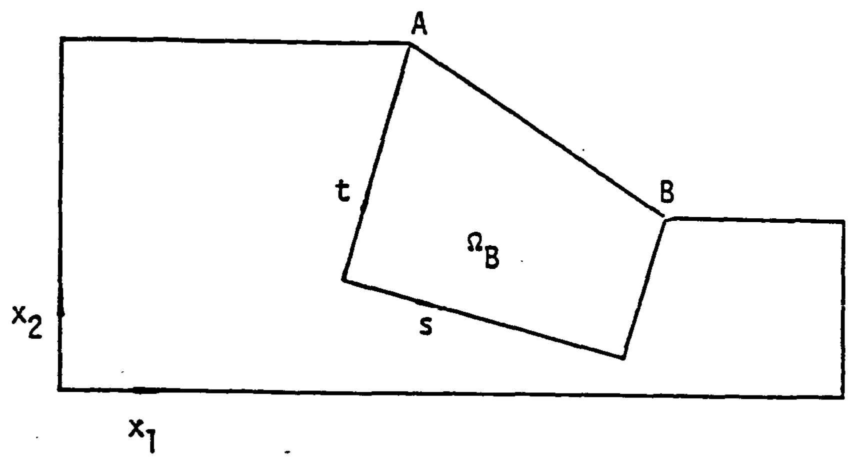

Figure 5.3.3 Boundary-Layer Ω_B and Boundary-Layer Coordinate System (s,t)

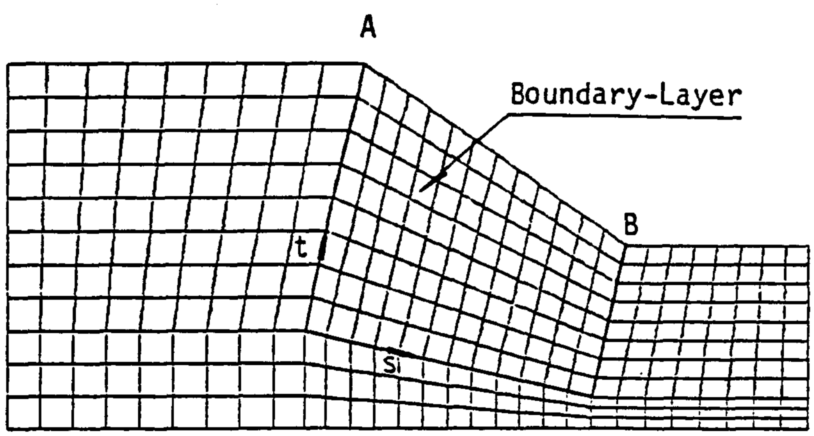

Figure 5.3.4 Finite Element Mesh for Fillet with Straight Boundary

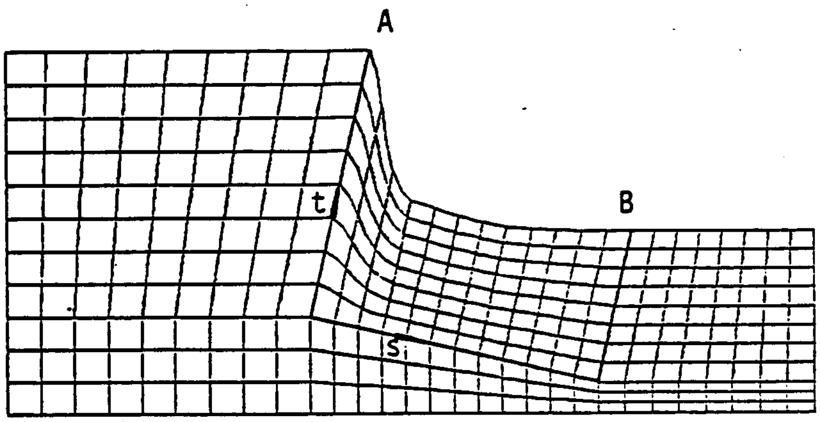

Figure 5.3.5 Finite Element Mesh for Fillet at Optimum

Velocity and derivative of velocity are evaluated using the velocity element idea explained in Section 2.3. Normally, a two dimensional velocity has two components, V^s and V^t the in s- and t-directions, respectively. However, the s-component of velocity is zero, since the domain is allowed to vary only in the t-direction. Note that $V^t_s = \partial V^t/\partial s$ is not necessarily zero in this velocity field. For velocity interpolation, velocity along the inner bounding surface γ and velocity along the outer bounding surface Γ must be specified. Velocity along γ is zero, since γ is not allowed to move. Velocity along Γ can be specified by perturbing the boundary Γ and V^t_s and V^t_t can be found using the isoparametric mapping given in Section 2.3. To evaluate the predicted change ψ', calculation is carried out over the boundary-layer Ω_B, due to zero velocity derivative in Ω Ω_B.

As noted previously, the ratio between predicted change ψ' and actual change $\Delta\psi$ times 100 is used as an accuracy measure of shape design sensitivity. The actual change $\Delta\psi$ is defined as $\Delta\psi = \psi(b^0+\delta b) = \psi(b^0)$, where b^0 is current design and δb is design change. Note that this accuracy measure may not give correct information when the actual change $\Delta\psi$ is very small, compared to $\psi(b^0)$, because the difference $\Delta\psi$ may lose precision, due to the subtraction $\psi(b^0+\delta b) - \psi(b^0)$.

Shape design sensitivity analysis results, with a 0.1% design perturbation, for a fillet with straight boundary are given in Table 5.3.1. For convenience, the same results are summarized in Fig. 5.3.6 graphically. One can see from Table 5.3.1 that very good accuracy can be obtained with the bounday-layer and velocity element approaches, except for elements 32, 105, 126, 133, 248, 256, 296, 301, 308 and 309. However, the magnitude of actual changes in the above elements is smaller than in others, so $\Delta\psi$ may lose precision. In Table 5.3.2, SDSA results obtained with the boundary approach [23] are listed and summarized graphically in Fig. 5.3.7. The boundary approach gives good design sensitivity results for this problem. Elements 28, 31, 33, 35, 37, 51, 52, 58, 73 thru 75, 79, and 84 show poorer accuracy than others, but this may be attributed to the smaller magnitudes of their actual changes.

In Tables 5.3.3 and 5.3.4, shape design sensitivity analysis results for a fillet at at near optimum design, which are obtained with 0.1% design perturbation by the boundary-layer and boundary approaches, respectively, are given. For comparison, summaries of these results are shown graphically in Figs. 5.3.8 and 5.3.9. Note that the shapes of the boundary are not exactly the same, partly because of differences in the design space and partly because of the different approximation methods used.

One can observe that better agreement with finite difference results is obtained with the boundary-layer approach than the boundary approach. However, one should consider the difference in gridding before interpreting results. Some elements (elements 9, 38, 237 thru 239, and 247 for the boundary-layer approach, and elements 25, 80, 84, 93, 98, 103 for boundary approach) show below marginal design sensitivities. However, for elements 9, 38, and 238 for the boundary-layer approach and element 25 for the boundary approach, the actual changes are smaller than for others. Poor sensitivities of elements 237, 239, and 247 in the boundary-layer approach and element 80 in the boundary approach may be caused by bad element aspect ratio (ratio between two adjcent sides for quadrilateral element).

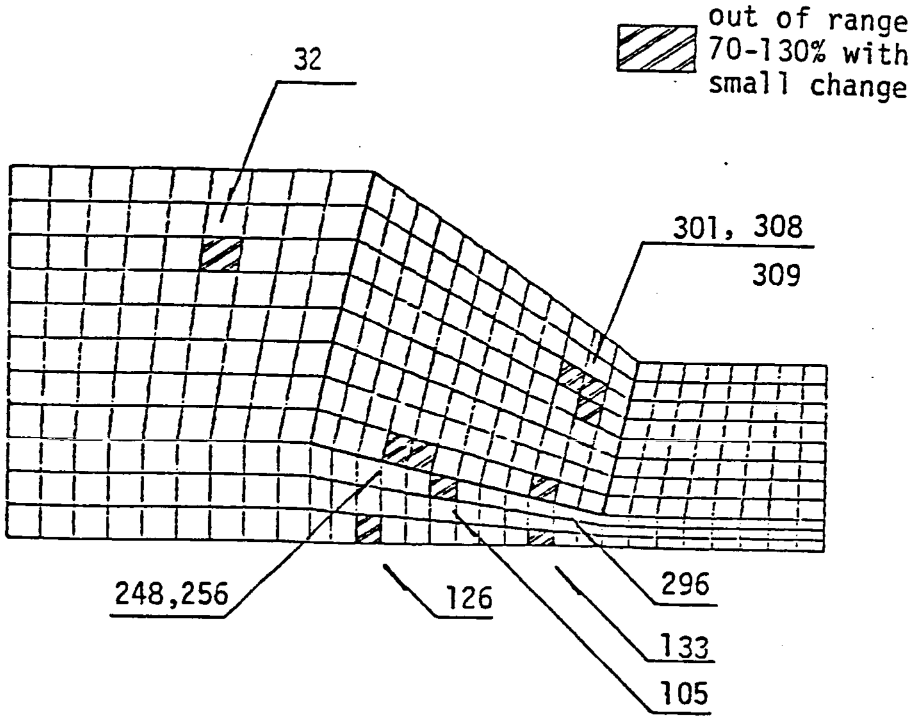

Figure 5.3.6 Summary of SDSA Result by Boundary-Layer Approach at Design with Straight Boundary

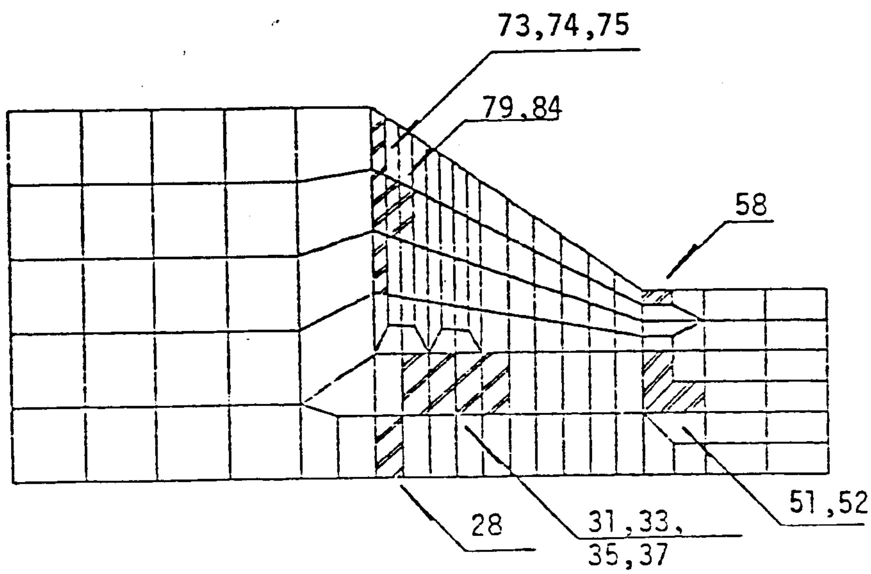

Figure 5.3.7 Summary of SDSA Result by Boundary Approach at Design with Straight Boundary

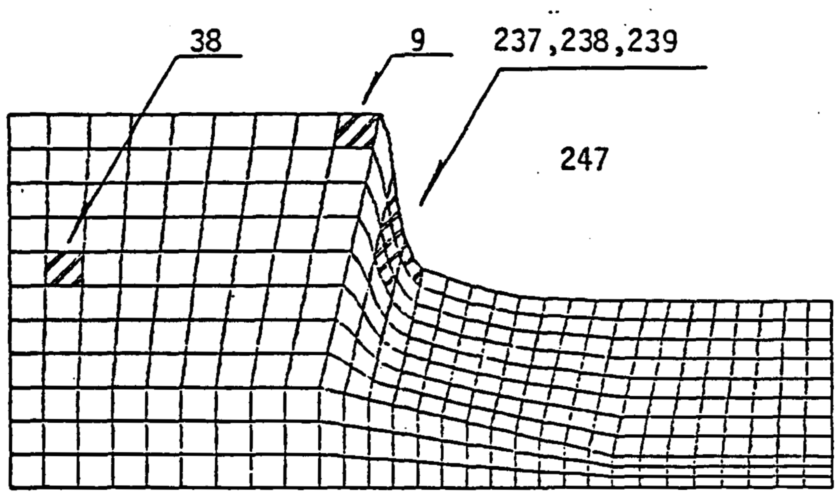

Figure 5.3.8 Summary of SDSA Result by Boundary-Layer Approach at Optimum of Ref. 23

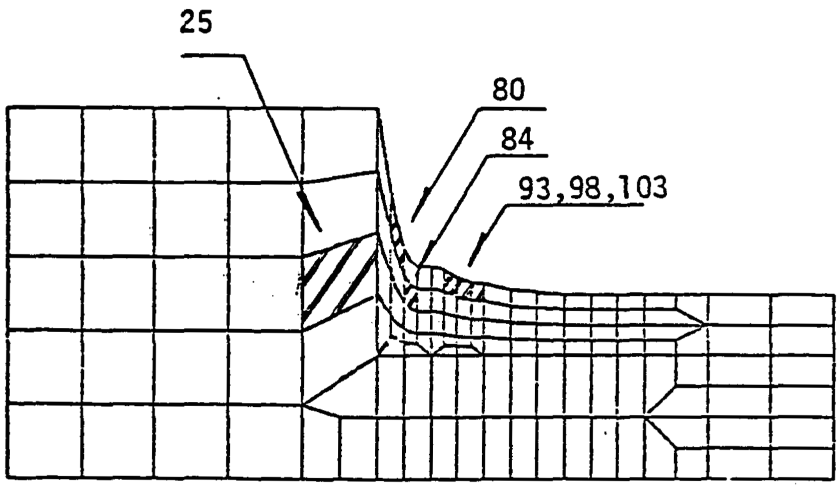

Figure 5.3.9 Summary of SDSA Result by Boundary Approach at Optimum of Ref. 23

Table 5.3.1 SDSA Result of Fillet with Straight Boundary Using Boundary-layer Approach

Elt #	von Mises Stress OLD	NEW	Actual Change	Predict Change	Ratio x 100 %
1	460.225940	460.350740	0.124800	0.125450	100.525
2	454.708990	454.843410	0.134420	0.135130	100.534
3	443.380220	443.534470	0.154250	0.155090	100.546
4	425.632450	425.817950	0.185500	0.186540	100.560
5	400.525300	400.755870	0.230570	0.231840	100.550
6	366.699190	366.990980	0.291790	0.293360	100.540
7	322.490570	322.866690	0.376120	0.377560	100.384
8	265.627070	266.100090	0.473020	0.474630	100.341
9	196.945070	197.554680	0.609620	0.608590	99.832
10	460.796120	460.901200	0.105080	0.105610	100.513
11	456.924230	457.034510	0.110290	0.110860	100.516
12	449.108250	449.228700	0.120450	0.121080	100.525
13	437.239910	437.374780	0.134870	0.135600	100.539
14	421.261880	421.413600	0.151720	0.152600	100.582
15	401.385180	401.552700	0.167530	0.168660	100.677
16	378.450110	378.623250	0.173140	0.175050	101.105
17	354.876240	355.040820	0.164580	0.168400	102.320
18	332.326810	332.461760	0.134950	0.144450	107.039
19	469.322020	469.395050	0.073030	0.073370	100.477
20	467.321060	467.394880	0.073820	0.074170	100.472
21	463.411370	463.486040	0.074680	0.075030	100.470
22	457.817900	457.891860	0.073960	0.074320	100.488
23	450.980340	451.049140	0.068800	0.069210	100.593
24	443.666440	443.721520	0.055080	0.055630	101.006
25	436.996520	437.024870	0.028350	0.029310	103.391
26	431.888270	431.878960	-0.009310	-0.007960	85.550
27	426.352600	426.313710	-0.038880	-0.039260	100.973
28	483.728570	483.762420	0.033850	0.033970	100.351
29	483.447360	483.478810	0.031450	0.031540	100.306
30	483.035810	483.061790	0.025970	0.026020	100.195
31	482.808910	482.824990	0.016080	0.016070	99.895
32	483.255410	483.255370	-0.000040	-0.000140	373.135
33	484.993980	484.970010	-0.023970	-0.024160	100.806
34	488.538740	488.483690	-0.055050	-0.055420	100.670
35	493.631890	493.545980	-0.085910	-0.086930	101.188
36	498.060230	497.961960	-0.098270	-0.101230	103.012
37	501.822780	501.815170	-0.007610	-0.007720	101.494
38	502.904160	502.892550	-0.011610	-0.011760	101.296
39	505.197510	505.177560	-0.019950	-0.020180	101.138
40	508.951300	508.918140	-0.033160	-0.033510	101.055
41	514.489690	514.438100	-0.051600	-0.052130	101.034
42	522.102190	522.027550	-0.074640	-0.075450	101.089
43	531.804730	531.705470	-0.099260	-0.100540	101.286
44	542.944160	542.825700	-0.118460	-0.120540	101.763
45	553.874000	553.752130	-0.121870	-0.125280	102.790

Table 5.3.1 continued

46	521.472370	521.424990	-0.047380	-0.047700	100.676
47	523.506730	523.455090	-0.051640	-0.052000	100.698
48	527.652710	527.592570	-0.060140	-0.060590	100.741
49	534.040910	533.968220	-0.072690	-0.073270	100.807
50	542.798360	542.709800	-0.088560	-0.089370	100.910
51	553.943880	553.837860	-0.106020	-0.107170	101.079
52	567.227450	567.105810	-0.121640	-0.123310	101.368
53	581.956790	581.826650	-0.130140	-0.132520	101.826
54	596.983620	596.857520	-0.126090	-0.129130	102.408
55	540.743510	540.660890	-0.082620	-0.083100	100.583
56	543.364530	543.278230	-0.086300	-0.086820	100.597
57	548.630270	548.536880	-0.093390	-0.093980	100.628
58	556.564430	556.461190	-0.103240	-0.103950	100.681
59	567.141110	567.026510	-0.114600	-0.115480	100.771
60	580.209020	580.083640	-0.125380	-0.126540	100.926
61	595.401290	595.268820	-0.132480	-0.134050	101.191
62	612.073960	611.941830	-0.132130	-0.134320	101.658
63	629.366870	629.245580	-0.121280	-0.124070	102.298
64	557.989290	557.877730	-0.111560	-0.112150	100.529
65	560.913630	560.799310	-0.114320	-0.114930	100.533
66	566.746520	566.627090	-0.119430	-0.120080	100.545
67	575.437510	575.311460	-0.126050	-0.126760	100.566
68	586.865110	586.732360	-0.132750	-0.133550	100.604
69	600.787730	600.650250	-0.137490	-0.138410	100.673
70	616.795760	616.658100	-0.137660	-0.138750	100.793
71	634.293440	634.162950	-0.130490	-0.131840	101.040
72	652.554930	652.440950	-0.113980	-0.115740	101.546
73	571.735950	571.602880	-0.133070	-0.133720	100.489
74	574.841290	574.706320	-0.134970	-0.135630	100.485
75	581.010830	580.872520	-0.138310	-0.138970	100.477
76	590.147510	590.005360	-0.142150	-0.142810	100.465
77	602.071270	601.926250	-0.145020	-0.145670	100.445
78	616.485820	616.340830	-0.144990	-0.145580	100.408
79	632.950610	632.810840	-0.139770	-0.140240	100.335
80	650.876510	650.749390	-0.127130	-0.127270	100.116
81	669.566560	669.461000	-0.105560	-0.105120	99.584
82	686.719050	686.639790	-0.079260	-0.076340	96.309
83	702.052950	702.001990	-0.050950	-0.050740	99.576
84	716.765290	716.745940	-0.019360	-0.016150	83.454
85	730.566360	730.579480	0.013130	0.017560	133.800
86	743.108560	743.152900	0.044340	0.049570	111.805
87	753.958250	754.028840	0.070590	0.076210	107.972
88	762.602790	762.689640	0.086850	0.092390	106.380
89	768.565320	768.652000	0.086690	0.091620	105.687
90	771.680660	771.744680	0.064020	0.067700	105.746
91	772.530720	772.547320	0.016600	0.018010	108.537
92	772.860930	772.813070	-0.047860	-0.040690	85.016
93	775.499150	775.383700	-0.115450	-0.115010	99.613
94	581.172890	581.025810	-0.147080	-0.147760	100.461
95	584.415920	584.267550	-0.148360	-0.149030	100.451

Table 5.3.1 continued

96	590.844670	590.694240	-0.150430	-0.151070	100.428
97	600.332060	600.179780	-0.152280	-0.152870	100.389
98	612.658950	612.506530	-0.152430	-0.152920	100.321
99	627.488410	627.339430	-0.148980	-0.149280	100.203
100	644.346030	644.206220	-0.139810	-0.139790	99.987
101	662.618950	662.495970	-0.122980	-0.122400	99.529
102	681.584770	681.487530	-0.097240	-0.095710	98.426
103	698.166420	698.098360	-0.068070	-0.066810	98.158
104	712.085750	712.047100	-0.038650	-0.036220	93.720
105	725.256790	725.250100	-0.006690	-0.003530	52.707
106	737.357500	737.383230	0.025730	0.029630	115.171
107	748.039730	748.095420	0.055690	0.060250	108.173
108	756.930640	757.009990	0.079350	0.084210	106.126
109	763.661810	763.753610	0.091800	0.096460	105.076
110	767.983580	768.071160	0.087580	0.091630	104.615
111	769.988690	770.050920	0.062230	0.064890	104.266
112	770.420260	770.435450	0.015180	0.017600	115.918
113	770.942640	770.895350	-0.047290	-0.042120	89.074
114	774.042640	773.930200	-0.112440	-0.109650	97.522
115	586.033940	585.879870	-0.154070	-0.154760	100.446
116	589.337690	589.182680	-0.155010	-0.155680	100.433
117	595.880190	595.723810	-0.156380	-0.157010	100.402
118	605.520130	605.362960	-0.157170	-0.157720	100.347
119	618.020110	617.864230	-0.155880	-0.156280	100.253
120	633.024260	632.873600	-0.150660	-0.150810	100.097
121	650.041680	649.902200	-0.139480	-0.139240	99.832
122	668.444960	668.324440	-0.120520	-0.119810	99.406
123	687.490560	687.397840	-0.092720	-0.091610	98.805
124	703.736710	703.674550	-0.062170	-0.060420	97.187
125	716.921560	716.889270	-0.032290	-0.029590	91.630
126	729.301040	729.300820	-0.000220	0.003490	-1612.521
127	740.540960	740.572820	0.031870	0.036040	113.102
128	750.298990	750.359950	0.060960	0.065380	107.240
129	758.235280	758.318450	0.083160	0.087640	105.387
130	764.055070	764.148790	0.093720	0.097940	104.501
131	767.616050	767.703700	0.087650	0.091250	104.108
132	769.123210	769.184410	0.061200	0.064710	105.725
133	769.384080	769.398430	0.014350	0.019870	138.484
134	770.011210	769.964370	-0.046840	-0.044700	95.419
135	773.332760	773.221910	-0.110850	-0.110090	99.317
136	1448.297520	1449.233560	0.936040	0.917880	98.060
137	1268.184480	1268.543660	0.359180	0.366160	101.942
138	1130.540300	1130.711710	0.171400	0.171080	99.814
139	1068.909820	1068.990310	0.080490	0.080890	100.494
140	1030.511320	1030.543650	0.032320	0.032360	100.122
141	1009.857070	1009.864820	0.007740	0.007790	100.636
142	1000.660140	1000.658720	-0.001420	-0.001400	98.583
143	999.751440	999.750850	-0.000590	-0.000590	99.354
144	1092.378200	1092.501350	0.123150	0.126220	102.492
145	1141.341490	1141.651140	0.309650	0.301950	97.513

Table 5.3.1 continued

146	1116.366540	1116.559930	0.193390	0.192710	99.650
147	1070.450880	1070.559520	0.108640	0.108120	99.518
148	1039.013640	1039.069870	0.056230	0.056030	99.657
149	1017.870040	1017.894610	0.024570	0.024480	99.645
150	1005.330910	1005.338100	0.007190	0.007170	99.628
151	1000.952770	1000.954730	0.001960	0.001950	99.455
152	944.428530	944.227510	-0.201020	-0.197880	98.440
153	1016.872820	1016.928380	0.055560	0.053600	96.471
154	1047.154970	1047.262080	0.107120	0.105380	98.374
155	1040.762720	1040.842750	0.080030	0.079120	98.864
156	1026.143840	1026.191470	0.047640	0.047190	99.072
157	1012.201320	1012.223240	0.021920	0.021730	99.111
158	1001.951340	1001.956380	0.005040	0.004980	98.753
159	998.551420	998.551320	-0.000100	-0.000110	115.988
160	877.729960	877.445410	-0.284540	-0.280700	98.650
161	930.708770	930.588760	-0.120010	-0.119410	99.503
162	976.693980	976.682190	-0.011790	-0.012760	108.229
163	997.395630	997.414200	0.018570	0.017740	95.523
164	1001.185310	1001.201330	0.016010	0.015540	97.052
165	998.165730	998.171100	0.005370	0.005140	95.848
166	993.803710	993.799250	-0.004450	-0.004520	101.417
167	993.120980	993.114430	-0.006540	-0.006540	100.005
168	838.605360	838.330050	-0.275310	-0.273860	99.472
169	878.283650	878.086450	-0.197200	-0.196280	99.531
170	922.658450	922.555240	-0.103210	-0.103330	100.112
171	954.996180	954.948440	-0.047740	-0.048160	100.869
172	972.785140	972.760140	-0.025000	-0.025310	101.246
173	980.678690	980.660200	-0.018490	-0.018640	100.790
174	983.469050	983.451060	-0.017990	-0.018010	100.115
175	985.818590	985.802660	-0.015930	-0.015890	99.760
176	814.601880	814.357350	-0.244520	-0.244830	100.128
177	845.254100	845.033510	-0.220590	-0.220120	99.787
178	884.327910	884.169940	-0.157970	-0.157680	99.814
179	920.186950	920.085500	-0.101460	-0.101430	99.977
180	946.544030	946.479370	-0.064650	-0.064690	100.053
181	963.335200	963.291460	-0.043750	-0.043740	99.991
182	972.897530	972.864850	-0.032680	-0.032620	99.823
183	977.974080	977.947770	-0.026320	-0.026220	99.643
184	799.235260	799.022610	-0.212650	-0.214550	100.891
185	824.044430	823.824910	-0.219530	-0.219410	99.946
186	858.174280	857.988980	-0.185290	-0.184780	99.725
187	894.063380	893.924960	-0.138420	-0.138020	99.707
188	925.067210	924.970220	-0.096990	-0.096720	99.725
189	948.303040	948.236740	-0.066300	-0.066120	99.719
190	963.451980	963.405710	-0.046270	-0.046120	99.667
191	970.750140	970.714190	-0.035950	-0.035800	99.569
192	789.360520	789.174080	-0.186440	-0.187450	100.544
193	810.413040	810.202820	-0.210220	-0.209700	99.756
194	840.834380	840.637890	-0.196490	-0.195660	99.580
195	875.712910	875.551790	-0.161110	-0.160360	99.535

Table 5.3.1 continued

196	909.089450	908.969210	-0.120240	-0.119700	99.551
197	936.656910	936.572990	-0.083920	-0.083560	99.569
198	955.989520	955.932300	-0.057220	-0.056970	99.569
199	964.999160	964.955570	-0.043590	-0.043380	99.518
200	784.883410	784.710260	-0.173150	-0.171700	99.161
201	804.257110	804.054090	-0.203020	-0.201970	99.483
202	832.799860	832.600760	-0.199100	-0.197920	99.407
203	866.826590	866.655860	-0.170740	-0.169770	99.435
204	900.998830	900.867220	-0.131610	-0.130900	99.464
205	930.551950	930.458790	-0.093150	-0.092690	99.499
206	951.988900	951.925760	-0.063140	-0.062840	99.520
207	961.875430	961.827710	-0.047720	-0.047480	99.493
208	783.555740	783.386870	-0.168870	-0.166950	98.860
209	802.474160	802.274170	-0.199990	-0.198430	99.219
210	830.318040	830.118870	-0.199160	-0.197820	99.324
211	863.854690	863.681020	-0.173670	-0.172600	99.382
212	898.100340	897.964690	-0.135650	-0.134870	99.427
213	928.233820	928.137120	-0.096690	-0.096180	99.470
214	950.374840	950.309290	-0.065550	-0.065220	99.500
215	960.532190	960.482710	-0.049480	-0.049220	99.482
216	782.904350	782.737510	-0.166840	-0.164330	98.499
217	801.600690	801.402240	-0.198450	-0.196580	99.060
218	829.102930	828.903800	-0.199130	-0.197680	99.274
219	862.393840	862.218770	-0.175060	-0.173930	99.353
220	896.665910	896.528290	-0.137620	-0.136810	99.409
221	927.078740	926.980290	-0.098450	-0.097920	99.455
222	949.564460	949.497710	-0.066750	-0.066410	99.489
223	959.852690	959.802330	-0.050360	-0.050100	99.477
224	670.357340	670.266400	-0.090940	-0.092620	101.848
225	647.393150	647.289780	-0.103380	-0.106480	102.999
226	614.436810	614.322390	-0.114420	-0.118610	103.661
227	569.515910	569.399920	-0.115980	-0.121590	104.839
228	510.326130	510.228900	-0.097230	-0.104350	107.328
229	433.622300	433.577820	-0.044480	-0.053090	119.345
230	332.650720	332.729660	0.078930	0.067910	86.038
231	186.625180	187.275810	0.650640	0.657360	101.033
232	687.402280	687.331930	-0.070350	-0.066830	94.999
233	666.179190	666.070870	-0.108320	-0.107570	99.302
234	634.965330	634.801550	-0.163780	-0.161900	98.849
235	591.514530	591.281560	-0.232970	-0.224400	96.322
236	533.462270	533.154440	-0.307830	-0.285740	92.826
237	458.177600	457.795030	-0.382560	-0.339060	88.629
238	361.999770	361.536920	-0.462850	-0.382380	82.614
239	241.168070	240.493170	-0.674900	-0.476450	70.595
240	704.068700	704.025000	-0.043710	-0.034120	78.056
241	685.025900	684.933850	-0.092050	-0.093270	101.331
242	656.184340	656.015490	-0.168850	-0.174150	103.141
243	614.986500	614.712580	-0.273920	-0.275940	100.736
244	558.997580	558.596120	-0.401460	-0.391720	97.574
245	486.457450	485.911060	-0.546380	-0.514040	94.081

Table 5.3.1 continued

246	397.035040	396.287820	-0.747210	-0.676680	90.560
247	297.264910	296.034610	-1.230300	-1.098780	89.310
248	720.164270	720.153150	-0.011120	-0.002650	23.873
249	703.962480	703.900730	-0.061750	-0.062260	100.837
250	678.496900	678.349260	-0.147640	-0.152610	103.364
251	640.872130	640.598130	-0.274010	-0.274280	100.101
252	588.516300	588.078790	-0.437510	-0.422240	96.508
253	520.391510	519.759280	-0.632230	-0.587400	92.910
254	438.721770	437.845400	-0.876370	-0.783140	89.362
255	353.044990	351.806240	-1.238760	-1.081230	87.284
256	735.395460	735.416970	0.021510	0.030350	141.127
257	722.864980	722.836150	-0.028830	-0.029460	102.201
258	702.100480	701.978940	-0.121540	-0.125990	103.660
259	669.830210	669.559720	-0.270490	-0.269300	99.559
260	623.060850	622.583330	-0.477530	-0.457640	95.834
261	560.848400	560.123000	-0.725400	-0.670280	92.401
262	486.460930	485.466980	-0.993950	-0.883530	88.890
263	409.774860	408.517960	-1.256890	-1.067160	84.904
264	749.278720	749.330500	0.051790	0.061490	118.735
265	741.280000	741.287250	0.007250	0.006820	94.024
266	726.729480	726.645880	-0.083600	-0.087960	105.221
267	701.987890	701.740910	-0.246980	-0.244900	99.160
268	663.207990	662.710940	-0.497040	-0.473490	95.262
269	608.499530	607.691400	-0.808130	-0.743770	92.036
270	540.746160	539.636320	-1.109840	-0.982210	88.500
271	469.192550	467.863750	-1.328790	-1.113190	83.775
272	761.097080	761.171940	0.074860	0.085810	114.627
273	758.273260	758.316800	0.043540	0.043510	99.935
274	751.373400	751.343450	-0.029950	-0.034860	116.395
275	736.633490	736.448710	-0.184780	-0.183170	99.131
276	708.996200	708.531500	-0.464700	-0.438610	94.387
277	664.312760	663.453630	-0.859130	-0.786690	91.568
278	603.214220	601.965030	-1.249190	-1.106040	88.540
279	533.948210	532.473860	-1.474350	-1.237720	83.950
280	769.983920	770.066520	0.082590	0.095130	115.173
281	772.392380	772.462130	0.069740	0.070310	100.815
282	773.971660	774.002220	0.030560	0.024130	78.944
283	771.630890	771.553720	-0.077170	-0.079180	102.600
284	759.425100	759.092370	-0.332730	-0.308240	92.639
285	729.458080	728.638690	-0.819390	-0.739240	90.218
286	677.295650	675.882370	-1.413280	-1.260830	89.213
287	607.928490	606.174560	-1.753930	-1.496780	85.339
288	775.261310	775.326430	0.065120	0.079920	122.724
289	781.978100	782.045860	0.067760	0.069390	102.397
290	791.380310	791.447510	0.067200	0.058770	87.457
291	802.425940	802.464910	0.038970	0.029150	74.798
292	810.550440	810.456290	-0.094150	-0.083790	88.998
293	804.052270	803.530960	-0.521310	-0.445230	85.406
294	767.633290	766.126510	-1.506780	-1.303330	86.497
295	699.520850	697.222700	-2.298150	-2.059110	89.599

Table 5.3.1 continued

296	777.116790	777.133970	0.017180	0.033510	195.093
297	786.185880	786.207920	0.022040	0.025870	117.342
298	800.547980	800.586860	0.038880	0.031210	80.268
299	822.019170	822.089660	0.070490	0.054600	77.455
300	851.149510	851.243410	0.093890	0.079750	84.934
301	882.383610	882.365300	-0.018310	0.005780	-31.567
302	886.252760	885.452810	-0.799950	-0.651770	81.476
303	819.420130	816.000120	-3.420010	-3.101070	90.674
304	777.384530	777.329830	-0.054710	-0.033010	60.336
305	786.667390	786.603100	-0.064290	-0.051580	80.230
306	801.827370	801.759080	-0.068290	-0.066450	97.298
307	826.220540	826.160750	-0.059800	-0.068570	114.670
308	865.789770	865.770730	-0.019040	-0.040940	215.064
309	930.718850	930.769820	0.050980	0.020270	39.768
310	1009.672510	1009.414690	-0.257820	-0.221050	85.739
311	1029.763760	1027.087350	-2.676410	-2.076330	77.579
312	779.599730	779.469730	-0.130000	-0.134900	103.768
313	788.256700	788.097650	-0.159060	-0.162400	102.105
314	802.017030	801.817440	-0.199600	-0.200630	100.519
315	823.822100	823.566980	-0.255120	-0.255400	100.112
316	859.881480	859.553390	-0.328090	-0.325410	99.184
317	921.305750	920.881610	-0.424140	-0.411440	97.006
318	1057.980240	1057.591970	-0.388270	-0.353050	90.927
319	1355.168670	1356.577950	1.409280	1.341410	95.184

Table 5.3.2 SDSA Result of Fillet with Straight Boundary Using Boundary Approach

Elt #	von Mises Stress OLD	NEW	Actual Change	Predict Change	Ratio x 100 %
1	5.8472E 02	5.8462E 02	-9.8457E-02	-9.9620E-02	101.2
2	5.6118E 02	5.6110E 02	-7.6042E-02	-7.6976E-02	101.2
3	5.2143E 02	5.2140E 02	-3.1542E-02	-3.1994E-02	101.4
4	4.8035E 02	4.8038E 02	2.7311E-02	2.7583E-02	101.0
5	4.5909E 02	4.5916E 02	7.6280E-02	7.7319E-02	101.4
6	5.9974E 02	5.9964E 02	-1.0007E-01	-1.0126E-01	101.2
7	5.7453E 02	5.7445E 02	-8.2602E-02	-8.3568E-02	101.2
8	5.2974E 02	5.2970E 02	-4.3296E-02	-4.3837E-02	101.2
9	4.7817E 02	4.7820E 02	2.1408E-02	2.1646E-02	101.1
10	4.4347E 02	4.4356E 02	9.2272E-02	9.3390E-02	101.2
11	6.2817E 02	6.2807E 02	-9.6188E-02	-9.7491E-02	101.4
12	6.0042E 02	6.0033E 02	-8.8724E-02	-8.9666E-02	101.1
13	5.4726E 02	5.4719E 02	-6.4247E-02	-6.4827E-02	100.9
14	4.7586E 02	4.7586E 02	2.4702E-03	2.0327E-03	82.3
15	4.1061E 02	4.1073E 02	1.2390E-01	1.2605E-01	101.7
16	6.6601E 02	6.6594E 02	-7.5820E-02	-7.7574E-02	102.3

Table 5.3.2 continued

17	6.3572E 02	6.3564E 02	-7.9878E-02	-8.0915E-02	101.3
18	5.7357E 02	5.7349E 02	-7.8812E-02	-7.9284E-02	100.6
19	4.7770E 02	4.7765E 02	-4.0955E-02	-3.7159E-02	90.7
20	3.5786E 02	3.5803E 02	1.7009E-01	1.7004E-01	100.0
21	6.9710E 02	6.9705E 02	-4.6633E-02	-4.8954E-02	105.0
22	7.1825E 02	7.1822E 02	-2.1667E-02	-2.4437E-02	112.8
23	6.9661E 02	6.9658E 02	-3.4476E-02	-3.7337E-02	108.3
24	6.5764E 02	6.5758E 02	-5.1717E-02	-5.4135E-02	104.7
25	5.8102E 02	5.8096E 02	-5.8213E-02	-6.1250E-02	105.2
26	4.6113E 02	4.6109E 02	-3.5838E-02	-4.5165E-02	126.0
27	2.7831E 02	2.7853E 02	2.1711E-01	2.4585E-01	113.2
28	7.3320E 02	7.3320E 02	-5.5668E-04	-3.4957E-03	628.0
29	7.1372E 02	7.1371E 02	-1.4117E-02	-1.7536E-02	124.2
30	7.4496E 02	7.4498E 02	1.4907E-02	1.2083E-02	81.1
31	7.2683E 02	7.2683E 02	-2.6504E-03	-5.9254E-03	223.6
32	7.5486E 02	7.5489E 02	2.6403E-02	2.3951E-02	90.7
33	7.3979E 02	7.3980E 02	3.6352E-03	7.3813E-04	20.3
34	7.6261E 02	7.6264E 02	3.2185E-02	3.0361E-02	94.3
35	7.5330E 02	7.5331E 02	4.2699E-03	2.0049E-03	47.0
36	7.6786E 02	7.6789E 02	3.0237E-02	2.9227E-02	96.7
37	7.6679E 02	7.6679E 02	-8.2116E-05	-1.6278E-03	1982.3
38	7.7083E 02	7.7085E 02	1.8665E-02	1.8496E-02	99.1
39	7.8030E 02	7.8029E 02	-8.5100E-03	-9.4092E-03	110.6
40	7.7220E 02	7.7220E 02	-3.9166E-03	-3.3413E-03	85.3
41	7.9258E 02	7.9256E 02	-2.2806E-02	-2.3068E-02	101.2
42	7.7396E 02	7.7392E 02	-3.6666E-02	-3.5606E-02	97.1
43	8.0246E 02	8.0241E 02	-5.0694E-02	-5.0720E-02	100.1
44	7.7936E 02	7.7928E 02	-7.4859E-02	-7.3769E-02	98.5
45	8.1129E 02	8.1119E 02	-1.0150E-01	-1.0170E-01	100.2
46	7.9207E 02	7.9196E 02	-1.0919E-01	-1.0866E-01	99.5
47	8.2856E 02	8.2841E 02	-1.5614E-01	-1.5726E-01	100.7
48	8.1229E 02	8.1217E 02	-1.2628E-01	-1.2669E-01	100.3
49	8.7653E 02	8.7637E 02	-1.6071E-01	-1.6511E-01	102.7
50	9.6294E 02	9.6279E 02	-1.4614E-01	-1.5889E-01	108.7
51	1.0618E 03	1.0618E 03	-2.7731E-02	-4.2805E-02	154.4
52	1.1814E 03	1.1816E 03	1.9755E-01	1.3362E-01	67.6
53	1.4505E 03	1.4513E 03	8.0147E-01	9.8812E-01	123.3
54	8.4589E 02	8.4576E 02	-1.2561E-01	-1.2727E-01	101.3
55	8.4880E 02	8.4867E 02	-1.2924E-01	-1.3139E-01	101.7
56	8.7496E 02	8.7483E 02	-1.2866E-01	-1.3244E-01	102.9
57	9.4940E 02	9.4932E 02	-8.2362E-02	-9.0174E-02	109.5
58	1.0360E 03	1.0360E 03	2.1150E-02	9.9812E-03	47.2
59	1.1757E 03	1.1760E 03	2.7348E-01	2.8391E-01	103.8
60	9.0223E 02	9.0213E 02	-9.5021E-02	-9.7820E-02	102.9
61	9.1490E 02	9.1482E 02	-8.6615E-02	-8.9951E-02	103.9
62	9.4206E 02	9.4200E 02	-6.3294E-02	-6.7537E-02	106.7
63	9.8482E 02	9.8480E 02	-1.7413E-02	-2.1861E-02	125.5
64	1.0336E 03	1.0337E 03	4.7816E-02	4.6460E-02	97.2
65	1.0508E 03	1.0508E 03	6.4612E-02	7.4788E-02	115.7
66	9.5391E 02	9.5386E 02	-5.1860E-02	-5.5044E-02	106.1

Table 5.3.1 continued

67	9.6080E 02	9.6075E 02	-4.4736E-02	-4.7812E-02	106.9
68	9.7339E 02	9.7335E 02	-3.1269E-02	-3.3909E-02	108.4
69	9.8928E 02	9.8927E 02	-1.2528E-02	-1.4404E-02	115.0
70	1.0021E 03	1.0021E 03	2.5947E-03	2.7839E-03	107.3
71	1.0033E 03	1.0033E 03	5.4674E-03	5.5965E-03	102.4
72	6.5150E 02	6.5147E 02	-3.4835E-02	-4.3554E-02	125.0
73	5.7123E 02	5.7120E 02	-3.2074E-02	-5.0166E-02	156.4
74	4.3689E 02	4.3692E 02	2.8959E-02	-3.3072E-02	-114.2
75	2.3246E 02	2.3252E 02	5.2253E-02	1.4734E-01	282.0
76	6.8278E 02	6.8275E 02	-2.6929E-02	-2.9217E-02	108.5
77	6.5023E 02	6.5019E 02	-3.3505E-02	-3.9074E-02	116.6
78	5.8080E 02	5.8076E 02	-3.8434E-02	-4.5093E-02	117.3
79	4.4891E 02	4.4890E 02	-9.2676E-03	-2.1597E-02	233.0
80	2.5724E 02	2.5683E 02	-4.1053E-01	-3.9519E-01	96.3
81	6.9411E 02	6.9409E 02	-2.3410E-02	-2.6525E-02	113.3
82	6.5909E 02	6.5905E 02	-3.8249E-02	-3.9128E-02	102.3
83	5.9088E 02	5.9083E 02	-5.2282E-02	-4.9861E-02	95.4
84	4.6213E 02	4.6206E 02	-7.0384E-02	-3.8428E-02	54.6
85	2.8408E 02	2.8340E 02	-6.8259E-01	-7.3049E-01	107.0
86	6.7732E 02	6.7728E 02	-3.6266E-02	-3.9646E-02	109.3
87	6.0183E 02	6.0177E 02	-6.4684E-02	-6.4156E-02	99.2
88	4.7693E 02	4.7682E 02	-1.0739E-01	-8.2539E-02	76.9
89	3.1242E 02	3.1170E 02	-7.1824E-01	-7.5366E-01	104.9
90	6.8648E 02	6.8644E 02	-4.0228E-02	-4.4847E-02	111.5
91	6.1412E 02	6.1404E 02	-8.0436E-02	-8.2375E-02	102.4
92	4.9370E 02	4.9356E 02	-1.3911E-01	-1.3250E-01	95.2
93	3.4163E 02	3.4094E 02	-6.8478E-01	-6.9505E-01	101.5
94	7.1586E 02	7.1583E 02	-2.7971E-02	-3.0594E-02	109.4
95	6.8901E 02	6.8896E 02	-5.7235E-02	-5.9934E-02	104.7
96	6.2816E 02	6.2806E 02	-1.0405E-01	-1.0340E-01	99.4
97	5.1280E 02	5.1261E 02	-1.8740E-01	-1.7829E-01	95.1
98	3.7164E 02	3.7094E 02	-7.0011E-01	-7.1850E-01	102.6
99	7.2978E 02	7.2975E 02	-3.6761E-02	-3.8931E-02	105.9
100	7.0140E 02	7.0134E 02	-6.9666E-02	-7.0822E-02	101.7
101	6.4398E 02	6.4385E 02	-1.3026E-01	-1.2740E-01	97.8
102	5.3431E 02	5.3407E 02	-2.3761E-01	-2.2293E-01	93.8
103	4.0249E 02	4.0176E 02	-7.2833E-01	-7.5729E-01	104.0
104	7.2171E 02	7.2164E 02	-7.2612E-02	-7.4042E-02	102.0
105	6.6186E 02	6.6170E 02	-1.5638E-01	-1.5376E-01	98.3
106	5.5832E 02	5.5804E 02	-2.7896E-01	-2.6738E-01	95.8
107	4.3436E 02	4.3363E 02	-7.3364E-01	-7.5935E-01	103.5
108	7.4656E 02	7.4648E 02	-8.0280E-02	-8.1695E-02	101.8
109	6.9300E 02	6.9281E 02	-1.9571E-01	-1.9392E-01	99.1
110	5.9934E 02	5.9901E 02	-3.3356E-01	-3.2718E-01	98.1
111	4.8463E 02	4.8390E 02	-7.3516E-01	-7.5475E-01	102.7
112	7.7840E 02	7.7831E 02	-9.7854E-02	-9.9726E-02	101.9
113	7.4416E 02	7.4392E 02	-2.4377E-01	-2.4520E-01	100.6
114	6.6588E 02	6.6547E 02	-4.0393E-01	-4.0039E-01	99.1
115	5.5962E 02	5.5887E 02	-7.5858E-01	-7.7189E-01	101.8
116	8.1496E 02	8.1486E 02	-1.0110E-01	-1.0252E-01	101.4

Table 5.3.2 continued

117	8.0828E 02	8.0802E 02	-2.6544E-01	-2.7164E-01	102.3
118	7.5057E 02	7.5008E 02	-4.9053E-01	-4.9405E-01	100.7
119	6.5019E 02	6.4938E 02	-8.1125E-01	-8.1443E-01	100.4
120	8.5084E 02	8.5074E 02	-9.6889E-02	-9.7769E-02	100.9
121	8.8459E 02	8.8437E 02	-2.1814E-01	-2.2146E-01	101.5
122	8.6715E 02	8.6662E 02	-5.2329E-01	-5.6106E-01	107.2
123	7.6924E 02	7.6827E 02	-9.6725E-01	-9.4236E-01	97.4
124	8.7609E 02	8.7596E 02	-1.3263E-01	-1.3443E-01	101.4
125	9.4734E 02	9.4715E 02	-1.8844E-01	-1.9434E-01	103.1
126	1.0189E 03	1.0184E 03	-4.5285E-01	-4.0735E-01	90.0
127	9.7359E 02	9.7208E 02	-1.5169E 00	-1.5908E 00	104.9
128	8.9835E 02	8.9813E 02	-2.1448E-01	-2.2030E-01	102.7
129	9.6573E 02	9.6546E 02	-2.6382E-01	-2.6761E-01	101.4
130	1.1268E 03	1.1265E 03	-2.8979E-01	-2.9140E-01	100.6
131	1.3703E 03	1.3692E 03	-1.0865E 00	-1.1314E 00	104.1

Table 5.3.3 SDSA Result of Fillet at Optimum Using Boundary-layer Approach

Elt #	von Mises Stress OLD	NEW	Actual Change	Predict Change	Ratio x 100 %
1	343.515150	343.759790	0.244640	0.249350	101.925
2	331.365630	331.620230	0.254610	0.259470	101.909
3	306.913410	307.186320	0.272910	0.278020	101.873
4	270.036600	270.332220	0.295620	0.300980	101.811
5	221.172710	221.487850	0.315140	0.320500	101.701
6	162.210080	162.529200	0.319120	0.323950	101.512
7	98.627940	98.915280	0.287340	0.290810	101.207
8	42.960540	43.112780	0.152240	0.155200	101.939
9	21.549280	21.546520	-0.002770	-0.006800	245.578
10	365.879780	366.077950	0.198170	0.201970	101.917
11	359.105100	359.306990	0.201890	0.205760	101.914
12	345.803600	346.012450	0.208850	0.212850	101.916
13	326.438890	326.657620	0.218730	0.222980	101.942
14	301.382400	301.615570	0.233160	0.237910	102.035
15	269.915720	270.174200	0.258480	0.264300	102.251
16	227.437390	227.742300	0.304910	0.312660	102.544
17	164.299510	164.666180	0.366670	0.377030	102.824
18	78.587680	78.928070	0.340390	0.351670	103.314
19	404.295720	404.434830	0.139110	0.141810	101.939
20	402.361860	402.501110	0.139250	0.141980	101.962
21	398.686760	398.827400	0.140640	0.143490	102.027
22	393.435400	393.581770	0.146370	0.149540	102.166
23	386.176640	386.339650	0.163010	0.166930	102.408
24	374.863840	375.065260	0.201420	0.206870	102.704
25	354.393860	354.669560	0.275700	0.283830	102.946
26	318.244380	318.634050	0.389670	0.402050	103.176

Table 5.3.3 continued

27	256.144300	256.680720	0.536420	0.554200	103.315
28	452.904690	452.977100	0.072410	0.073870	102.021
29	454.408350	454.479450	0.071100	0.072580	102.089
30	457.419190	457.489390	0.070200	0.071780	102.249
31	461.777350	461.850830	0.073480	0.075330	102.509
32	466.859250	466.946230	0.086980	0.089410	102.791
33	471.265430	471.384150	0.118720	0.122190	102.921
34	473.093340	473.270510	0.177170	0.182190	102.830
35	471.503560	471.771280	0.267720	0.274520	102.540
36	465.888710	466.323830	0.435120	0.443880	102.013
37	506.225050	506.227230	0.002190	0.002340	106.746
38	509.765180	509.765440	0.000260	0.000410	156.414
39	516.721640	516.719500	-0.002140	-0.001960	91.615
40	526.794860	526.792570	-0.002290	-0.002000	87.519
41	539.469850	539.473210	0.003360	0.003860	114.795
42	554.172150	554.190150	0.018010	0.018780	104.277
43	570.915180	570.957270	0.042090	0.042940	102.031
44	591.604000	591.676100	0.072100	0.072250	100.205
45	622.427670	622.530500	0.102830	0.101220	98.436
46	559.408820	559.341290	-0.067530	-0.068710	101.752
47	563.885600	563.815700	-0.069900	-0.071110	101.731
48	572.649250	572.575480	-0.073770	-0.075020	101.702
49	585.330040	585.252340	-0.077690	-0.079010	101.699
50	601.440030	601.359670	-0.080360	-0.081800	101.793
51	620.580020	620.498050	-0.081970	-0.083720	102.129
52	642.834100	642.747990	-0.086120	-0.088620	102.909
53	669.263090	669.160350	-0.102740	-0.106930	104.079
54	701.945860	701.790010	-0.155850	-0.162940	104.549
55	608.457200	608.324520	-0.132680	-0.135130	101.843
56	613.112980	612.977550	-0.135420	-0.137920	101.842
57	622.189280	622.048790	-0.140480	-0.143080	101.850
58	635.234310	635.087030	-0.147280	-0.150050	101.884
59	651.632940	651.477310	-0.155630	-0.158700	101.974
60	670.702630	670.536010	-0.166620	-0.170220	102.164
61	691.803840	691.620160	-0.183680	-0.188230	102.480
62	714.217760	714.004550	-0.213220	-0.219390	102.897
63	736.392640	736.129220	-0.263410	-0.271870	103.211
64	650.321730	650.132320	-0.189410	-0.192960	101.874
65	654.710070	654.517720	-0.192350	-0.195960	101.878
66	663.212230	663.014190	-0.198040	-0.201780	101.889
67	675.286500	675.080280	-0.206220	-0.210170	101.915
68	690.141100	689.924220	-0.216880	-0.221150	101.968
69	706.753380	706.522820	-0.230560	-0.235310	102.061
70	723.859730	723.611150	-0.248580	-0.254050	102.200
71	739.843430	739.570910	-0.272520	-0.279000	102.379
72	752.562560	752.260250	-0.302310	-0.310140	102.592
73	682.495070	682.261220	-0.233850	-0.238260	101.888
74	686.532000	686.295130	-0.236870	-0.241350	101.891
75	694.288720	694.045960	-0.242770	-0.247370	101.897
76	705.127740	704.876460	-0.251270	-0.256070	101.910

Table 5.3.3 continued

77	718.087820	717.825720	-0.262100	-0.267160	101.929
78	731.883720	731.608770	-0.274950	-0.280330	101.954
79	744.921540	744.632180	-0.289360	-0.295090	101.978
80	755.367940	755.063720	-0.304220	-0.310220	101.973
81	761.453530	761.136160	-0.317370	-0.323590	101.961
82	762.987860	762.661590	-0.326270	-0.332910	102.033
83	761.773040	761.443910	-0.329130	-0.339210	103.062
84	760.750730	760.415650	-0.335070	-0.336570	100.447
85	763.253410	762.904820	-0.348590	-0.347780	99.767
86	771.074040	770.708980	-0.365060	-0.362460	99.286
87	784.187360	783.813760	-0.373600	-0.369660	98.945
88	801.451600	801.086990	-0.364610	-0.359600	98.626
89	821.634780	821.296600	-0.338180	-0.332780	98.402
90	843.730560	843.424830	-0.305730	-0.301600	98.649
91	866.750610	866.464700	-0.285910	-0.286940	100.358
92	889.660680	889.365830	-0.294850	-0.292870	99.326
93	911.475610	911.142480	-0.333140	-0.338690	101.668
94	704.002700	703.738690	-0.264010	-0.269010	101.894
95	707.777850	707.510800	-0.267050	-0.272110	101.895
96	714.968430	714.695480	-0.272960	-0.278130	101.896
97	724.846570	724.565230	-0.281340	-0.286670	101.897
98	736.307470	736.015910	-0.291560	-0.297070	101.891
99	747.881730	747.579130	-0.302600	-0.308260	101.871
100	757.816200	757.503320	-0.312880	-0.318580	101.821
101	764.325150	764.004960	-0.320200	-0.325690	101.715
102	766.158120	765.835860	-0.322250	-0.327070	101.494
103	764.321050	764.001380	-0.319670	-0.324240	101.431
104	761.366190	761.050760	-0.315420	-0.317380	100.621
105	759.240840	758.927600	-0.313240	-0.313570	100.105
106	760.250330	759.935090	-0.315240	-0.314750	99.846
107	766.038310	765.718820	-0.319490	-0.317670	99.432
108	777.160470	776.839960	-0.320510	-0.317480	99.053
109	793.209310	792.896270	-0.313040	-0.309260	98.794
110	813.247370	812.950540	-0.296830	-0.293110	98.747
111	836.104070	835.825010	-0.279060	-0.277180	99.325
112	860.462270	860.189770	-0.272500	-0.272320	99.933
113	884.951730	884.662700	-0.289020	-0.287880	99.603
114	908.281540	907.952220	-0.329320	-0.332380	100.928
115	714.907240	714.627790	-0.279450	-0.284750	101.896
116	718.519090	718.236620	-0.282470	-0.287830	101.896
117	725.360080	725.071780	-0.288300	-0.293760	101.894
118	734.654630	734.358180	-0.296450	-0.302050	101.887
119	745.226640	744.920580	-0.306060	-0.311780	101.868
120	755.527060	755.211340	-0.315720	-0.321480	101.826
121	763.763410	763.440070	-0.323340	-0.328960	101.739
122	768.245210	767.918850	-0.326360	-0.331530	101.584
123	768.063010	767.740160	-0.322850	-0.327150	101.331
124	764.805230	764.490030	-0.315200	-0.317780	100.820
125	761.117220	760.809840	-0.307380	-0.308010	100.207
126	758.479670	758.178530	-0.301130	-0.300330	99.733

Table 5.3.3 continued

127	758.838460	758.540390	-0.298070	-0.296780	99.567
128	763.740840	763.443610	-0.297230	-0.295380	99.376
129	773.947240	773.651930	-0.295310	-0.292700	99.118
130	789.369070	789.080260	-0.288810	-0.285720	98.928
131	809.251090	808.973650	-0.277450	-0.274580	98.967
132	832.402380	832.135890	-0.266480	-0.264060	99.089
133	857.371130	857.105060	-0.266070	-0.262490	98.654
134	882.614320	882.328310	-0.286010	-0.287600	100.557
135	906.689340	906.361980	-0.327360	-0.332630	101.610
136	1013.278680	1014.923580	1.644910	1.593660	96.885
137	1004.323000	1005.198280	0.875270	0.868310	99.204
138	999.636320	1000.178890	0.542570	0.534450	98.503
139	997.563100	997.870600	0.307490	0.303890	98.829
140	997.209990	997.371580	0.161590	0.159370	98.627
141	997.881110	997.948000	0.066890	0.065900	98.529
142	998.982410	998.997890	0.015480	0.015170	97.989
143	999.878280	999.878750	0.000470	0.000450	95.410
144	1021.965700	1022.113240	0.147530	0.186090	126.135
145	1010.780050	1011.263380	0.483330	0.478090	98.915
146	1004.718880	1005.087850	0.368960	0.367260	99.540
147	1001.498580	1001.751690	0.253120	0.250810	99.089
148	1000.000720	1000.151510	0.150800	0.149390	99.065
149	999.580790	999.655860	0.075070	0.074290	98.956
150	999.793130	999.816480	0.023350	0.023100	98.921
151	1000.284420	1000.284670	0.000250	0.000290	116.101
152	1014.099910	1013.683260	-0.416660	-0.392020	94.086
153	1009.583790	1009.522430	-0.061370	-0.050710	82.635
154	1005.272870	1005.360420	0.087550	0.090560	103.441
155	1002.587160	1002.691860	0.104710	0.105170	100.448
156	1001.089330	1001.164870	0.075540	0.075400	99.816
157	1000.423260	1000.459330	0.036070	0.035940	99.630
158	1000.355560	1000.355900	0.000350	0.000440	126.961
159	1000.763810	1000.747890	-0.015910	-0.015640	98.285
160	1000.456210	999.926520	-0.529680	-0.522360	98.617
161	1001.950360	1001.601710	-0.348650	-0.338680	97.141
162	1001.654790	1001.495220	-0.159570	-0.154260	96.672
163	1000.990600	1000.929600	-0.061000	-0.058630	96.121
164	1000.515760	1000.489140	-0.026620	-0.025580	96.104
165	1000.322900	1000.297650	-0.025250	-0.024700	97.797
166	1000.464470	1000.427370	-0.037100	-0.036600	98.651
167	1001.099050	1001.056010	-0.043040	-0.042460	98.651
168	984.528990	984.019440	-0.509550	-0.512750	100.628
169	991.255930	990.806790	-0.449150	-0.445370	99.158
170	995.198590	994.886050	-0.312540	-0.308320	98.650
171	997.363250	997.167690	-0.195560	-0.192810	98.591
172	998.606270	998.482020	-0.124250	-0.122630	98.697
173	999.424060	999.334300	-0.089760	-0.088730	98.850
174	1000.161070	1000.082750	-0.078310	-0.077480	98.933
175	1001.223180	1001.147460	-0.075720	-0.074830	98.827
176	968.237360	967.767890	-0.469460	-0.476790	101.560

Table 5.3.3 continued

177	979.578960	979.111430	-0.467530	-0.468800	100.272
178	987.451840	987.064650	-0.387190	-0.385560	99.579
179	992.591370	992.305980	-0.285390	-0.283410	99.307
180	995.866540	995.665120	-0.201430	-0.199840	99.213
181	997.999370	997.853520	-0.145850	-0.144640	99.171
182	999.570680	999.454200	-0.116480	-0.115430	99.103
183	1001.155870	1001.047060	-0.108810	-0.107660	98.948
184	953.128980	952.696500	-0.432470	-0.441610	102.113
185	968.370520	967.913930	-0.456590	-0.460740	100.909
186	979.664360	979.248030	-0.416330	-0.417020	100.166
187	987.555720	987.217990	-0.337720	-0.336920	99.762
188	992.848460	992.593390	-0.255070	-0.253900	99.542
189	996.366410	996.177590	-0.188830	-0.187680	99.391
190	998.848230	998.700420	-0.147810	-0.146680	99.234
191	1000.963460	1000.825260	-0.138190	-0.136860	99.037
192	940.358340	939.955160	-0.403190	-0.411480	102.058
193	958.700440	958.261240	-0.439190	-0.444160	101.131
194	972.790960	972.367050	-0.423910	-0.426030	100.501
195	983.002360	982.637060	-0.365300	-0.365520	100.062
196	990.060400	989.771450	-0.288950	-0.288290	99.774
197	994.830180	994.611660	-0.218520	-0.217540	99.552
198	998.148610	997.977850	-0.170770	-0.169630	99.332
199	1000.730790	1000.569780	-0.161010	-0.159560	99.101
200	933.468600	933.080180	-0.388420	-0.393820	101.392
201	953.382750	952.954720	-0.428030	-0.432930	101.143
202	968.943900	968.520520	-0.423370	-0.425940	100.606
203	980.407470	980.032160	-0.375310	-0.376070	100.201
204	988.445780	988.141910	-0.303870	-0.303540	99.889
205	993.929110	993.696320	-0.232790	-0.231940	99.637
206	997.732370	997.549890	-0.182480	-0.181350	99.385
207	1000.579630	1000.406380	-0.173250	-0.171750	99.134
208	931.182510	930.798600	-0.383920	-0.388880	101.293
209	951.548570	951.125060	-0.423510	-0.427970	101.053
210	967.561780	967.140080	-0.421700	-0.424370	100.633
211	979.437940	979.060460	-0.377470	-0.378410	100.247
212	987.820890	987.512410	-0.308490	-0.308280	99.934
213	993.570910	993.333040	-0.237870	-0.237080	99.671
214	997.564110	997.376960	-0.187150	-0.186040	99.406
215	1000.513710	1000.335160	-0.178550	-0.177020	99.148
216	930.038190	929.656520	-0.381670	-0.386010	101.137
217	950.625630	950.204400	-0.421230	-0.425410	100.992
218	966.864160	966.443410	-0.420760	-0.423460	100.642
219	978.946810	978.568400	-0.378420	-0.379430	100.268
220	987.503200	987.192530	-0.310680	-0.310540	99.956
221	993.388220	993.147880	-0.240340	-0.239590	99.687
222	997.477900	997.288430	-0.189470	-0.188370	99.416
223	1000.479200	1000.297980	-0.181220	-0.179690	99.154
224	759.841920	759.512380	-0.329530	-0.336660	102.162
225	754.260510	753.934110	-0.326410	-0.338310	103.647
226	740.940650	740.657280	-0.283370	-0.295250	104.194

Table 5.3.3 continued

227	694.688710	694.643440	-0.045270	-0.052910	116.891
228	557.871840	558.317460	0.445620	0.450770	101.155
229	323.106040	323.844010	0.737970	0.767140	103.953
230	92.890180	93.345520	0.455340	0.491140	107.861
231	35.083260	34.964610	-0.118650	-0.131240	110.608
232	761.895870	761.551660	-0.344210	-0.375990	109.234
233	762.375990	762.015220	-0.360760	-0.404030	111.993
234	762.652080	762.278250	-0.373840	-0.419210	112.137
235	762.306930	761.912570	-0.394360	-0.437160	110.854
236	757.034320	756.683330	-0.350980	-0.359520	102.431
237	696.431200	696.281610	-0.149590	0.016850	-11.267
238	500.720130	500.665760	-0.054370	0.453240	-833.600
239	233.601980	233.426030	-0.175950	0.363650	-206.675
240	762.881480	762.521780	-0.359700	-0.356070	98.990
241	765.735980	765.353150	-0.382830	-0.386530	100.968
242	770.401620	769.989980	-0.411640	-0.424950	103.233
243	778.193890	777.749140	-0.444750	-0.458370	103.061
244	788.507600	788.038590	-0.469010	-0.469050	100.008
245	807.003600	806.468450	-0.535140	-0.494580	92.420
246	872.904840	872.181390	-0.723450	-0.564050	77.967
247	987.671500	986.529380	-1.142120	-0.543410	47.579
248	767.955940	767.568650	-0.387290	-0.385440	99.521
249	774.698740	774.271920	-0.426820	-0.428560	100.409
250	785.240870	784.765130	-0.475740	-0.483080	101.544
251	801.969970	801.434680	-0.535290	-0.543090	101.456
252	829.725720	829.113380	-0.612340	-0.612130	99.966
253	881.292260	880.573870	-0.718380	-0.694880	96.728
254	989.507140	988.646230	-0.860910	-0.777290	90.288
255	1216.525880	1215.613140	-0.912740	-0.779690	85.424
256	779.379520	778.958330	-0.421190	-0.416180	98.809
257	791.601060	791.120970	-0.480090	-0.479830	99.945
258	810.180950	809.627600	-0.553350	-0.556450	100.559
259	838.792160	838.150600	-0.641550	-0.645610	100.633
260	883.742670	883.001060	-0.741610	-0.741950	100.046
261	954.827320	953.992270	-0.835050	-0.825250	98.827
262	1060.707650	1059.838640	-0.869010	-0.849310	97.732
263	1220.226630	1219.475200	-0.751430	-0.721580	96.028
264	796.041940	795.601510	-0.440430	-0.430750	97.802
265	813.260850	812.750280	-0.510570	-0.505480	99.003
266	838.303250	837.706230	-0.597020	-0.595570	99.756
267	874.597690	873.900840	-0.696850	-0.697940	100.155
268	926.793410	925.993820	-0.799590	-0.802190	100.326
269	1000.394070	999.514730	-0.879330	-0.882920	100.408
270	1099.525730	1098.639570	-0.886160	-0.890210	100.457
271	1202.637680	1201.890120	-0.747560	-0.752620	100.678
272	815.514450	815.085030	-0.429430	-0.413620	96.320
273	835.722730	835.225440	-0.497290	-0.485550	97.640
274	863.580330	862.998520	-0.581810	-0.573400	98.554
275	901.439310	900.756880	-0.682430	-0.677090	99.218
276	952.070080	951.275900	-0.794190	-0.792410	99.776

Table 5.3.3 continued

277	1018.494780	1017.592640	-0.902140	-0.905230	100.342
278	1104.810060	1103.841610	-0.968450	-0.977660	100.951
279	1225.766450	1224.842630	-0.923820	-0.939110	101.654
280	836.460250	836.071020	-0.389230	-0.366470	94.152
281	857.940800	857.498170	-0.442630	-0.422810	95.524
282	886.302390	885.790180	-0.512210	-0.494530	96.549
283	922.898340	922.293810	-0.604530	-0.588460	97.341
284	969.207970	968.477290	-0.730680	-0.716370	98.041
285	1027.268100	1026.367740	-0.900350	-0.890570	98.913
286	1101.912410	1100.812380	-1.100030	-1.099870	99.986
287	1207.434550	1206.217500	-1.217060	-1.217250	100.016
288	858.150750	857.814180	-0.336560	-0.306640	91.108
289	879.726950	879.360860	-0.366090	-0.338200	92.382
290	907.427240	907.021290	-0.405950	-0.379260	93.425
291	941.978300	941.509950	-0.468360	-0.439790	93.901
292	984.005950	983.422970	-0.582980	-0.549810	94.310
293	1033.881040	1033.073520	-0.807520	-0.771330	95.518
294	1090.767920	1089.547990	-1.219930	-1.184320	97.081
295	1148.262330	1146.525160	-1.737170	-1.747450	100.592
296	879.885460	879.587020	-0.298440	-0.262870	88.081
297	900.454860	900.151280	-0.303580	-0.270920	89.241
298	926.306420	926.000130	-0.306290	-0.274600	89.652
299	957.546570	957.233790	-0.312780	-0.277360	88.674
300	993.896210	993.548950	-0.347260	-0.302140	87.008
301	1034.148610	1033.659880	-0.488730	-0.420560	86.050
302	1073.136050	1072.085030	-1.051020	-0.946190	90.026
303	1093.408670	1090.747020	-2.661650	-2.674830	100.495
304	900.886600	900.583950	-0.302660	-0.276550	91.376
305	919.335760	919.032140	-0.303620	-0.282730	93.120
306	941.992830	941.695020	-0.297810	-0.282320	94.799
307	968.233580	967.950600	-0.282970	-0.270960	95.754
308	996.717560	996.459570	-0.257990	-0.249150	96.573
309	1024.849030	1024.598270	-0.250770	-0.240040	95.724
310	1049.963070	1049.604250	-0.358830	-0.335310	93.447
311	1078.494590	1076.451580	-2.043010	-1.607990	78.707
312	920.594620	920.248050	-0.346570	-0.356840	102.963
313	936.385420	936.015730	-0.369690	-0.379200	102.572
314	955.396730	954.998920	-0.397810	-0.406560	102.202
315	976.519280	976.087770	-0.431520	-0.442390	102.521
316	997.982090	997.509290	-0.472800	-0.484130	102.397
317	1017.347190	1016.825410	-0.521780	-0.523120	100.256
318	1032.722000	1032.360310	-0.361690	-0.320900	88.722
319	1039.737220	1041.679120	1.941900	1.912430	98.482

Table 5.3.4 SDSA Result of Fillet at Optimum
Using Boundary Approach

Elt #	von Mises Stress OLD	New	Actual Change	Predict Change	Ratio x 100 %
1	7.1348E 02	7.1331E 02	-1.6878E-01	-1.4733E-01	87.3
2	6.5911E 02	6.5899E 02	-1.2209E-01	-1.0575E-01	86.6
3	5.5968E 02	5.5964E 02	-3.9794E-02	-3.3762E-02	84.8
4	4.4105E 02	4.4111E 02	5.5723E-02	4.8161E-02	86.4
5	3.4984E 02	3.4997E 02	1.3963E-01	1.1888E-01	85.1
6	7.2892E 02	7.2874E 02	-1.7547E-01	-1.5506E-01	88.4
7	6.7769E 02	6.7756E 02	-1.2937E-01	-1.1275E-01	87.2
8	5.7717E 02	5.7713E 02	-4.3532E-02	-3.6705E-02	84.3
9	4.4401E 02	4.4407E 02	5.6628E-02	4.9339E-02	87.1
10	3.1938E 02	3.1953E 02	1.5139E-01	1.2898E-01	85.2
11	7.5125E 02	7.5107E 02	-1.8421E-01	-1.6772E-01	91.0
12	7.0910E 02	7.0895E 02	-1.4457E-01	-1.2734E-01	88.1
13	6.0921E 02	6.0916E 02	-4.5148E-02	-3.6188E-02	80.2
14	4.4736E 02	4.4744E 02	7.7085E-02	6.7049E-02	87.0
15	2.6003E 02	2.6020E 02	1.6836E-01	1.4359E-01	85.3
16	7.6520E 02	7.6501E 02	-1.8310E-01	-1.7672E-01	96.5
17	7.4161E 02	7.4144E 02	-1.6393E-01	-1.4695E-01	89.6
18	6.5226E 02	6.5219E 02	-7.2275E-02	-5.5553E-02	76.9
19	4.4626E 02	4.4641E 02	1.5784E-01	1.4958E-01	94.8
20	1.6907E 02	1.6925E 02	1.8455E-01	1.4864E-01	80.5
21	7.6311E 02	7.6295E 02	-1.6060E-01	-1.6507E-01	102.8
22	7.5938E 02	7.5923E 02	-1.4921E-01	-1.5729E-01	105.4
23	7.5982E 02	7.5965E 02	-1.7762E-01	-1.8667E-01	105.1
24	7.5764E 02	7.5741E 02	-2.2665E-01	-2.1449E-01	94.6
25	6.9135E 02	6.9132E 02	-3.2621E-02	2.5778E-02	-79.0
26	3.4246E 02	3.4281E 02	3.4492E-01	3.0472E-01	88.3
27	5.2213E 01	5.2303E 01	9.0667E-02	9.9984E-02	110.3
28	7.5894E 02	7.5879E 02	-1.5128E-01	-1.5552E-01	102.8
29	7.6659E 02	7.6640E 02	-1.8394E-01	-1.9222E-01	104.5
30	7.6518E 02	7.6502E 02	-1.6579E-01	-1.6206E-01	97.7
31	7.8331E 02	7.8308E 02	-2.3080E-01	-2.2156E-01	96.0
32	7.7792E 02	7.7773E 02	-1.8635E-01	-1.7301E-01	92.8
33	8.1051E 02	8.1021E 02	-3.0049E-01	-2.7236E-01	90.6
34	7.9624E 02	7.9604E 02	-2.0412E-01	-1.8338E-01	89.8
35	8.4214E 02	8.4180E 02	-3.4741E-01	-3.1397E-01	90.4
36	8.1900E 02	8.1879E 02	-2.1213E-01	-1.8811E-01	88.7
37	8.7360E 02	8.7324E 02	-3.5742E-01	-3.2975E-01	92.3
38	8.4465E 02	8.4444E 02	-2.0855E-01	-1.8513E-01	88.8
39	9.0267E 02	9.0233E 02	-3.3462E-01	-3.1638E-01	94.5
40	8.7158E 02	8.7138E 02	-1.9771E-01	-1.7744E-01	89.7
41	9.2816E 02	9.2788E 02	-2.8423E-01	-2.7394E-01	96.4
42	8.9817E 02	8.9798E 02	-1.8845E-01	-1.7234E-01	91.4
43	9.4990E 02	9.4968E 02	-2.1904E-01	-2.1483E-01	98.1
44	9.2283E 02	9.2264E 02	-1.8939E-01	-1.7709E-01	93.5
45	9.6752E 02	9.6734E 02	-1.8070E-01	-1.7945E-01	99.3
46	9.4412E 02	9.4391E 02	-2.0135E-01	-1.9196E-01	95.3

Table 5.3.4 continued

47	9.8004E 02	9.7984E 02	-2.0352E-01	-2.0099E-01	98.8
48	9.5984E 02	9.5962E 02	-2.1140E-01	-2.0402E-01	96.5
49	9.9143E 02	9.9120E 02	-2.2750E-01	-2.2442E-01	98.6
50	1.0086E 03	1.0084E 03	-2.0521E-01	-2.0524E-01	100.0
51	1.0114E 03	1.0113E 03	-6.9032E-02	-7.4673E-02	108.2
52	1.0118E 03	1.0120E 03	1.7063E-01	1.4186E-01	83.1
53	1.0101E 03	1.0111E 03	1.0119E 00	1.1085E 00	109.5
54	9.7460E 02	9.7440E 02	-2.0375E-01	-1.9877E-01	97.6
55	9.7653E 02	9.7632E 02	-2.0924E-01	-2.0465E-01	97.8
56	9.8548E 02	9.8527E 02	-2.1007E-01	-2.0703E-01	98.6
57	9.9850E 02	9.9834E 02	-1.6589E-01	-1.6631E-01	100.2
58	1.0047E 03	1.0046E 03	-3.8143E-02	-4.1313E-02	108.3
59	1.0016E 03	1.0020E 03	4.3657E-01	4.3558E-01	99.8
60	9.8890E 02	9.8874E 02	-1.5872E-01	-1.5670E-01	98.7
61	9.9139E 02	9.9124E 02	-1.5139E-01	-1.5002E-01	99.1
62	9.9545E 02	9.9532E 02	-1.2651E-01	-1.2644E-01	99.9
63	9.9958E 02	9.9951E 02	-6.5606E-02	-6.7161E-02	102.4
64	1.0013E 03	1.0014E 03	4.5266E-02	4.2634E-02	94.2
65	9.9853E 02	9.9867E 02	1.4035E-01	1.4507E-01	103.4
66	9.9880E 02	9.9869E 02	-1.0675E-01	-1.0717E-01	100.4
67	9.9930E 02	9.9921E 02	-9.5022E-02	-9.5581E-02	100.6
68	1.0001E 03	1.0000E 03	-7.1633E-02	-7.2355E-02	101.0
69	1.0006E 03	1.0006E 03	-3.6898E-02	-3.7660E-02	102.1
70	1.0004E 03	1.0004E 03	-1.0972E-03	-1.1074E-03	100.9
71	9.9936E 02	9.9937E 02	1.3883E-02	1.3537E-02	97.5
72	7.6621E 02	7.6597E 02	-2.3827E-01	-2.4628E-01	103.4
73	7.5626E 02	7.5598E 02	-2.8732E-01	-2.2988E-01	80.0
74	4.0619E 02	4.0695E 02	7.6283E-01	8.2264E-01	107.8
75	5.6629E 01	5.6589E 01	-4.0020E-02	-3.6689E-02	91.7
76	7.7654E 02	7.7632E 02	-2.1809E-01	-2.3139E-01	106.1
77	7.8064E 02	7.8038E 02	-2.5953E-01	-2.6923E-01	103.7
78	7.9341E 02	7.9294E 02	-4.6884E-01	-5.4161E-01	115.5
79	8.2903E 02	8.2852E 02	-5.1069E-01	-4.7843E-01	93.7
80	5.0835E 02	5.0887E 02	5.2571E-01	1.0243E 00	194.8
81	8.0069E 02	8.0039E 02	-2.9558E-01	-2.8017E-01	94.8
82	7.9665E 02	7.9639E 02	-2.6252E-01	-2.5325E-01	96.5
83	8.2977E 02	8.2928E 02	-4.8937E-01	-4.5928E-01	93.9
84	8.6576E 02	8.6507E 02	-6.8731E-01	-3.9711E-01	57.8
85	1.2008E 03	1.1984E 03	-2.4295E 00	-2.9116E 00	119.8
86	8.3184E 02	8.3143E 02	-4.0881E-01	-3.6058E-01	88.2
87	8.7361E 02	8.7301E 02	-5.9955E-01	-4.8429E-01	80.8
88	9.7568E 02	9.7462E 02	-1.0613E 00	-8.2982E-01	78.2
89	1.2003E 03	1.1988E 03	-1.5543E 00	-1.9347E 00	124.5
90	8.5908E 02	8.5858E 02	-4.9900E-01	-4.4503E-01	89.2
91	9.1622E 02	9.1549E 02	-7.3539E-01	-6.3187E-01	85.9
92	1.0242E 03	1.0229E 03	-1.2795E 00	-1.3476E 00	105.3
93	1.0546E 03	1.0547E 03	1.0742E-01	4.8463E-01	451.2
94	8.6134E 02	8.6087E 02	-4.6770E-01	-4.1540E-01	88.8
95	8.9480E 02	8.9423E 02	-5.6582E-01	-5.0033E-01	88.4
96	9.4550E 02	9.4479E 02	-7.0984E-01	-6.4016E-01	90.2

Table 5.3.4 continued

97	1.0351E 03	1.0342E 03	-9.1180E-01	-8.8138E-01	96.7
98	1.1139E 03	1.1136E 03	-2.5416E-01	-4.7332E-01	186.2
99	8.9720E 02	8.9669E 02	-5.1128E-01	-4.6699E-01	91.3
100	9.1816E 02	9.1758E 02	-5.7527E-01	-5.2682E-01	91.6
101	9.6707E 02	9.6640E 02	-6.7384E-01	-6.3559E-01	94.3
102	1.0533E 03	1.0526E 03	-7.1123E-01	-6.7148E-01	94.4
103	1.2005E 03	1.1997E 03	-7.4768E-01	-1.1593E 00	155.1
104	9.3432E 02	9.3376E 02	-5.6393E-01	-5.2885E-01	93.8
105	9.8997E 02	9.8930E 02	-6.6820E-01	-6.4750E-01	96.9
106	1.0773E 03	1.0765E 03	-7.9243E-01	-8.3829E-01	105.8
107	1.2000E 03	1.1995E 03	-5.3825E-01	-6.1813E-01	114.8
108	9.5435E 02	9.5381E 02	-5.3831E-01	-5.2012E-01	96.6
109	1.0144E 03	1.0138E 03	-6.3541E-01	-6.3578E-01	100.1
110	1.0964E 03	1.0957E 03	-7.2912E-01	-7.7003E-01	105.6
111	1.2001E 03	1.1997E 03	-4.5831E-01	-5.5195E-01	120.4
112	9.8241E 02	9.8191E 02	-5.0158E-01	-5.0218E-01	100.1
113	1.0357E 03	1.0352E 03	-5.9292E-01	-6.1349E-01	103.5
114	1.1060E 03	1.1053E 03	-6.6831E-01	-7.1596E-01	107.1
115	1.2000E 03	1.1994E 03	-5.2892E-01	-5.7500E-01	108.7
116	9.9968E 02	9.9924E 02	-4.3597E-01	-4.4060E-01	101.1
117	1.0437E 03	1.0431E 03	-5.4828E-01	-5.6052E-01	102.2
118	1.0990E 03	1.0983E 03	-6.7922E-01	-6.9766E-01	102.7
119	1.1668E 03	1.1662E 03	-5.7666E-01	-5.9707E-01	103.5
120	1.0090E 03	1.0087E 03	-3.0901E-01	-3.1716E-01	102.6
121	1.0401E 03	1.0397E 03	-4.3952E-01	-4.5294E-01	103.1
122	1.0775E 03	1.0768E 03	-6.7458E-01	-7.0266E-01	104.2
123	1.1314E 03	1.1307E 03	-7.9667E-01	-7.9720E-01	100.1
124	1.0144E 03	1.0142E 03	-1.6283E-01	-1.7156E-01	105.4
125	1.0362E 03	1.0360E 03	-1.9490E-01	-2.0054E-01	102.9
126	1.0549E 03	1.0545E 03	-4.1929E-01	-3.8934E-01	92.9
127	1.0582E 03	1.0569E 03	-1.3215E 00	-1.4021E 00	106.1
128	1.0129E 03	1.0127E 03	-1.8775E-01	-1.9073E-01	101.6
129	1.0242E 03	1.0240E 03	-1.7384E-01	-1.7806E-01	102.4
130	1.0303E 03	1.0301E 03	-1.3788E-01	-1.4788E-01	107.3
131	1.0278E 03	1.0276E 03	-2.4327E-01	-2.4824E-01	102.0

5.3.4 Discussion

Shape design sensitivity analysis is performed using the boundary-layer approach and results obtained are compared to previous SDSA results by the boundary approach [23]. Due to differences in meshes used, one-to-one comparison is not possible. However, one can see general trends by comparing these results. Both methods give acceptable shape design sensitivities for a fillet with straight boundary, but both approaches show poor design sensitivities near point A of Fig. 5.3.10, mainly due to ill-proportioned elements in contrast to good initial element shapes (see Figs. 5.3.4 and 5.3.5). For the boundary-layer approach, this may be avoided by adjusting the boundary-layer coordinate system and adopting a curved inner bounding surface, as shown in Fig. 5.3.10.

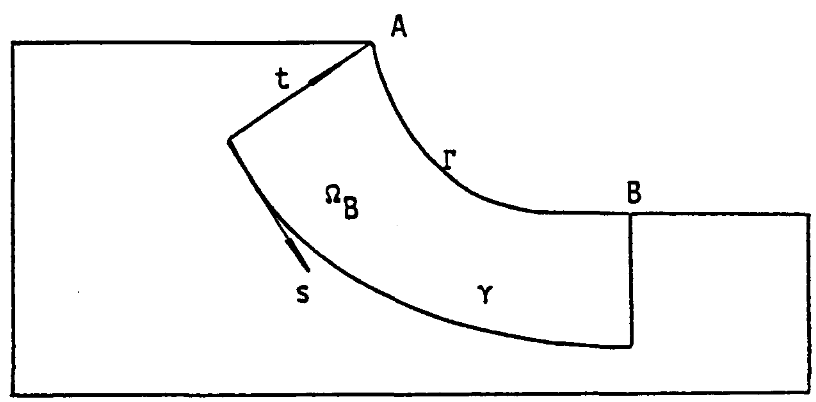

Figure 5.3.10 Boundary-Layer with Curved Inner Bounding Surface

This problem also shows the reliability of the velocity element approach, which can add generality and convenience to the boundary-layer approach. Velocity elements can greatly simplify the process of evaluating velocity and derivatives of velocity within the boundary-layer.

In the present work, only guidelines for locating a boundary-layer in the domain are given. To make the boundary-layer approach more attractive, this area must be studied further, since accuracy and efficiency of shape design sensitivity analysis by the boundary-layer approach depends largely on size and location of the boundary-layer.

B-splines are used to approximate the boundary. They prove to be easy to manupulate and approximate the original boundary well. However, they still have the basic characteristics of the spline family, such as fluctuating when chord length changes rapidly from one segment to another. One must sellect joint positions cautiously to avoid this.

VI. CONCLUSION

Shape design sensitivity formulas for domain and boundary approaches are mathematically identical. However, numerical results obtained by each approach can be quite different, depending on numerical methods used. The domain approach can be coupled better with the finite element method, taking advantage of the finite element method as a domain type approximation method. Results of the present work show that accuracy of shape design sensitivity is improved significantly by using domain information, especially for problems with singular behavior; e.g., along interfaces due to non-smooth boundaries or data.

Futhermore, the derivation of shape design sensitivity formula can be simplified, avoiding use of intergration by parts and interface boundary conditions. Consequently, shape design sensitivity formulas for a built-up structures can be easily obtained by adding contributions from each structural component of the structural system. In other words, one can derive the shape design sensitivity formulas for any built-up structure by assembling shape design sensitivty formulas of each prototype structural components, taking care to enforce compatible design velocity fields throughout the domain.

Results presented show the effectiveness of the boundary-layer approach to shape design sensitivity analysis, which is introduced for ease of generating the design velocity field and for efficiency of numerical calculation. The design velocity field is constructed using local-othogonality imposed on a pre-set inner bounding surface, allowing only non-zero velocity in one direction (normal to the inner bounding surface). The velocity element idea provides convience and generality to the boundary-layer approach, evaluating velocity and its derivatives, using velocity shape functions.

The present work concentrates on testing the domain approach of SDSA, using relatively simple structures such as a square box and a truss-beam-plate built-up structure in which velocity fields can be easily defined over the domain. A fillet is studied to generate a more general velocity field, using B-spline and isoparametric mappings. Results are quite encouriging. To apply the present method to more general structures, velocity field specification throughout the domain should be further studied.

Accuracy and efficiency of the boundary-layer approach depend on size and location of the boundary-layer in the domain. The present work gives only guidelines for sizing and locating the boundary-layer. This area should be futher studied to make the boundary-layer idea more attractive.

REFERENCES

1. Babuska, I. and Aziz, A. K. "Survey Lectures on the Mathematical Foundations of the Finite Element Method", The Mathematical Foundation of the Finite Element Method with Application to Partial Differential Equations (Edit. A. K. Aziz), Academic Press, 1972, pp. 1-359.

2. Zienkiewicz, O. C. and Campbell, J. S. "Shape Optimization and Sequential linear Programming" Optimum Structural Design (Ed. R. H. Gallagher and O. C. Zienkiewicz) John Wiley and Sons, 1973, pp. 109-126.

3. Ramakrishnan, C. V. and Francavilla, A. "Structural Shape Optimization using Penalty Functions", Journal of Structural Mechanics, Vol. 3, NO. 4, 1975, pp. 403-432.

4. Francavilla, A., Ramakrishnan, C. V. and Zienkiewicz, O. C. "Optimization of Shape to Minimize Stress Concentration", Journal of Strain Analysis, Vol. 10, 1975, pp. 63-70.

5. Schnack, E. "An Optimization Procedure for Stress Concentration by the Finite Element Technique", International Journal for Numerical Methods in Engineering, Vol.14, 1979, pp. 115-124.

6. Oda, J. "On A Technique to Obtain an Optimum Strength Shape by the Finite Element Method", Bulletine of JSME, Vol. 20, 1977, pp. 160-167.

7. Tvergaard, V. " On the Optimum Shape of Fillet in a Flat Bar with Restrictions", Optimizations in Structural Design (Ed. A. Sawczuk and M. Mroz), Springer-Verlag, 1975, pp. 181-195.

8. Kristensen, E. S. and Madsen, N. F. "On the Optimum Shape of Fillet Fillets in Plates Subjected to Multiple In-plane Loading Cases", International Journal for Numerical Methods in Engineering, Vol. 10, 1976, pp. 1007-1019.

9. Queau, J. P. and Trompette, P. H., "Two-Dimensional Shape Optimal Design by Finite Element Methods", International Journal for Numerical Methods in Engineering, Vol. 15, 1980, pp. 1603-1612.

10. Bhavikatti, S. S. and Ramakrishnan, C. V. "Optimum Design of Fillets in Flat and Round Tension Bars", ASME paper, 77-DET-45, 1977.

11. Dems, K. and Mroz, Z. "Multi-parameter Structural Shape Optimization by the Finite Element Method", International Journal for Numerical Method in Engineering, Vol. 13, 1978, pp. 247-263.

12. Dems, K. "Multi-parameter Shape Optimization of Elastic Bars in Torsion", International Journal for Numerical Methods in Engineering, Vol. 15, 1980, pp. 1517-1539.

13. Chun, Y. W. and Haug, E. J. "Two Dimensional Shape Optimal Design", International Journal for Numerical Methods in Engineering, Vol. 13, 1978, pp. 311-336.

14. Rousellet, B. and Haug, E. J. "Design Sensitivity Analysis of Shape Variation", Optimization of Distributed Parameter Structures (Ed. E. J. Haug, and J. Cea) Sijthoff & Noordhoff, Alphen aan den Rijn, Netherland, 1981, pp. 1415-1460.

15. Haug, E. J. and Arora, J. S., Applied Optimal Design, John Wiley & Sons, New York, 1979.

16. Yoo, Y. M., Haug, E. J. and Choi, K. K. "Shape Optimal Design of an Engine Connecting Rod", ASME Journal of Mechanisms, Transmissions and Automation in Design, Vol. 106, No. 3, 1984, pp. 415-419.

17. Lam, H. L. and Choi, K. K. and Haug, E. J., "A Sparce Matrix Finite Element Technique for Iterative Structural Optimization", Computers and Structures, Vol. 16, No. 1-4, 1983, pp. 289-295.

18. Hou, J. W. and Benedict R. L. "Shape Optimal Design and Free Boundary Value Problems", Technical Report No. 83-9, Center for Computer Aided Design, The Univ. of Iowa, Iowa City, May, 1983.

19. Choi, K. K. and Haug, E. J. "Shape Design Sensitivity Analysis of Elastic Structures", J. of Structural Mechanics, Vol. 11, No. 2, 1983, pp. 231-269.

20. Choi, K. K. "Shape Design Sensitivity of Displacement and Stress Constraint", J. of Structural Mechanics, Vol. 13, No. 1, 1985.

21. Haug, E. J., Choi, K. K. and Komkov, V. Design Sensitivity Analysis of Structural Systems, Academic Press, in press.

22. Lee, H. G., Choi, K. K. and Haug, E. J. "Shape Optimal Design of Build-up Structures", Technical Report No. 84-12, Center for Computer Aided Design, The Univ. of Iowa, Iowa City.

23. Yang, R. J. and Choi, K. K. "Accuracy of Finite Element Based Design Sensitivity Analysis", Journal of Struct. Mechanics, Vol. 13, No. 2, 1985.

24. Szabo, B. A., Chen, K. C. and Tsai, C-T "Conforming Finite Elements Based on Complete Polynomials", Computers and Structures, Vol. 4, pp. 521-530, 1974.

25. Strang, G. and Fix, G. J. An Analysis of the Finite Element Method, 3rd Ed., John Wiley & Sons, N.Y., 1981.

26. Barsky B. A. and Greenberg, D. P. "Interactive Surface Representation System using B-spline Formulation with Interpolation Capability", Computer Aided Design, Vol. 14, No. 4, July, 1984, pp. 187-194.

27. Zienkiewicz, O. C. The Finite Element Method, 3rd Ed., McGraw-Hill (UK), 1977.

28. Heubner, K. H. The Finite Element Method for Engineers, 4th Ed., John Wiley & Sons, N.Y., 1975.

29. Cook, R. D. Concepts and Applications of Finite Element Analysis, 2nd Ed., John Wiley & Sons, N.Y., 1981.

30. do Carmo, M. P. Differential Geometry of Curves and Surfaces, Prentice-Hall, N.J., 1976.

31. Faux, I. D. and Pratt, M. J. Computational Geometry for Design and Manufacturing, Wiley, N.Y., 1979.

32. Foley, J. D. and Van Dam, A. Fundamental Eelement for Computer Graphics, McGraw-Hill, N.Y., 1976.

33. Gordon, W. J. and Riesenfeld, R. F. "B-Spline Curves and Surfaces", Proc. of a Conference on Computer Aided Geometric Design (Editted by Barnhill and Riesenfeld), pp. 95-126, Univ. of Utah, March 1974.

34. Nowacki, H. "Curve and Surface Generation and Fairing", Computer Aided Design, Modelling, System Engineering, CAD-System (Ed. G. Goos and J. Hartmanis), Lecture Notes in Computer Science No. 89, pp. 137-176.

35. Rogers, D. F. and Adams J. A. Mathematical Eelement for Computer Graphics, McGraw-Hill, N.Y., 1976.

36. Schoenberg, I. J. "Contributions to the Problem of Approximation of Equidistant Data by Analytic Functions", Quater. Appl. Math. Vol. 4, 1946, pp. 49-99.

37. deBoor, C. "On Calculation with B-splines", J, Approx. Theory, Vol. 6, 1972,pp. 50-62.

38. Barsky, B. A. and Greenberg, D. P. "Determining a Set of B-spline Control Vertices to Generate an Interpolating Surface", Computer Graphics and Image Processing, Vol. 14, 1980, pp. 203-226.

39. Riesenfeld, R. F. "Application of B-spline Approximation to Geometric Problems of Computer Aided Design", Ph.D Thesis, Syracuse Univ., 1973.

40. Schoenberg, I. J. "On Spline Functions" with Supplement by T. N. F. Greville, Inequalities (Ed. O. Shisha), Acdemic Press, 1967, pp. 255-291.

41. Cox, M. G. "The Numerical Evaluation of B-splines", National Physical Lab. (Teddington, England), DNAC 4, Aug., 1971.

42. Gordon, W. J. "Spline Blending Surface Interpolation Through Curve Network", J. of Mech. Math., Vol. 18, 1969, pp. 931-952.

43. Coons, S. A. "Surfaces for Computer Aided Design", Design Div., Mech. Eng. Dept., MIT, 1964, Revised in 1967.

44. Choi, K. K., Haug, E. J., Hou, J. W. and Sohoni, V. N., "Pshenichny's Linearization Method for Mechanical System Optimization", ASME Journal of Mechanical Design, Vol. 105, No. 1, 1983, pp. 97-103.

45. Dym, C. and Shames, I. H. <u>Solid Mechanics - A Variational Approach</u>, McGraw-Hill, N.Y., 1973.